Enhancing microalgal biomass harvesting efficiency using thermoresponsive polymers

by

Xuexue Wang

B.S., Jiangnan University, 2012
M.S., Nanjing Tech University, 2019

AN ABSTRACT OF A DISSERTATION

submitted in partial fulfillment of the requirements for the degree

DOCTOR OF PHILOSOPHY

Department of Grain Science and Industry
College of Agriculture

KANSAS STATE UNIVERSITY
Manhattan, Kansas

2024

Abstract

Microalgae-based biorefining presents significant potential; however, the high costs associated with the harvesting of algal biomass pose substantial challenges to its commercialization. This research aims to develop innovative technology for algal cell harvesting, facilitating a cost-competitive and environmentally sustainable biorefinery. Poly(N-isopropylacrylamide) (PNIPAM), known for its temperature-induced phase transition properties, is explored as a means to capture algal cells within the cultivation medium.

This study investigates PNIPAM and its derivatives to elucidate the fundamental principles and potential applications of thermoresponsive polymers (TRPs) for the harvesting of microalgae. Variants of PNIPAM were synthesized, and the impacts of charge, molecular weight, amine content, and polymer concentration on the phase transition temperature and degree of phase separation were systematically examined. Results indicated that the lower critical solution temperature (LCST) of PNIPAM decreases with increasing concentration, with the rate of decrease attenuating at higher molecular weights. Notably, amine content did not exert a significant influence on the LCST. The efficacy of these properties on the harvesting of *Chlorella vulgaris* was assessed, achieving a remarkable 92% algae harvesting efficiency (AHE) with PNIPAM (300 kDa). However, amine-modified TRPs did not enhance harvesting performance. These findings underscore the potential of TRPs as a viable polymer class for microalgae harvesting, thereby advancing the microalgae industry.

To broaden the applicability of TRPs, additional algal strains with varying sizes, culture media, and cell wall compositions were evaluated. In addition to *C. vulgaris*, strains such as

Chlorococcum oleofaciens, *Chlorella protothecoides*, and *Nannochloropsis oculata* were investigated. Results demonstrated that both higher molecular weight and concentration positively influenced cell harvesting efficacy. PNIPAM (300 kDa) consistently harvested over 90% of algal cells across all four strains within the cultivation medium. PNIPAM was found to be particularly effective for *N. oculata*, which thrives in seawater and possesses a cell size of 2-10 μm with a cell wall primarily composed of glucosamine. Notably, the introduction of amine-induced positive charge did not facilitate harvesting even when the charge-shielding effect is diminished. Structural transitions of TRPs following phase changes indicated that algal cells may become encapsulated within the polymer meshwork, facilitating their extraction. The harvesting process resulted in a vitality reduction of more than 50% in algal cells, alongside noticeable shrinkage and damage to the cell wall.

Furthermore, the grafting of PNIPAM onto various substrate materials, including cotton fabric, polyester fabric, polyester sheets, and polystyrene flexible sheets, was explored to enhance the convenience and cost-effectiveness of PNIPAM recycling and reuse. Among the tested grafted PNIPAMs, PNIPAM (300 kDa) grafted onto cotton fabric exhibited the highest grafting yield (2.38 ± 0.39 mg/cm^2) and optimal AHE of 72.31 ± 0.56%. Allowing the polymer to dissolve completely prior to heating significantly improved AHE during the harvesting process. Moreover, PNIPAM-grafted cotton fabrics demonstrated the capacity for reuse across more than 20 cycles before a decline in AHE was observed. The implementation of grafted PNIPAM on substrate materials presents a promising cost-effective strategy for algal harvesting, thereby promoting the commercialization of microalgae biorefineries.

Overall, this study demonstrates the significant potential of PNIPAM as a novel approach

for the efficient harvesting of microalgae, addressing key challenges in the commercialization of microalgae-based biorefineries. This research lays the groundwork for future developments in algae biorefining processes, encouraging further exploration and optimization of thermoresponsive polymers to foster a more cost-effective and environmentally friendly approach to microalgae harvesting and biorefinery commercialization.

Enhancing microalgal biomass harvesting efficiency using thermoresponsive polymers

by

Xuexue Wang

B.S., Jiangnan University, 2012
M.S., Nanjing Tech University, 2019

A DISSERTATION

submitted in partial fulfillment of the requirements for the degree

DOCTOR OF PHILOSOPHY

Department of Grain Science and Industry
College of Agriculture

KANSAS STATE UNIVERSITY
Manhattan, Kansas

2024

Approved by:

Major Professor
Dr. Yonghui Li

Copyright

Abstract

Microalgae-based biorefining presents significant potential; however, the high costs associated with the harvesting of algal biomass pose substantial challenges to its commercialization. This research aims to develop innovative technology for algal cell harvesting, facilitating a cost-competitive and environmentally sustainable biorefinery. Poly(N-isopropylacrylamide) (PNIPAM), known for its temperature-induced phase transition properties, is explored as a means to capture algal cells within the cultivation medium.

This study investigates PNIPAM and its derivatives to elucidate the fundamental principles and potential applications of thermoresponsive polymers (TRPs) for the harvesting of microalgae. Variants of PNIPAM were synthesized, and the impacts of charge, molecular weight, amine content, and polymer concentration on the phase transition temperature and degree of phase separation were systematically examined. Results indicated that the lower critical solution temperature (LCST) of PNIPAM decreases with increasing concentration, with the rate of decrease attenuating at higher molecular weights. Notably, amine content did not exert a significant influence on the LCST. The efficacy of these properties on the harvesting of *Chlorella vulgaris* was assessed, achieving a remarkable 92% algae harvesting efficiency (AHE) with PNIPAM (300 kDa). However, amine-modified TRPs did not enhance harvesting performance. These findings underscore the potential of TRPs as a viable polymer class for microalgae harvesting, thereby advancing the microalgae industry.

To broaden the applicability of TRPs, additional algal strains with varying sizes, culture media, and cell wall compositions were evaluated. In addition to *C. vulgaris*, strains such as

Chlorococcum oleofaciens, *Chlorella protothecoides*, and *Nannochloropsis oculata* were investigated. Results demonstrated that both higher molecular weight and concentration positively influenced cell harvesting efficacy. PNIPAM (300 kDa) consistently harvested over 90% of algal cells across all four strains within the cultivation medium. PNIPAM was found to be particularly effective for *N. oculata*, which thrives in seawater and possesses a cell size of 2-10 μm with a cell wall primarily composed of glucosamine. Notably, the introduction of amine-induced positive charge did not facilitate harvesting even when the charge-shielding effect is diminished. Structural transitions of TRPs following phase changes indicated that algal cells may become encapsulated within the polymer meshwork, facilitating their extraction. The harvesting process resulted in a vitality reduction of more than 50% in algal cells, alongside noticeable shrinkage and damage to the cell wall.

Furthermore, the grafting of PNIPAM onto various substrate materials, including cotton fabric, polyester fabric, polyester sheets, and polystyrene flexible sheets, was explored to enhance the convenience and cost-effectiveness of PNIPAM recycling and reuse. Among the tested grafted PNIPAMs, PNIPAM (300 kDa) grafted onto cotton fabric exhibited the highest grafting yield (2.38 ± 0.39 mg/cm^2) and optimal AHE of 72.31 ± 0.56%. Allowing the polymer to dissolve completely prior to heating significantly improved AHE during the harvesting process. Moreover, PNIPAM-grafted cotton fabrics demonstrated the capacity for reuse across more than 20 cycles before a decline in AHE was observed. The implementation of grafted PNIPAM on substrate materials presents a promising cost-effective strategy for algal harvesting, thereby promoting the commercialization of microalgae biorefineries.

Overall, this study demonstrates the significant potential of PNIPAM as a novel approach

for the efficient harvesting of microalgae, addressing key challenges in the commercialization of microalgae-based biorefineries. This research lays the groundwork for future developments in algae biorefining processes, encouraging further exploration and optimization of thermoresponsive polymers to foster a more cost-effective and environmentally friendly approach to microalgae harvesting and biorefinery commercialization.

Table of Contents

List of Figures xv

List of Tables xx

Acknowledgements xxi

Chapter 1 - Introduction 1

1.1 Microalgae 1

1.1.1 Chlorococcum oleofaciens 2

1.1.2 Chlorella protothecoides 4

1.1.3 Nannochloropsis oculata 5

1.1.4 Chlorella vulgaris 7

1.2 Microalgae biorefinery 10

1.3 Microalgae harvesting 12

1.3.1 Centrifugation 13

1.3.2 Sedimentation 14

1.3.3 Chemical flocculation 15

1.3.4 Particle-based flocculation 17

1.3.5 Bio-flocculation 18

1.4 Utilization of Thermo-responsive polymers to separate algal biomass 19

1.5 Conclusions and prospects 21

Chapter 2 - Microalgae Aggregation induced by Thermoresponsive Polymers 23

Abstract 24

2.1. Introduction 25

2.2. Materials and Methods 28

2.2.1 Materials 28

2.2.2 Synthesis of thermoresponsive polymers 28

2.2.3 Characterization of thermoresponsive polymers 30

2.2.4 Microalgae harvesting by using thermoresponsive polymers 31

2.2.5 Data analysis 32

2.3. Results and Discussion 33

2.3.1 Synthesis of thermoresponsive polymers 33

2.3.2 Characterization of thermoresponsive polymers 34

2.3.3 Thermoresponsive polymer-induced microalgae harvesting 40

2.4. Conclusions 43

Chapter 3 - Innovative Microalgae Harvesting via Thermoresponsive Polymers: Insights into Poly(N-isopropylacrylamide) Efficacy and Mechanisms 45

Abstract 45

3.1. Introduction 47

3.2. Materials and Methods 49

3.2.1 Materials 49

3.2.2 Synthesis of PNIPAM, PNIPAM-AA, and PNIPAM-MTAC 50

3.2.3 Characterization of the synthesized thermoresponsive polymers 51

3.2.4 Microalgae harvesting by using thermoresponsive polymers 51

3.2.5 Scanning electron microscope 53

3.2.6 Algae cell property evaluation after harvesting with thermoresponsive polymers 54

3.2.7 Data analysis 55

3.3 Results and Discussion 56

3.3.1 Characterization of the synthesized thermoresponsive polymers 56

3.3.2 Microalgae harvesting by using thermoresponsive polymers 59

3.3.3. Scanning electron microscope 65

3.3.4. Algae cell property evaluation after harvesting with thermoresponsive polymers..... 66

3.4. Conclusions..... 70

Chapter 4 - Temperature-Induced Algae Harvesting with Grafted Poly(N-isopropylacrylamide) 72

Abstract..... 72

4.1. Introduction..... 73

4.2. Materials and Methods..... 75

4.2.1 Materials 75

4.2.2 Polymer grafting 76

4.2.3 Algae harvesting 77

4.2.4 Data analysis 79

4.3. Results and Discussion 79

4.3.1 PNIPAM grafting on fabric substrate materials..... 79

4.3.2 Characterization of grafted substrate materials..... 81

4.3.3 Microalgae harvesting by using grafted PNIPAM on different substrate materials.... 86

4.4. Conclusions 91

Chapter 5 - Conclusions and recommendations 93

References 97

Appendix A - Copyright permission for Figure 1.1 131

Appendix B - Copyright permission for Figure 1.3 132

Appendix C - Copyright permission for Chapter 2 133

List of Figures

Figure 1.1. Nomarski interference microscopy of *Chlorococcum oleofaciens* Trainor & H.C. Bold in liquid or on agar AF-6 medium (Kawasaki et al. 2015). (A, B) Vegetative cells on agar medium. (A) Optical section. (B) Surface view. (C, D) Ellipsoidal vegetative cell C), and stigma of a zoospore (D) in liquid medium. (E, F) Artificially compressed pyrenoid by coverslip in a vegetative cell showing a continuous starch sheath (E), and an aplanosporangium with eight aplanospores (F) on agar medium. (G–K) Mature cells and oil droplets in liquid medium. (G) Mature cell. (H) Brownish oil droplet. (I) Colorless oil droplet. (J, K) Mature cell stained with Nile red. (J) Light field. (K) Fluorescence microscopy. (L, M) Zoospore (L), and a zoosporangium with eight zoospores (M) in liquid medium. An asterisk indicates the anterior direction of the zoospore. Bar = 10 μm (F, G, J, K, M), 5 μm (A–C, H, I), 2 μm (E, L), or 1 μm (D). cv, contractile vacuole; d, oil droplet; e, stigma; n, nucleus; p, pyrenoid. CC BY. Used with permission. 3

Figure 1.2. Image of *Nannochloropsis oculata* (Malakootian et al. 2016). CC BY-NC-ND. 6

Figure 1.3. Schematic ultrastructure of *C. vulgaris* representing different organelles (Safi et al. 2014). Copyright (2014), with permission from Elsevier. 8

Figure 1.4. Overview of microalgae biorefinery to produce value-added bioproducts. 11

Figure 1.5. Auto-flocculation harvesting of algal biomass. Three vials contain algal samples cultured in different nitrate concentrations: (left) 0.5×; (middle) 1× (original); and (right) 2× (Nguyen et al. 2017). CC BY-NC-ND. 15

Figure 2.1. (a) Phase change of TRPs; (b) Chemical formula of NIPAM and TRPs and (c) FT-IR spectra of NIPAM and TRPs. 34

Figure 2.2. (a) Standard curve for the calculation of TRPs' MWs with PMMA as a standard; (b) LCST of TRPs with different MWs at different concentrations; and (c) DSC curves for PNIPAM-300 kDa and PNIPAM-100 kDa. 37

Figure 2.3. LCST of PNIPAM copolymers with AA (a) and MTAC (b) at the concentration of 100 mg/mL. 38

Figure 2.4. Zeta potentials of PNIPAM copolymers with varied AA (a) and MTAC (b) contents with different MWs. 40

Figure 2.5. (a) UV-vis spectra for algae (UTEX 2714) and PNIPAM; and (b) standard curve for algae BDW vs. OD430 in its cultivation medium. 40

Figure 2.6. (a) Schematic diagram of the TRP-induced algae harvesting; (b) Effects of the MW and PNIPAM concentration on algae harvesting efficiency (AHE); (c) Effects of the AA content and PNIPAM-AA concentration on AHE; and (d) Effects of the MTAC content and PNIPAM-MTAC concentration on AHE. 43

Figure 3.1. ^{1}H NMR spectrum of NIPAM (a), PNIPAM (b), PNIPAM-AA (c), and PNIPAM-MTAC (d) 57

Figure 3.2. TRPs' LCST in water (a-b), Bristol medium (c-d), and modified artificial sea water (MASW) (e-f) 58

Figure 3.3. UV-vis spectra for algae strains and PNIPAM (a); and standard curve for algal BDW vs. OD_{430} in their cultivation media (b: *Cc. oleofaciens*; c: *C. protothecoides*; d: *N. oculata*; e: *C. vulgaris*)..... 59

Figure 3.4. Algae harvest efficiency induced by TRPs (a: *Cc. oleofaciens* harvested by PNIPAM; b: *C. protothecoides* harvested by PNIPAM; c: *N. oculata* harvested by PNIPAM; d: *C. vulgaris* harvested by PNIPAM. e-h: algae harvested by PNIPAM-AA; i-l: algae harvested by PNIPAM-MTAC) 63

Figure 3.5. Algae harvest efficiency induced by TRPs in salt-free buffer (a: *Cc. oleofaciens* harvested by PNIPAM-AA; b: *C. protothecoides* harvested by PNIPAM-AA; c: *N. oculata* harvested by PNIPAM-AA; d: *C. vulgaris* harvested by PNIPAM-AA. e-h: algae harvested by PNIPAM-MTAC) 65

Figure 3.6. SEM of PNIPAM (a: unheated PNIPAM ×50; b: unheated PNIPAM ×100; c: unheated PNIPAM ×3000; d: heated PNIPAM ×50; e: heated PNIPAM ×100; f: heated PNIPAM ×3000)..... 66

Figure 3.7. MTT assay of algae cells after harvesting (a: *Cc. oleofaciens* harvested by PNIPAM-AA; b: *C. protothecoides* harvested by PNIPAM-AA; c: *N. oculata* harvested by PNIPAM-AA; d: *C. vulgaris* harvested by PNIPAM-AA. e-h: algae harvested by PNIPAM-MTAC)67

Figure 3.8. LSM images of algae cells (a: normal *Cc. oleofaciens* cells; b: normal *C. protothecoides* cells; c: normal *N. oculata* cells; d: normal *C. vulgaris* cells. e-h: algae harvested by PNIPAM. i-l: algae harvested by PNIPAM-AA. m-p: algae harvested by PNIPAM-MTAC) 69

Figure 3.9. Transmission electron micrographs of (a) normal *Cc. oleofaciens* cells, (b) *Cc. oleofaciens* incubated with PNIPAM-300 kDa (32℃ for 30 min), (c) normal *C. protothecoides* cells, (d) *Cc. oleofaciens* incubated with PNIPAM-15 kDa (46℃ for 30 min), (e) normal *N. oculata* cells, (f) *N. oculata* incubated with PNIPAM-100 kDa (31℃ for 30 min), (g) normal *C. vulgaris* cells, (h) *C. vulgaris* incubated with PNIPAM-100 kDa (31℃ for 30 min), (i) *C. vulgaris* incubated at 31℃ for 30 min and (j) *C. vulgaris incubated* incubated with PNIPAM-100 kDa at 25℃ for 30 min. CW denotes the cell wall of algal cells. The arrows show the formation of villi-like structures on the cell wall after harvesting. 70

Figure 4.1. Grafting yield of PNIPAM onto cotton by using various methods (a); grafting yield of PNIPAM with various MWs onto cotton (b); grafting yield of PNIPAM-300 kDa onto various substrate materials (c). 80

Figure 4.2. FTIR spectra for PNIPAM-grafted cotton fabric (a), PNIPAM-grafted PET sheet (b), PNIPAM-grafted PET fabric (c), and PNIPAM-grafted PS sheet (d). 83

Figure 4.3. SEM images for the original (a-c), RT grafted (d-f), heated grafted (g-i), and plasma initiated grafted (j-l) cotton fabrics. Scale bar: 500 μm for ×100 (a, d, g, j), 50 μm for ×1000 (b, e, h, k), and 10 μm for ×3000 (c, f, I, l). 85

Figure 4.4. SEM images for the original and grafted PET sheet (a-b), PET fabric (c-d), and PS sheet (e-f). Scale bar: 500 μm for ×100 and 50 μm for ×1000. 86

Figure 4.5. Immediate algae harvesting efficiency by using PNIPAM-grafted cotton fabric with different MW (a) and using different substrate materials with grafted PNIPAM (b). 88

Figure 4.6. Effect of PNIPAM dissolution on algae harvesting efficiency by using PNIPAM-grafted cotton fabric with different MW (a) and using PNIPAM-grafted other materials (b). 89

Figure 4.7. Algae harvesting efficiency (AHE) of consecutive harvesting cycles using PNIPAM-300 kDa grafted on cotton fabric (a); Schematic for the improved continuous algae harvesting process using grafted cotton (b); and AHE of consecutive multiple harvest with addition of the elution step (c). 91

List of Tables

Table 1.1. Lipid production of commercial algae. 2

Table 2.1. Recipe for the synthesis of different thermoresponsive polymers 29

Table 2.2. Actual MW of PNIPAM copolymers with AA and MTAC 36

Table 3.1. Properties of algae used in this research 52

Acknowledgements

This work was supported by the National Science Foundation [Grant numbers 1846827].

The authors are grateful for the NMR analysis to Dr. Mi Li and Kailong Zhang from Department of Chemical and Biomolecular Engineering, University of Tennessee.

We would also like to thank Dr. Daniel L. Boyle from KSU Microscopy Facility in the Division of Biology for his support in LSM, SEM and TEM.

I am deeply indebted to Dr. Yi Zheng, my former major advisor, who is a very patient and supportive to my academic and mentally life. Also, words cannot express my gratitude to my now major advisor, Dr. Yonghui Li, for his invaluable kindness in being willing to take care of me as my advisor after Dr. Zheng resigned. Additionally, this endeavor would not have been possible without my defense committee, Dr. Xiuzhi Sun, Dr. Lisa Wilken and Dr. Donghai Wang, who generously provided knowledge and expertise.

I am also grateful to my friends, especially my lab mates, for their feeding, late night feedback and moral support. Thanks should also go to the staff from our department, who made my life here easier.

Lastly, I would be remiss in not mentioning my family, especially my mom. Their belief in me has kept my spirits and motivation high during this process.

Chapter 1 - Introduction

1.1 Microalgae

Microalgae are a diverse class of photosynthetic eukaryotic microorganisms, which are mostly found in widely dispersed and unconnected water bodies (Randrianarison and Ashraf 2017). Algae are the main producers of food in the ocean. Not only does the production of all seafood in nature depend on algae, but also plants derived from algae (such as bryophytes and vascular plants) are the source of all our food and feed. In short, all life can ultimately be traced back to algae and its predecessors. Microalgae have great economic potentials and contribute to human society in many ways (Gallardo-Rodríguez et al. 2012; Kay and Barton 1991; Wells et al. 2017). They can be used to produce pigments, colorants, biofertilizers/inoculants and cosmeceuticals, as well as feed, human food/food supplements, nutraceuticals (e.g., β-carotene and provitamin A), biofuels, and polyunsaturated fatty acids. They can also be used for wastewater treatment and phytoremediation (Borowitzka 1995, 2013; Gantar and Svirčev 2008; Lee 1997; Specht and Mayfield 2014). Four algae strains used in this work are described in detail.

Technologies for converting algal biomass into valuable commodities, including fuels, have garnered increasing attention recently (Sharmila et al. 2022). The production of biofuels from algal biomass presents a viable long-term solution for climate change mitigation and energy sustainability. Algal biomass has emerged as a promising alternative to traditional energy sources, offering potential for sustainable and reliable products (Narayanan 2024). One of the key advantages of algae is their ability to grow abundantly in saline and harsh environments,

positioning them as one of the most promising non-food sources for biofuels. The composition of algal biomass, which includes varying amounts of sugars, proteins, and lipids, differs between species and is influenced by both biotic and abiotic factors, such as sunlight and temperature (Anbuchezhian, Karuppiah, and Li 2015). This variability highlights the potential of algal biomass as a versatile resource for biofuel production. Several commercial algae strains used in this work have been shown in Table 1.1.

Table 1.1. Lipid production of commercial algae.

Strain	Class	Medium	Lipid Production
Chlorococcum oleofaciens (Trainor and Bold 1953)	Chlorophyceae	Freshwater	198.3 ± 4.61mg/L.d (Rayati, Rajabi Islami, and Shamsaie Mehrgan 2020)
Chlorella protothecoides (Huss et al. 1986)	Chlorophyceae	Freshwater	1068.11 mg/L.d (Li et al. 2024)
Nannochloropsis oculata (Hibberd 1981)	Eustigmatophyceae	Seawater	0.037 ± 0.007 g/L.d (Abdelkarim, Wijffels, and Barbosa 2024)
Chlorella vulgaris (González, Cañizares, and Baena 1997)	Chlorophyceae	Freshwater	149.0 ± 24.0 mg/L.d (Shen et al. 2019)

1.1.1 Chlorococcum oleofaciens

Chlorococcum is one of the largest genera in the order *Chlamydomonadales*, with approximately 50 species (Ettl and Gärtner 2013; Maltseva et al. 2024), which are widely distributed in various ecosystems (Maltsev, Maltseva, and Maltseva 2022; Scherbina, Maltseva, and Solonenko 2014). *Chlorococcum oleofaciens* was first described by Trainor and Bold (Trainor and Bold 1953). It occurs as vegetative cells, mature cells, zoospores, zoosporangia, aplanospores, and aplanosporangia (Kawasaki, Nakada, and Tomita 2015). The maximum size of *Cc. oleofaciens* mature cells is 20-46 μm with cell wall thickness of 0.5-6.5 μm (Kawasaki et al.

2015). *Cc. oleofaciens* is a freshwater unicellular microalga that accumulates large amounts of lipids in mature cells (Rajabi Islami and Assareh 2020). These oil droplets turn yellow orange during aging of the culture (Rayati et al. 2020). Morphologies of *Cc. oleofaciens* have been shown in Figure 1.2.

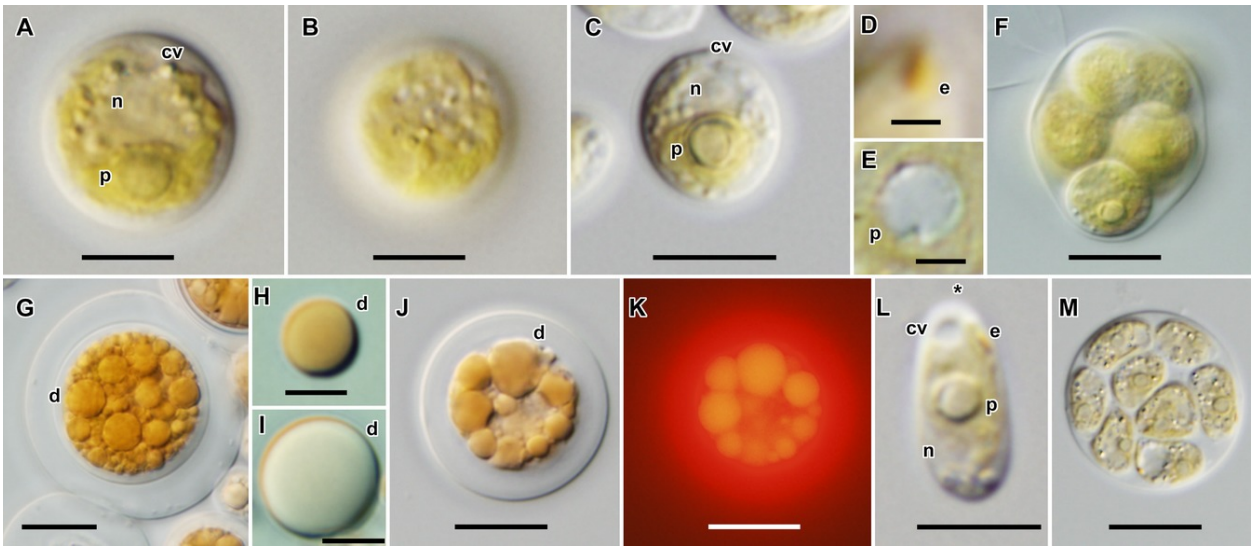

Figure 1.1. Nomarski interference microscopy of *Chlorococcum oleofaciens* Trainor & H.C. Bold in liquid or on agar AF-6 medium (Kawasaki et al. 2015). (A, B) Vegetative cells on agar medium. (A) Optical section. (B) Surface view. (C, D) Ellipsoidal vegetative cell C), and stigma of a zoospore (D) in liquid medium. (E, F) Artificially compressed pyrenoid by coverslip in a vegetative cell showing a continuous starch sheath (E), and an aplanosporangium with eight aplanospores (F) on agar medium. (G–K) Mature cells and oil droplets in liquid medium. (G) Mature cell. (H) Brownish oil droplet. (I) Colorless oil droplet. (J, K) Mature cell stained with Nile red. (J) Light field. (K) Fluorescence microscopy. (L, M) Zoospore (L), and a zoosporangium with eight zoospores (M) in liquid medium. An asterisk indicates the anterior direction of the zoospore. Bar = 10 µm (F, G, J, K, M), 5 µm (A–C, H, I), 2 µm (E, L), or 1 µm (D). cv, contractile vacuole; d, oil droplet; e, stigma; n, nucleus; p, pyrenoid. CC BY. Used with permission.

Several previous studies attempted to evaluate the potential of *Cc. oleofaciens* as a biodiesel producer. Halim et al. (2011) proposed that the fatty acid composition of *Cc. oleofaciens* is

dominated by oleic acid (C 18:1, 63 wt %) and palmitic acid (C 16:0), making it suitable for biodiesel production. Del Río et al. (2017) found that limited nitrate supply led to increased fatty acid level but reduced biomass productivity in *Cc. oleofaciens* in continuous culture, and the maximum fatty acid productivity (111 $mg \cdot L^{-1} \cdot d^{-1}$) was obtained at 2 mM nitrate. Rayati et al. (2020) studied the effects of light intensity on the growth performance and lipid accumulation of *Cc. oleofaciens* and found that when the algae were grown at 400 μmol photons$\cdot m^{-2} \cdot s^{-1}$, it had a lipid content of up to 59.2% and a lipid productivity of 198.3 $mg \cdot L^{-1} \cdot day^{-1}$. The fatty acid profile contained 82.3% saturated fatty acids, with palmitic acid, stearic acid, and myristic acid being the major three fatty acids. Islami and Assareh (2020) added iron ions to the culture medium for *Cc. oleofaciens*, the algal growth rate increased by 2.19 times and the exponential growth period was extended by 10 days compared with the normal culture medium when the iron ion concentration was increased to 10^{-6} $mol \cdot L^{-1}$. Also, the highest biomass and lipid productivity were 310 $mg \cdot L^{-1} \cdot d^{-1}$ and 139 $mg \cdot L^{-1} \cdot d^{-1}$, respectively.

1.1.2 Chlorella protothecoides

Among oil-producing microalgae, *Chlorella* species produces high levels of triacylglycerols (TAGs), which are ideal precursors for biodiesel production (Přibyl, Cepák, and Zachleder 2012; Sun et al. 2015; Yang et al. 2011). *Chlorella protothecoides* is a microalga that can grow photoautotrophically or heterotrophically, and it can adapt to different culture conditions (Xu, Miao, and Wu 2006). The heterotrophic growth of *Chlorella* strain requires an organic carbon source, usually acetic acid (CH_3COOH), glucose ($C_6H_{12}O_6$), glycerol ($C_3H_5(OH)_3$), or other organic compounds, resulting in high cell biomass concentration and high intracellular lipid content (Endo 1977; Heredia-Arroyo, Wei, and Hu 2010; Wu et al. 1994). In heterotrophic

growth, cells lose chloroplasts and photosynthetic capacity, thereby increasing the efficiency of fatty acid production (Rodríguez-Castillo et al. 2016).

Many studies have improved the cultivation methods of *C. protothecoides* in an attempt to increase its growth rate and oil production. Sun et al. (2015) conducted the first comprehensive study of lipid production in indoor and outdoor photoautotrophic *C. protothecoides* cultures. *C. protothecoides* CS-41 accumulated lipids up to 55% of dry weight, with triacylglycerols and oleic acid accounting for 71% of total lipids and 59% of total fatty acids, respectively. The optimal biomass and lipid productivity achieved in the outdoor panel photobioreactor were 1.25 g L^{-1} day^{-1} and 0.59 g L^{-1} day^{-1}, respectively. O'Grady and Morgan (2011) showed that *C. protothecoides* obtained specific growth rates and final lipid yields of 0.1/h and 0.31 g lipid/g substrate, respectively, using low-cost glycerol as the sole carbon source. *C. protothecoides* has been cultivated in a tetracycline environment (S. Wang et al. 2023). The results proved that *C. protothecoides* had a biosorption effect on low-concentration tetracycline and increased the biomass production by 13.26% with the addition of biochar. The study by Li et al. (2024) explored the possibility of co-cultivation of *C. protothecoides* and *Ellipsodium ellipsoidea* in enhancing cell growth and lipid accumulation. The biomass yield was 6.91 g L^{-1}, and the lipid productivity was 1.07 g L^{-1} d^{-1}, which were increased by 1.41 to 1.70 times and 3.05 to 3.10 times, respectively, compared with the single culture. The supplementation of exogenous metabolite melatonin (50 μM) increased the biomass and lipid content of the co-cultured algae to 9.27 g L^{-1} and 69.86%.

1.1.3 Nannochloropsis oculata

Nannochloropsis oculata is a species of marine unicellular algae belonging to the genus

Nannochloropsis, family Monodopsidaceae, order Eustigmatales, class Eustigmatophyceae (Hibberd 1981; Kagan and Matulka 2015). They are usually simple, non-flagellated, non-zoospore producing, free-floating, and spherical to slightly ovoid cells (Al-Hoqani, Young, and Purton 2016; Zanella and Vianello 2020) with the size of 2-8 μm (Figure 1.3). *N. oculata* is promising for biodiesel production and can also be used as a food source in aquaculture due to its ability to produce high-value oil containing omega-3 fatty acids (Chua and Schenk 2017; Sukenik, Carmeli, and Berner 1989). In addition, *N. oculata* contains high levels of protein, polyunsaturated fatty acids, and antioxidant pigments, making it safe for use in human dietary supplements (Kagan and Matulka 2015; Kent et al. 2015).

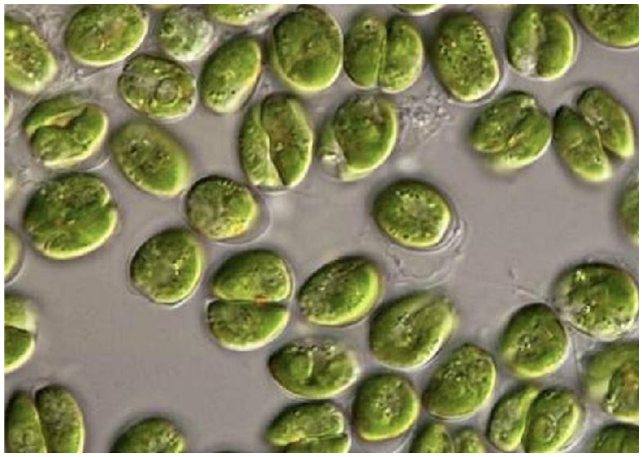

Figure 1.2. Image of *Nannochloropsis oculata* (Malakootian et al. 2016). CC BY-NC-ND.

A two-stage cultivation strategy was developed to enhance lipid production by *N. oculata* (Su et al. 2011). Cell biomass growth and lipid production were divided into two independent and non-interacting stages. The algae were first cultivated under conditions suitable for cell growth and then transferred to a growth-restricted environment to improve lipid production. The

final lipid yield was 2.82 times higher than that of the traditional single-stage batch culture system, at 0.324 g L^{-1} d^{-1}. Rasdi and Qin (2015) evaluated the growth of *N. oculata* by manipulating the ratio of nitrogen (N) to phosphorus (P) in the culture medium. The results showed that the N:P ratio did not affect the growth rate of the algae but affected the synthesis of proteins as well as lipids. *N. oculata* has been successfully inoculated in medium containing oilfield produced water (PW) and obtained effective growth (Ammar, Khadim, and Mohamed 2018). At 25% PW, the biomass yields of *N. oculata* were 0.856 g/L and 89% of the oil content could be removed. In addition, a two-pronged strategy of random mutagenesis and adaptive laboratory evolution has been used to greatly improve the thermotolerance of *N. oculata* (Arora, Lo, and Philippidis 2022). The best mutant not only survived at 35°C, but also had 1.43-fold and 2.24-fold higher biomass and lipid productivity than the wild type at 25°C, respectively. Metabolomics and lipidomics showed that the central carbon metabolism and membrane lipid synthesis of the thermotolerant strain were rewired to ensure cellular homeostasis without compromising productivity. In summary, various approaches have been investigated to enhance the growth and lipid production of *N. oculata.*

1.1.4 Chlorella vulgaris

Chlorella vulgaris is a species of microalgae belonging to the order *Chlorococcalales*, family *Oocystaceae*, genus *Chlorella* (Coronado-Reyes et al. 2020). Its shape is spherical with a size from 2 to 10 μm, and its structure is similar to that of higher plants, containing cell walls, mitochondria, and chloroplasts (Safi et al. 2014). Figure 1.4 shows the *C. vulgaris* structure. The cell wall of *C. vulgaris* changes with the growth stage and environmental conditions, from a thin electron-dense monolayer of 2 nm in the sporangium stage to 17-21 nm after maturity

(Yamamoto et al. 2004; Yamamoto, Kurihara, and Kawano 2005).

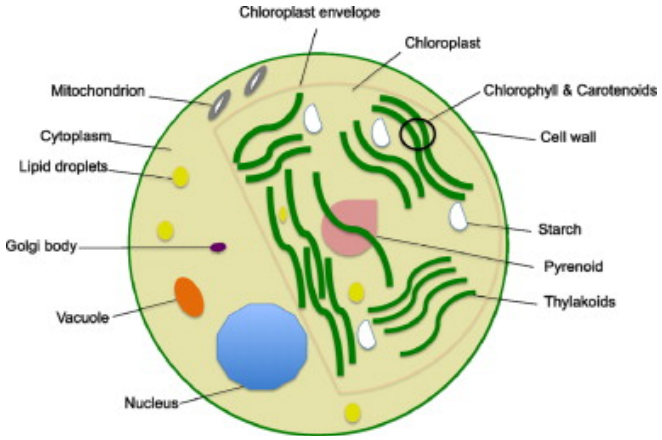

Figure 1.3. Schematic ultrastructure of *C. vulgaris* representing different organelles (Safi et al. 2014). Copyright (2014), with permission from Elsevier.

C. vulgaris reproduces asexually by autospore formation, which is common among algae. In this case, four daughter cells with their own cell walls are formed within the cell wall of a mother cell. The mother cell wall then ruptures, releasing the mature daughter cells (Yamamoto et al. 2004, 2005). *C. vulgaris* is one of the most commonly used microalgae in aquaculture and can be used as feed, growth promoter, and immunostimulant (Ahmad et al. 2020). *C. vulgaris* can also be used to produce lipids (e.g., triglycerides, phospholipids, glycolipids) (Maliwat et al. 2017; Ru et al. 2020; Yeh and Chang 2011), proteins and amino acids (Gouveia et al. 2006; Liu and Chen 2016), carbohydrates (e.g., starch, cellulose, β-1-3-glucans, and sulphonated polysaccharides) (Lordan, Ross, and Stanton 2011; Mohamed 2008; Tabarsa et al. 2015), pigments (e.g., β-carotene, astaxanthin, cantaxanthin, lutein, and chlorophyll) (Cha et al. 2010; Ru et al. 2020), vitamins, and minerals (Maruyama et al. 1997).

Sharma et al. (2012) determined the effects of culture conditions on the growth of *C. vulgaris* and the contents of chlorophyll a, chlorophyll b, total carotene, total protein, and total free amino acids under different temperature and light conditions. The results showed that *C. vulgaris* had the highest biomass (30.2 mg/50 ml), chlorophyll-a (2.16%), chlorophyll-b (0.59%), and total protein contents when the temperature was 25-30°C and natural sunlight was exposed to the north-facing windows of the growth chamber. However, the contents of total carotenoids and free amino acids reached their maximum values of 0.440% and 834 μg/mg fresh weight, respectively, under continuous light at 30-35°C. Candido and Lombardi (2017) presented results on the growth and biomass yield of *C. vulgaris* in conventional and biodigested vinasse, a residue of the sugarcane industry. Comparable to the growth in normal medium, *C. vulgaris* could grow in 60% filtered conventional vinasse and 80% biodigested vinasse with the growth rate up to 1.2 day^{-1}. Organic food waste compost medium was also investigated to substitute inorganic medium for the cultivation of *C. vulgaris* (Chew et al. 2018). The use of 25% compost mixture combination resulted in higher biomass concentration (11.1%), more lipid (10.1%) and protein (2.0%) contents compared to the culture grown in complete inorganic medium. Ratomski and Hawrot-Paw (2021) used aquaculture wastewater (AWW) as a nutrient source to improve the lipid accumulation of *C. vulgaris* during growth. The biomass obtained with 80% AWW was the largest (727 $mg \cdot L^{-1}$), which was almost 5 times that of the synthetic medium while the lipid content ranged from 5.75% (80% AWW) to 11.81% (20% AWW). Peter et al. (2023) developed a mobile/digital app [FindAlgae] to replace the traditional UV-visible spectrophotometry to monitor the growth of *C. vulgaris*. Experimental results showed that the combination of recycled medium and fresh medium with a mixing ratio of 40% produced the greatest biomass growth (4.52 g/L), lipid (317.40 mg/g), protein (280.57 mg/g), and carbohydrate (451.37 mg/g). In the

process, the iterative model explained the results of each data set with an accuracy of more than 92% based on the performance of the trained model.

1.2 Microalgae biorefinery

Microalgae have gained increasing attention as a third-generation feedstock for biorefinery due to their high carbon density (including carbohydrates, proteins, and lipids), fast growth rate, short life cycle, and tolerance to a variety of environmental conditions (e.g., temperature, pH, salinity, and light intensity) (Okeke et al. 2022). Under right conditions, microalgae can accumulate metabolites through photosynthesis that serve as potential feedstocks for the production of various biofuels (Chisti 2018). For example, carbohydrates and various types of oils can be accumulated. The starch produced by algae is easily hydrolyzed into glucose and then fermented into biofuels (Harun et al. 2014). Genetically modified algae have long been used to directly produce ethanol through photosynthesis (Lü, Sheahan, and Fu 2011; Williams 2009). The triglyceride oil recovered from algal biomass can be easily converted into biodiesel by transesterification with methanol (Chisti 2007). Algal biomass can be fermented to produce biogas, or to generate energy-rich hydrogen (Montingelli, Tedesco, and Olabi 2015). In addition, it is possible to directly use live algae to produce hydrogen (Dubini and Gonzalez-Ballester 2016; Melis and Happe 2001). The conversion of algal biomass into liquid and gaseous fuels is feasible through chemical-physical processes, such as pyrolysis, hydrothermal treatment, and gasification (Chisti 2013). All of the above productions have been proven to be technically feasible.

Gendy and El-Temtamy (2013) pointed out that algae are the fastest-growing plants in the

world. The microalgal oil yield per unit area was estimated to be 7-31 times higher than palm oil. Biodiesel derived from microalgae shares similar physicochemical and functional properties to diesel, indicating the potential of microalgae as a green alternative feedstock to petroleum (Elkelawy et al. 2021; G. Li et al. 2020). For instance, *C. vulgaris* grown under nutrient-deficient conditions had oil content up to 70% of dry cell weight (Yun et al. 2019). Microalgae can produce 58,700 L/hac microalgae oil, which could be converted to 121,104 L/hac biodiesel (X. Wang et al. 2023). Thus, microalgae biorefinery is expected to be a platform for the conversion of microalgal biomass into a variety of value-added products, such as biofuels, bio-based chemicals, biomaterials, and bioactive substances. Advanced biotechnology, engineering technology, and green process engineering are able to achieve efficient, clean, and cyclic conversion and utilization of microalgal biomass (Tan et al. 2018). Figure 1.4 illustrates the concept of microalgae biorefinery to produce multiple products (Wang et al. 2022).

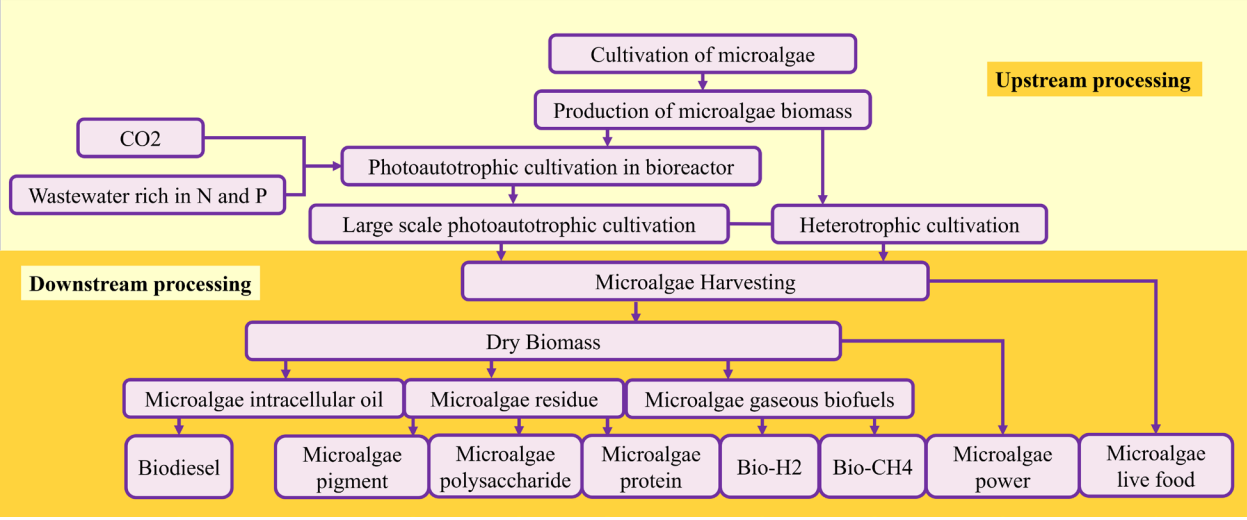

Figure 1.4. Overview of microalgae biorefinery to produce value-added bioproducts.

However, due to high infrastructure and downstream operation costs, the production of biodiesel from microalgae hasn't yet been an economically viable alternative to other fossil fuels. The cost of microalgae biodiesel ($3.52-3.75/L) is significantly higher than that of the biodiesel produced from other crops, such as soybean ($0.93~1.48/L) (Bhatt et al. 2022; Valverde et al. 2016). Hence, the concept of a microalgae biorefinery holds the potential to establish a sustainable green economy, while the cost should be well addressed through technique advancement.

1.3 Microalgae harvesting

Microalgae biorefinery suffers from several technical barriers at different stages of the upstream and downstream processes (Tan et al. 2018). Microalgal cells usually grow with very dilute concentrations (~0.2-0.5 g/L) such that algal biomass must be concentrated before downstream processing (Danquah et al. 2009). This is particularly important when the compounds of interest are restrained within the cells (e.g., cellular lipids and pigments). Harvesting of algal biomass is one of the biggest obstacles for downstream processing, as it involves significant energy consumption and cost contribution. Microalgal cells were found in different shape, size, and density, e.g., spherical, filamentous, and elongated ranging from 0.5 to 200 μm with cell density within 1070-1140 $kg \cdot m^{-3}$ (Henderson, Parsons, and Jefferson 2008). The cell surface charge can vary from -2 to -75 mV (Zeta potential) under the influence of chemical functional groups of cell wall, which changes with culture conditions and cell age (Roy and Mohanty 2019). Also, some species, such as *Chlamydomonas reinhardtii* are found to be flagellated and can evade flocculation by swimming out of flocs (Gerardo et al. 2015). The challenge for algal cell isolation from water is a result of the above-mentioned inherent

properties of algae, all of which lead to the formation of stable algal suspensions. Almost 80%-90% of the equipment cost is spent in dewatering microalgal biomass from open ponds (Amer, Adhikari, and Pellegrino 2011; Roy and Mohanty 2019). The technoeconomic analysis pointed out that reducing the cost of microalgae harvesting is the most effective way to reduce the total production cost and increase the profit of microalgae products (Sui et al. 2020).

Algae can be harvested by using different types of methods: centrifugation, filtration, flocculation, and a combination of some of these methods (Singh et al. 2023). Each process has its own advantages and limitations (Ahmad et al. 2022).

1.3.1 Centrifugation

Centrifugation is a proven dewatering technology in multiple industries because it can achieve solid concentrations of more than 90% within 2-5 min (Hussian and Ellatif 2018; Javed et al. 2019; Pahl et al. 2013). Heasman et al. (2000) conducted centrifugation tests on 9 different microalgae strains and found that the harvest efficiency using super centrifugation (a centrifuge designed to operate at higher than normal speeds) was between 94% and 100%, while the efficiency of cream separation and bucket centrifugation were significantly reduced. Japar et al. (2017) compared three different algae species using four different speeds of 1000, 3000, 5000, and 7000 rpm for 5 min each. The results showed that the highest harvesting efficiency of 98%, 96%, and 90% were achieved at 7,000 rpm (about 6000 g force) for *Chlorella sp*. UKM2, *Coelastrella sp*. UKM4, and *Chlamydomonas sp*. UKM6, respectively. Centrifugation also provides contaminant-free algal biomass that can be stored for long periods of time without purification before entering downstream processing (Radin Mohamed, Al-Gheethi, and Mohd Kassim 2019). However, centrifugation is energy-intensive, resulting in high cost for algal

biomass production (Kumar et al. 2019; Najjar and Abu-Shamleh 2020). Based on a feasibility analysis for microalgae-based biofuel, the total investment cost of centrifuges can reach 30% of the total investment in the industry (Alam, Wang, and Yuan 2017). Filtration has similar shortcomings to centrifugation. Therefore, new technologies that are environmentally friendly and low-cost for algae harvesting are still needed to promote the commercial microalgae biorefinery.

1.3.2 Sedimentation

Sedimentation, also known as auto-flocculation, refers to the spontaneous aggregation of suspended algae under the influence of gravity (Figure 1.5). This phenomenon is often observed under non-ideal culture conditions, such as pH changes and culture aging (Shen, Cui, and Yuan 2013). Yoo et al. (2015) studied the freshwater alga *Ettlia sp.* and found that its flocculation activity showed an S-shaped pattern with increasing pH. In the pH range of 6.5-8.5, the harvesting efficiency was very low, about 11%, while it increased dramatically to 83% and 94% when the pH increased to 10.5 and 12.5, respectively. Yoo believed that the negative charge on algae cell surface can be neutralized by multivalent metals salts which actively precipitate at high pH. However, for *Scenedesmus obliquus*, the self-flocculation efficiency only increased from 10.4% to 33.2% when the pH value increased from 7 to 10 (Matter, Darwesh, and Eida 2018). Liu et al. (2013) studied the flocculation efficiency of three types of freshwater microalgae cells. When the pH dropped from 6.7 to about 5.0, the microalgae cells began to coagulate. When the pH was further reduced to 4.0, the cells further coagulated and quickly settled within a few minutes, with a higher flocculation efficiency of 90%. Addition of synthetic seawater to cultures of the freshwater alga *Scenedesmus quadricauda* increased the flocculation activity from 82.13%

to 88.79% at low algae concentration (0.52 g/L) and from 82.92% to 95.60% at high concentration (2.66 g/L) (Huo et al. 2014). It has been reported that the freshwater microalga *C. vulgaris* can be harvested by self-flocculation, which is caused by the precipitation of magnesium or calcium compounds due to a slow increase in pH in the absence of CO_2 input (Nguyen et al. 2014). Algae harvesting based on sedimentation is a low-cost and environmentally friendly biomass recovery strategy. However, this harvesting process is often very slow (up to several days) and highly species-specific. And compared with centrifugation, the dehydration degree and dehydration efficiency of sedimentation are greatly reduced.

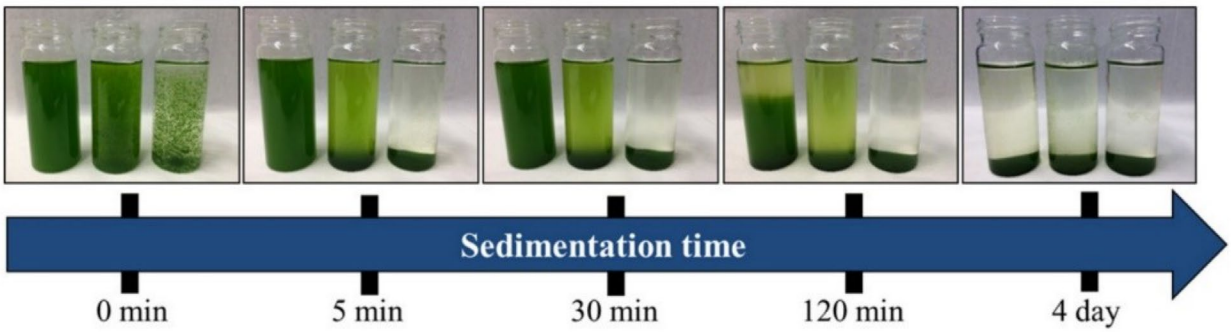

Figure 1.5. Auto-flocculation harvesting of algal biomass. Three vials contain algal samples cultured in different nitrate concentrations: (left) 0.5×; (middle) 1× (original); and (right) 2× (Nguyen et al. 2017). CC BY-NC-ND.

1.3.3 Chemical flocculation

In situations where natural settling is difficult, flocculation is often used to speed up sedimentation. Adding flocculants can neutralize the negatively charged cell surface and allow microalgal cells to aggregate (Caetano et al. 2020; Matter et al. 2019). Commonly used inorganic chemical flocculants, such as aluminum sulfate, ferric chloride, and ferric sulfate can form flocs

with algae cells through charge neutralization and electrostatic bridging (Kumar et al. 2023). Organic polymers, such as chitosan, cationic starch, modified tannins, and polyacrylamide are also widely used (Shen et al. 2013).

Kwon et al. (2014) optimized and compared the harvesting efficiency of aluminum sulfate, iron sulfate, and chitosan for *Tetraselmis sp.* at different pH values. The optimal dosage and pH level of aluminum sulfate were 1.2 g/L and pH 5-6, iron sulfate was 0.7 g/L and pH 4-8, and chitosan was 5.0 mg/mL and pH 7-8. The highest harvesting efficiencies were 85.6%, 92.6%, and 93%, respectively. Kim et al. (2017) used $Fe_2(SO_4)_3$ and sulfuric acid to harvest *C. vulgaris*. The large release of such chemicals into the environment is a critical environmental and health concern. Lowering the pH successfully released the precipitate attached to the microalgae, and the remaining acidic solution containing the recovered iron ions could be reused up to three times with an efficiency of more than 98%. 120 mg/L chitosan could harvest 92% *C. vulgaris* within 3 min, and the harvesting efficiency increased to 99% when the pH was adjusted to 6.0 (Rashid, Rehman, and Han 2013). Cationic starch was used to harvest *C. pyrenoidosa* and *Botryococcus braunii*, with the amount of cationic starch required to recover 1 g of algal biomass being 89 mg and 119 mg, respectively (Peng et al. 2017). Even though the harvesting efficiency of chemical flocculants is usually pretty high, up to 85% within one hour, the final product can have a serious impact on the environment (Matter et al. 2019).

In electrochemical systems, a sacrificial metal anode (usually iron and aluminum. Magnesium, copper, zinc, and brass are also used) is used to release positively charged metal cations. These dissolved metal cations electrostatically attract negatively charged algal cells, resulting in flocculation (Rahmani et al. 2017). The electrical energy requirement for harvesting

1 kg of *C. pyrenoidosa* biomass using aluminum electrodes was 0.28 kWh, and the maximum harvesting efficiency was 95.83 ± 0.87%. Electrochemical algae harvesting is generally carried out by passing a direct electrical current through electrodes into a culture broth wherein algal cells act as negatively charged colloids (Krishnamoorthy et al. 2021). Electric current in an aqueous solution can cause a water electrolysis reaction through a sacrificial or non-sacrificial electrode, which will release hydrogen and oxygen from the cathode and anode, respectively. For the practical application of the electrochemical flocculation process, further research is needed to develop optimal electrodes with high efficiency, scale-free, and low toxicity properties, as well as scale-up and process optimization to reduce equipment and power costs.

1.3.4 Particle-based flocculation

Particle-based flocculation can potentially circumvent some drawbacks of conventional chemical flocculation, such as bio-toxicity and difficulties related to chemical recovery (Kumar et al. 2023). Cationic starch nanoparticles (CSNPs) were used for the harvesting of *C. vulgaris* (Bayat Tork, Khalilzadeh, and Kouchakzadeh 2017). The maximum flocculation efficiency of 90% was achieved under the optimal conditions of microalgae concentration of 0.75 g dry weight/L, CSNPs concentration of 7.1 mg dry weight/L, and pH of 11.8. Almost 100% of algal cells (1.7 g cells/L) can be harvested in 30 min using 0.6 g/L aluminum aminoclay (Al-AC) and Mg-AC but is less effective in seawater media (Y.-C. Lee et al. 2013). Magnetic nanoparticles (MNPs) are also designed for algae separation (Wang et al. 2020). The harvesting of raw magnetic nanoparticles achieved a high efficiency of 99.6% with the dosage of 0.58 g MNPs/g dried-biomass (Lin et al. 2015). Due to the high cost of magnetic particles, their separation and recovery from the culture medium has become a problem.

1.3.5 Bio-flocculation

Bio-flocculation is the harvesting of target algae by adding self-flocculating microorganisms (or their extracellular biopolymers) to the culture solution. Bacteria, fungi, yeasts, as well as their exudate-rich culture supernatants can be used as bio-flocculants (Li, Hu, and Zhu 2021; Matter et al. 2019).

Zhang and Hu (2012) demonstrated the co-cultivation of *Aspergillus niger* with *C. vulgaris* to form cell pellets, facilitating algae harvesting. For the co-culture with autotrophic microalgae, around 60% of algae cells were pelletized with fungal cells. Similarly, Yang et al. highlighted the benefits of co-cultivating *Chlorella sp.* with *Aspergillus sp.* to enhance algae biomass production and harvesting efficiency (Yang, Li, and Wang 2019). The results showed that the highest biomass yield (4.215 g/L) was obtained when the inoculation ratio of fungi to microalgae was 100 to 1. The co-cultivation system produced biomass with a higher lipid content (35.2%) and produced microbial cell oil with a lower degree of unsaturation compared with the single microalgae system. Extensive research supports fungal bioflocculants as reliable methods for achieving high biomass harvesting efficiencies (Chu et al. 2021; Lin et al. 2022).

Yen et al. co-cultured *Scenedesmus obliquus* with *Rhodotorula glutinis* and achieved an increase in biomass of approximately 40-50% and total lipids of 60-70% compared to the single culture batches (Yen, Chen, and Chen 2015). Díaz-Santos et al. (2015) studied the effect of the self-flocculating yeast strain *Saccharomyces bayanus* var. *uvarum* on a freshwater microalga *Chlamydomonas reinhardtii* and a marine microalga *Picochlorum sp.* HM1. The addition of yeast induced cell aggregation in both microalgae studied, and 80% of *C. reinhardtii* and 60% of *Picochlorum sp.* were harvested. After separation and addition of 0.1 mg mL^{-1} of concentrated

flocculated excreted proteins, the recovery efficiency values for *C. reinhardtii* and *Picochlorum sp.* were 95% and 75%, respectively.

Bacteria sometimes play an important role in flocculation, which leads to the sedimentation of microalgae by increasing the size of flocs. The flocculation activity of xenic *C. vulgaris* culture was 94%, while it was only 2% (J. Lee et al. 2013). Wan et al. (2013) isolated a bacterial strain *Solibacillus silvestris* from activated sludge, and the bio-flocculant in its culture broth had a flocculation efficiency of 90% on the marine microalga *Nannochloropsis oceanica*. These researchers claimed that the bio-flocculant had no effect on the growth of microalgae cells and could be reused to economically harvest *N. oceanica*. Úbeda et al. (2017) found that using *Coelastrum* exudates as a bio-flocculant for *Scenedesmus* sp. could achieve good harvesting efficiency of 97%.

Bio-flocculation method can be considered as a sustainable and highly efficient technique for algal biomass harvesting since no chemical is required in this process, while possible environmental pollution caused by fungi, bacteria, etc. and process amplification issues need to be noted. Moving from lab-scale to commercial-scale applications still requires extensive developments for reliable, cheap, and eco-friendly algae harvesting processes.

1.4 Utilization of Thermo-responsive polymers to separate algal biomass

Existing algae harvesting methods have their own shortcomings, including but not limited to long time, high cost, product contamination, environmental pollution, etc. Therefore, innovative cost-efficient and environmentally benign algae harvesting technologies are urgently needed. Interest in thermo-responsive polymers (TRPs) has persisted decades and it represents a

series of polymers of which physical property (e.g., solubility) change can be triggered by temperature (Doberenz et al. 2020). It has been investigated for a variety of applications, such as controlled drug delivery, injectable biomaterials, and tissue engineering (Hogan and Mikos 2020). Poly-(N-isopropylacrylamide) (PNIPAM) is a TRP which undergoes a phase transition in water when temperature changes across its lower critical solution temperature (LCST) (Cao et al. 2019; Liu et al. 2022).

Our previous work involving a one-pot microalgae separation and intracellular product extraction (Zheng et al. 2015; Zheng, Xiao, and Roberts 2016), demonstrated that the phase transition behavior of PNIPAM and its derivatives can be used to separate microalgae efficiently via some interaction mechanism(s) between the polymer and cells. After algae separation from the growth media, the polymer can be recovered by gentle washing with water. The recovered polymer can then be added to a new culture to repeat the process without generating or wasting additional material. While neutral PNIPAM homopolymers are effective for harvesting *C. protothecoides* cells from their growth media, these systems require high dosage (50-100 mg/mL). By introducing allylamine (AA) randomly into PNIPAM to make positively charged copolymers, nearly quantitative separation of algae was achieved using 25 mg/mL NIPAM copolymers with 2.6 mol% AA. Additionally, TRPs of PNIPAM and PNIPAM-AA were studied to enhance enzymatic cell wall disruption of *C. protothecoides* to recover lipids and reducing sugars. Results indicated that polymers were also able to disrupt microalgal cell walls for lipid extraction without enzymes, but unable to hydrolyze cell walls. By adding PNIPAM-AA in the medium, 68% and 33% cell disruption can be achieved with and without enzyme, respectively, resulting in respective lipid and reducing sugar yields of 59% and 50% (g/g, reducing sugar/dry

algal cell wall). The use of TRPs in addition to enzymes results in faster cell disruption with higher breakdown efficiency for improved lipid yield. The polymer was shown to function by stressing and disrupting the cell wall to improve the susceptibility to enzymatic cleavage as well as protecting the enzyme from denaturation. The use of TRPs provides a simple and energy-efficient approach in assisting the production of biofuels and bioproducts from microalgae. More importantly, the polymer can be readily recovered and reused, thereby reducing overall material cost. In short, the foreseen advantages of using TRPs for microalgae separation include: (a) high energy efficiency, (b) simplicity of operation, (c) low capital/operational cost, (d) reduction of chemical contamination, (e) ability to recycle and reuse polymers, (f) enhancement of enzymatic microalgal cell disruption for intracellular product extraction, and (g) increased efficiency of subsequent microalgal biomass processing and utilization.

1.5 Conclusions and prospects

Microalgae-based biorefinery provides various advantages to meet the rising demand for biofuel, food, and feed, as well as pharmaceuticals. Although microalgae technology is renewable and carbon-neutral, the cost of the renewable fuel derived from microalgae is prohibitive. This dilemma makes current microalgae biorefinery unprofitable compared to the conventional petroleum fuel. Of the microalgae processing, the algal cell harvesting accounts for a major proportion of the cost. This is because algal cells are generally small in size with negative charge on cell surface while their density is similar to water such that they usually form a uniform suspension in the culture medium. As a result, the development of cost-efficient algal cell separation technology is essential to scale up the microalgae biorefinery.

Many previous studies reported methods and materials for algae harvesting. But more

universal and reliable ways are crucial for large-scale applications. Previous studies have some of the following common technical issues and concerns which compromise their reliability: 1) several studies use flocculation to speed up the precipitation of algae cells. This process can cause irreversible environmental pollution, and the need for subsequent biomass purification is also worth considering; 2) a number of new materials have been developed to help harvest algae. The preparation process of most materials is cumbersome and expensive. Also, some materials are highly strain-specific, i.e., one material may be very effective for some strains but not for others; 3) even though the efficiency of PNIPAM and its copolymers have been proven to harvest algae successfully. Its scope of application and durability are still not clear. Meanwhile, the mechanisms of the interaction between TRP and algal cells need to be further investigated. In understanding the mechanisms, we can modify the TRP to make it suitable for a wide range of algae strains. Therefore, this dissertation project is to establish a new TRP-induced algae harvesting system in which proper TRP can be specifically chosen to achieve high algal cell harvesting efficiency based on the properties of different algae. To achieve this goal, this project aims at three objectives: (1) establish relationships between TRP features and algae enrichment; (2) understand the fundamentals behind the interactions between TRP and algal cells; and (3) graft polymers onto suitable surfaces to enable large-scale reuse of TRP.

Chapter 2 - Microalgae Aggregation induced by Thermoresponsive Polymers

Paper title:

Microalgae Aggregation Induced by Thermoresponsive Polymers

Published in:

Bioresource Technology, Volume 415, 21 Oct 2024, Pages 131650

Authors' names:

Xuexue Wang, Donovan Mafukidze, Yi Zheng

Authors' affiliations:

Department of Grain Science and Industry, Kansas State University, 1980 Kimball Avenue, Manhattan, KS 66506, USA

Abstract

Algal biomass harvesting is one of key technical hurdles impeding the commercialization of algae-based biorefinery. The goal of this work is to develop an innovative technology for algae cell harvesting. Thermoresponsive polymers (TRPs) such as poly(N-isopropylacrylamide) (PNIPAM) and its derivatives were studied on their properties and potential applications for microalgae harvesting. Various PNIPAM was synthesized, and the effects of charge, molecular weight (MW), amine content, and polymer concentration on the polymer phase transition temperature, the degree of phase separation, and the harvesting of microalgae (*Chlorella vulgaris*) were investigated. The lower critical solution temperature (LCST) of PNIPAM decreased with the increase of polymer concentration, while the decline rate reduced under high MW. The amine content didn't significantly affect the LCST of TRPs. Approx. 92 % of algae cells were harvested by PNIPAM-300 kDa. Modified TRPs showed few benefits in enhancing algae harvesting. TRPs are a promising class of polymers for microalgae harvesting.

Keywords: Bioenergy; Algae harvesting; Poly-(N-isopropylacrylamide); Phase transition; Lower critical solution temperature

2.1. Introduction

Energy security and environmental impact associated with the consumption of petroleum fuels have prompted the production and use of renewable energy for sustainable future (Sakarika and Kornaros 2019). Biomanufacturing that utilizes microorganisms as factories to produce fuels and chemicals has received increasing research interest (Deckers et al. 2020; Negassa, Mohiuddin, and Tiruye 2021). Microalgae are considered as one of promising renewable feedstocks for the third-generation biofuels and chemicals because of its faster growth, higher energy density, higher productivity, and lower land/fertilizer requirements than terrestrial plants (Brennan and Owende 2010; Hossain, Mahlia, and Saidur 2019; Moshood, Nawanir, and Mahmud 2021). *Chlorella vulgaris* has been one of the most commonly studied microalga species for biofuel production (e.g., biodiesel). It can grow under nutrient-deficient conditions to accumulate lipid up to 70% of dry cell weight (Yun et al. 2019).

Despite the potential benefits of microalgae, there are several technical barriers preventing the commercialization of microalgal biorefinery, e.g., algal biomass harvesting (Branco-Vieira et al. 2020; Hajinajaf, Mehrabadi, and Tavakoli 2021). Microalgal cells usually grow in medium at very low concentration (0.2-0.5 g/L, dry weight basis) and need to be concentrated before downstream processing. However, harvesting algal biomass is usually energy-intensive and time-consuming, making the current microalgae biorefinery economically unfit (Park, Craggs, and Shilton 2011). In addition, microalgal cells are small (2~50 μm) and have a similar density to water (1.08-1.13 g/mL) (Lavoie and de la Noüe 1987). Furthermore, the cell carries strong negative surface charge (Zhang et al. 2020), making it difficult to separate them from the cultivation medium, particularly during the exponential growth phase (Kumar et al. 2023).

Gravity sedimentation is the most common method for algal biomass harvesting, but it could take up to 1-2 days with the harvesting efficiency of only 60-70% (Nurdogan and Oswald 1996; Ortiz et al. 2021). In addition, various chemical and mechanical methods have also been extensively investigated (S. Li et al. 2020; Roy and Mohanty 2019; Suparmaniam et al. 2019), most of which are costly and have potential negative environmental impacts. For instance, Zhu et al. (2018) used aluminum sulfate as a flocculant to harvest more than 90% *C. vulgaris* biomass. Using metallic salts is useful to enhance the electro-flocculation process for concentrating *C. vulgaris*, but it increases the overall cost and might cause product contaminations (Chatsungnoen and Chisti 2019). High-speed centrifugation has been used to effectively recover microalgae. Farooq et al. (2015) isolated ~100% *C. vulgaris* biomass in four consecutive times while recycling medium. But the high energy and capital costs of the centrifugation prevent its use on a large scale. Savvidou et al. (2021) investigated magnetic harvesting of *C. vulgaris* using microwave-synthesized magnetite (Fe_3O_4) particles and achieved approx. 99% harvesting efficiency. The recovered particles could be reused five times, but the specific service life is still unclear. The high cost, high energy consumption, chemical contamination, and/or algal species-dependence make it challenging to scale up the existing technologies. Therefore, more research is needed to develop microalgal biomass harvesting technologies that are cost-effective, environmentally friendly, energy-efficient, and compatible with a broad range of microalga species.

Research interest in thermoresponsive polymer (TRP) has persisted over decades. TRP represents a series of polymers of which physical property changes (e.g., solubility) can be triggered by temperature shift (Doberenz et al. 2020). It has been investigated for a variety of applications, such as controlled drug delivery, injectable biomaterials, and tissue engineering

(Hogan and Mikos 2020). Poly-(N-isopropylacrylamide) (PNIPAM) is a typical TRP which undergoes a phase transition in water when temperature changes across its lower critical solution temperature (LCST) (Cao et al. 2019; Liu et al. 2022). The previous work involving a one-pot microalgae separation and intracellular product extraction (Zheng et al. 2015, 2016), demonstrated that the phase transition behavior of PNIPAM and its derivatives can be used to separate microalgae efficiently. The potential stages of TRPs for microalgae separation include high energy efficiency, simplicity of operation, low capital/operational cost, elimination of chemical contamination, and easy recycling and reuse of polymers.

This study is to investigate the properties (e.g., molecular weight, charge and concentration) of PNIPAM-based TRPs and their effects on the thermoresponsive behavior and microalgae harvesting performance. The three objectives aim at: 1) synthesizing three types of TRPs such as PNIPAM, PNIPAM-allylamine (AA), and PNIPAM-2-(Methacryloyloxy) ethyl trimethylammonium chloride (MTAC) with different properties; 2) characterizing the TRPs for LCST, enthalpy during phase change, and zeta potential under different molecular weights (MWs)/concentrations/functional groups; and 3) studying the impacts of TRPs' properties on the microalgae (*C. vulgaris*) harvesting. This work also correlates the molecular characteristics and microalgae harvesting performance of TRPs with their thermoresponsive behaviors. The results are expected to assist in selecting suitable TRPs for specific microalgae and lay a foundation for the development of a new class of TRP-based approach to harvest microalgae.

2.2. Materials and Methods

2.2.1 Materials

N-isopropylacrylamide (NIPAM), ammonia persulfate (APS), allylamine (AA), 2-(Methacryloyloxy) ethyl trimethylammonium chloride (MTAC), tetramethylethylenediamine (TEMED), N, N-dimethylformamide (DMF), and lithium bromide (LiBr) were purchased from Fisher Scientific (Hampton, NH, USA). Polymethyl methacrylate (PMMA) was purchased from MilliporeSigma (St. Louis, MO). The microalgae, *C. vulgaris* (UTEX 2714) culture and the Bristol medium were purchased from the Culture Collection of Algae at the University of Texas at Austin (Austin, TX, USA).

2.2.2 Synthesis of thermoresponsive polymers

TRPs such as PNIPAM, PNIPAM-AA, and PNIPAM-MTAC were prepared for studies. The recipe for TRP synthesis is shown in Table 2.1. PNIPAM was synthesized via the free radical emulsion polymerization of NIPAM using APS as an initiator. A series of amount of NIPAM (0.01-10 g) were dissolved in 200 mL deionized (DI) water. The solution was extensively purged with N_2 for 10 min and constantly stirred at room temperature to remove dissolved oxygen before 100 µL of TEMED and 1 g of APS were added. The N_2 purging and stirring continued for 5 min, and the glass bottle was sealed. The reaction was then carried out at room temperature for another 24 h without bubbling or stirring. The MWs of the synthesized TRPs were measured on a high-pressure liquid chromatograph (HPLC). Three of the TRPs (300, 100, and 15 kDa) were chosen for further analysis. To make the TRPs with positive charge, AA and MTAC (1, 5, and 10 mol%) were dissolved with NIPAM in 200 mL DI water following by

repeating the above synthesis steps. The resultant TRPs were purified via dialysis against DI water by using regenerated cellulose dialysis membrane tubing (Spectra/Por®, Fisher Scientific, Hampton, NH) with the MW cutoff (MWCO) of 10 and 50 kDa for 7 days to remove unreacted monomers. TRP solutions after dialysis were freeze-dried and stored in a refrigerator until used.

Table 2.1. Recipe for the synthesis of different thermoresponsive polymers

Sample	NIPAM (g)	AA (μL)	MTAC (μL)
PNIPAM-300kDa	5		
PNIPAM-100kDa	1		
PNIPAM-85kDa	0.6		
PNIPAM-56kDa	0.4		
PNIPAM-27kDa	0.2		
PNIPAM-15kDa	0.1		
PNIPAM-AA-1-300kDa	5	33	
PNIPAM-AA-5-300kDa	5	165	
PNIPAM-AA-10-300kDa	10	660	
PNIPAM-AA-1-100kDa	1	6.6	
PNIPAM-AA-5-100kDa	1	33	
PNIPAM-AA-10-100kDa	1	66	
PNIPAM-AA-1-15kDa	0.1	0.66	
PNIPAM-AA-5-15kDa	0.1	3.3	
PNIPAM-AA-10-15kDa	0.1	6.6	
PNIPAM-MTAC-1-300kDa	5		110
PNIPAM-MTAC-5-300kDa	5		550
PNIPAM-MTAC-10-300kDa	10		2200
PNIPAM-MTAC-1-100kDa	1		22
PNIPAM-MTAC-5-100kDa	1		110

PNIPAM-MTAC-10-100kDa	1	220
PNIPAM-MTAC-1-15kDa	0.1	2.2
PNIPAM-MTAC-5-15kDa	0.1	11
PNIPAM-MTAC-10-15kDa	0.1	22

Note: The number after AA and MTAC represents how much % mol of AA and MTAC were added to the monomer solution, respectively. The number before kDa means the MW of TRPs. For example, PNIPAM-AA-1-300kDa means PNIPAM was modified with 1 mol% AA and had a MW 300 kDa.

2.2.3 Characterization of thermoresponsive polymers

The MWs of TRPs synthesized in Section 2.2 were measured by using HPLC (1100 Series, Agilent Technologies, Santa Clara, CA, USA) which was equipped with a refractive index (RI) detector and an analytical column (PL1113-6500, Agilent PLgel, 5 μm × 7.5 mm × 300 mm, Agilent Technologies, Santa Clara, CA, USA). The mobile phase was DMF with 0.05 M LiBr at a flow rate of 1 mL/min, and the analysis temperature was 42°C. The powder polymer was dissolved in the mobile phase at 5 mg/mL and filtered through a 0.2-μm syringe filter into an HPLC vial. The MWs of TRPs were calculated against PMMA as a standard. The chemical structure and functional groups of TRPs were analyzed by using Fourier-transform infrared (FT-IR) spectroscopy (Spectrum 400, PerkinElmer, Austin, TX) in the range of 380-4000 cm^{-1}. Low critical solution temperatures (LCSTs) of TRPs were determined by using differential scanning calorimetry (DSC) (Q200, TA Instrument, Schaumburg, IL). Approximately 40 μL of TRP solutions at various concentrations were weighed in aluminum pans, heated from 20 to 55℃ at a rate of 5℃·min^{-1}, and then cooled to 20℃. Three cycles were recorded to determine the TRPs'

LCSTs with DI water as a reference. The charge of TRPs was measured as Zeta potential. The TRP solutions of 10 mg/mL were prepared in DI water, and their Zeta potential was measured on a Zetasizer (Nano-ZS, Malvern Panalytical Inc., Westborough, MA) at 25℃. The measurements were repeated three times.

2.2.4 Microalgae harvesting by using thermoresponsive polymers

The microalgae used in this study was *C. vulgaris* which was cultivated in Bristol medium (Bold 1949) supplemented with 1 g/L of proteose peptone. The medium was sterilized by autoclave at 121℃ for 20 min. All media were stored at 4℃ for at least 24 h for gas equilibrium before stock culture inoculation according to the vendor's instruction. The stock algae culture was scraped from the agar slant and transferred to the liquid medium at an optical density of 0.1 at 670 nm (OD_{670}) to prepare a seed culture and incubated at room temperature under light/dark (12 h/12 h) cycles. After the OD_{670} of the seed culture reached 0.2, all the seed culture was transferred to a 500-mL flask, mixed with fresh medium at a ratio of 1: 5 (v/v), and incubated at room temperature under light/dark (12 h/12 h) cycles. The flask was aerated with an air pump at an air flow rate of 0.15 liter per minute (LPM) and stirred at 400 rpm with a magnetic bar for 12 days. Algal biomass dry weight (BDW) was determined by filtration, washing with DI water three times, and weighing after drying at 80°C overnight. The BDW was calculated by subtracting the dry weight of filter paper from the total dry weight of filter paper with algal biomass.

The wavelength for the maximum absorption (λ_{max}= 430 nm) of the algae suspension was determined using the scan mode on a microplate reader (BioTek Epoch2, BioTek Instrument Inc., Winooski, VT). The OD of algae suspension was then measured at 430 nm. To build the

calibration curve for BDW vs. OD, the algae suspensions with a series of BDW (0.05-1 mg/mL) were prepared, and their corresponding OD were measured. With this curve, the algae BDW was determined in subsequent experiments by measuring OD of the algae suspension. All the algae culture samples were diluted with medium if their OD values exceeded 1.0.

The TRP solutions were prepared in DI water at the concentration of 200 mg/mL at room temperature and mixed with the algae suspension (1:1, v/v). The mixture was vortexed and heated to specific LCST of the corresponding TRPs for 30 min to induce the phase transition from soluble to insoluble. The supernatant of the mixture was collected for OD measurement after cooling down. The OD values were converted to BDW using the calibration curve. The algae harvesting efficiency (AHE) was calculated as Eq 2.1:

$$\mathrm{AHE}(\%) = \left[{}^{(BDW_i - BDW_f)}\Big/_{BDW_i}\right] \times 100\%$$

(Equation 2.1)

where BDW_i and BDW_f are the initial and final algae BDW (mg/L), respectively.

2.2.5 Data analysis

The statistical significance of data was determined using analysis of variance (ANOVA) and least significant difference (LSD) at $\alpha = 0.05$ using SAS OnDemand for Academics analysis. All reported values in this study were the average of three replicates, unless specified otherwise.

2.3. Results and Discussion

2.3.1 Synthesis of thermoresponsive polymers

All TRPs (i.e., PNIPAM, PNIPAM-AA, and PNIPAM-MTAC) were soluble in water, and their solutions were transparent and clear at the temperature below their LCST, while the TRP solutions turned turbid white when the temperature was increased over the LCST (Figure 2.1a). The chemical formulas of NIPAM, PNIPAM, PNIPAM-AA and PNIPAM-MTAC are shown in Figure 2.1b. In the FT-IR spectrum of NIPAM (Figure 2.1c), the peak at 1620 cm^{-1} corresponds to the C=C stretching vibration, and the peak at around 3300 cm^{-1} corresponds to the deformation vibration of the hydrogen atoms of the alkene group swinging out of the plane. The spectra of PNIPAM, PNIPAM-AA, and PNIPAM-MTAC lack the peak at 1620 cm^{-1}, which indicates that the C=C in NIPAM was completely reacted and the monomer successfully polymerized into TRPs (Ningrum et al. 2022; Shi et al. 2015). In the spectra of NIPAM and 3 TRPs, the absorption band at 1656 cm^{-1} corresponds to the C=O stretching vibration of the amide group, peaks at 1546 cm^{-1} and 3300 cm^{-1} ascribe to the typical signals of N-H, and the peak at 2876 cm^{-1} reflects the $-CH_3$ unsymmetrical bending vibration. The grafting of AA did not bring new functional groups to PNIPAM such that PNIPAM-AA showed a similar spectrum to PNIPAM with slight differences in the fingerprint region (1450-500 cm^{-1}). In addition to the functional groups of PNIPAM, the spectrum of PNIPAM-MTAC exhibits the signals of other functional groups, such as C=O (1728 cm^{-1}) of the ester and the stretching of C-O-C (1250 cm^{-1}) linkage which confirm the presence of MTAC in the polymer.

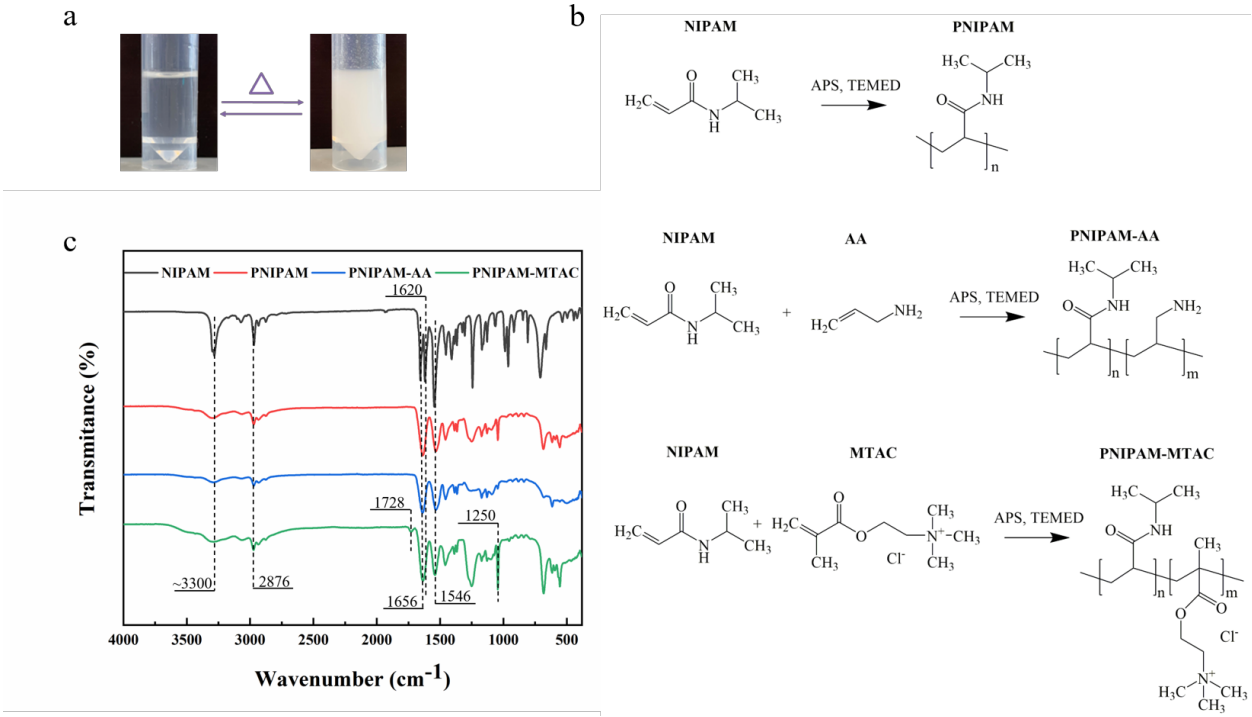

Figure 2.1. (a) Phase change of TRPs; (b) Chemical formula of NIPAM and TRPs and (c) FT-IR spectra of NIPAM and TRPs.

2.3.2 Characterization of thermoresponsive polymers

The TRPs with different designated MWs in the range of 15 ~ 300 kDa were verified for their MWs (Table 2.2) which were calculated based on the standard curve with PMMA as a standard (Figure 2.2a). As depicted in Figure 2.2b, the LCST of each TRP varied with its MW and concentration. During the LCST analysis, the heating-cooling cycle was repeated three times and achieved a consistent LCST of the TRP, which shows that the TRP phase change is reversible. The LCST of all TRPs decreased linearly with the increase of the TRP concentration, and the decreasing rate (~0.089°C/mg/mL) was similar among the TRPs with the MW of 15- 85 kDa, while the decreasing rate became smaller for the TRPs with MW of 100 (0.060°C/mg/mL)

and 300 kDa (0.026°C/mg/mL). The phase change process is mainly controlled by the hydrophobic hydration, and the increase of PNIPAM concentration increases the number of hydrophobic groups in solution, leading to a lower LCST (Bischofberger, Calzolari, and Trappe 2014). At the same concentration, higher MW PNIPAM showed lower LCST within the MW range of 15~85 kDa since individual polymer chains undergo a hydrated coil to dehydrated globule transition during heating resulting in PNIPAM precipitation (Yanase, Buchner, and Sato 2020). The higher MW PNIPAM had longer polymer chains than the lower MW one such that it was more likely to precipitate out of water. Surprisingly, the TRP with MW of 100 kDa had slightly higher (0.19°C) LCST than that with MW of 85 kDa at the concentration of 100 mg/mL while the TRP with MW of 300 kDa had a higher LCST than those with MW of 100 kDa at >40 mg/mL, of 85 kDa at >60 mg/mL, and of 56 kDa at 100 mg/mL, respectively. Yanase et al. (2020) reported that at higher polymer concentrations, the PNIPAM chains are highly crowded and the LCST converges to similar values that are independent of MW. That could be the reason why the LCST of PNIPAM with MW >85 kDa did not decrease as the MW increase at high concentrations.

In comparison, the DSC curve (heat flow vs. temperature) for PNIPAM-100 kDa was flatter and showed a wider range of LCST than that for PNIPAM-300 kDa during the heating process (Figure 2.2c). Meanwhile, PNIPAM-300 kDa showed a larger enthalpy peak during the phase transition, i.e., it needs more energy to drive the phase transition. The temperature induced phase transitions of PNIPAM are driven by hydrophobic interaction between the isopropyl groups of the side chains. PNIPAM with higher MW has more side chains, resulting in a larger enthalpy required for the phase transition process. In addition, the repeatability of PNIPAM-300 kDa in the phase transition was better than that of PNIPAM-100 kDa. After the 1st or 2nd heating-cooling

cycle, the enthalpy peaks slightly decreased for both PNIPAM-100 kDa and PNIPAM-300 kDa, while the former needed more time to recover from its insoluble state.

Table 2.2. Actual MW of PNIPAM copolymers with AA and MTAC

AA and MTAC (% mol)	MW (kDa) of PNIPAM copolymers with AA or MTAC		
	PNIPAM-300 kDa	PNIPAM-100 kDa	PNIPAM-15 kDa
No AA/MTAC	303.18 ± 3.35	110.01 ± 0.25	17.16 ± 0.09
AA-1	370.98 ± 2.18	165.49 ± 0.92	16.34 ± 0.10
AA-5	338.39 ± 2.96	159.86 ± 1.17	16.83 ± 0.02
AA-10	279.54 ± 0.66	124.40 ± 0.55	15.71 ± 0.16
MTAC-1	340.01 ± 3.19	144.78 ± 0.58	15.56 ± 0.15
MTAC-5	289.39 ± 0.96	129.71 ± 0.64	13.05 ± 0.11
MTAC-10	231.20 ± 1.79	90.23 ± 0.94	14.23 ± 0.11

Note: The number after AA and MTAC represents how much % mol of AA and MTAC have been added to the monomer solution. The number after PNIPAM means the MW of PNIPAM which were modified with AA or MTAC.

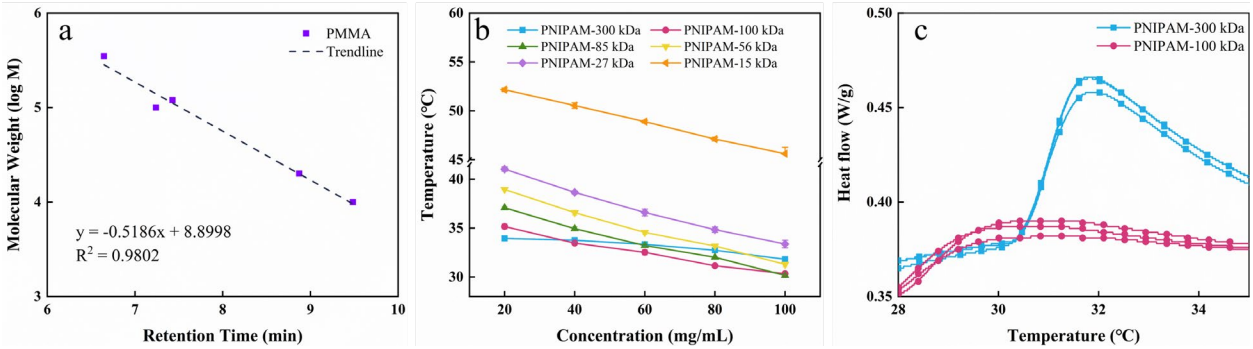

Figure 2.2. (a) Standard curve for the calculation of TRPs' MWs with PMMA as a standard; (b) LCST of TRPs with different MWs at different concentrations; and (c) DSC curves for PNIPAM-300 kDa and PNIPAM-100 kDa.

Since *C. vulgaris* cells have negative surface charge, PNIPAM was modified by copolymerization of NIPAM with two types of amine compounds (AA and MTAC), respectively to render the PNIPAM copolymers positive charge. Both AA and MTAC have positive charge groups that could form complexes with negatively charged cells through electrostatic interactions (Gatenby 2019; Tran et al. 2014). Adding amine decreased the MW of the TRPs (Table 2.2), therefore, the upper limit of the amine content in the copolymers was set to 10% mol to maintain a similar MW to PNIPAM without amine. As shown in Figure 2.3a, the incorporation of AA into the PNIPAM did not significantly affect the LCST even though it slightly changed the MW compared to PNIPAMs with the same MW at the same concentration. Only PNIPAM-AA-10-300 kDa showed a significant increase in LCST with addition of 10% mol of AA. In comparison to PNIPAM, the copolymerization of MTAC with NIPAM increased the LCST in the presence of 1% mol MTAC in the copolymers with MW of 15 and 300 kDa, while further increase of MTAC content caused little change of the LCST (Figure 2.3b). In addition, the LCST for the PNIPAM-MTAC copolymer with the MW of 100 kDa increased with the increase of MTAC content to 5% mol followed by a negligible change. Slight changes in the molecular structure of PNIPAM can greatly affect its chain conformation and thus its LCST (Tang et al. 2009). Inomata, Goto, and Saito (1990) modified the isopropyl group of NIPAM with cyclopropyl group, decreased the surface (contact) area of hydrophobic group, eliminated the phase change properties of poly (N-cyclopropylacrylamide). Also, the poly (N-n-propylacrylamide) which has larger surface area of its n-propyl group showed a lower LCST. Therefore, insignificant change

in LCST of the PNIPAM-AA copolymers could be because the addition of AA had little effect on the hydrophobic groups of PNIPAM. Meanwhile, the significant change in LCST of PNIPAM by the introduction of MTAC could suggest that the addition of MTAC at the designated contents might be enough to weaken the hydrophobic interaction.

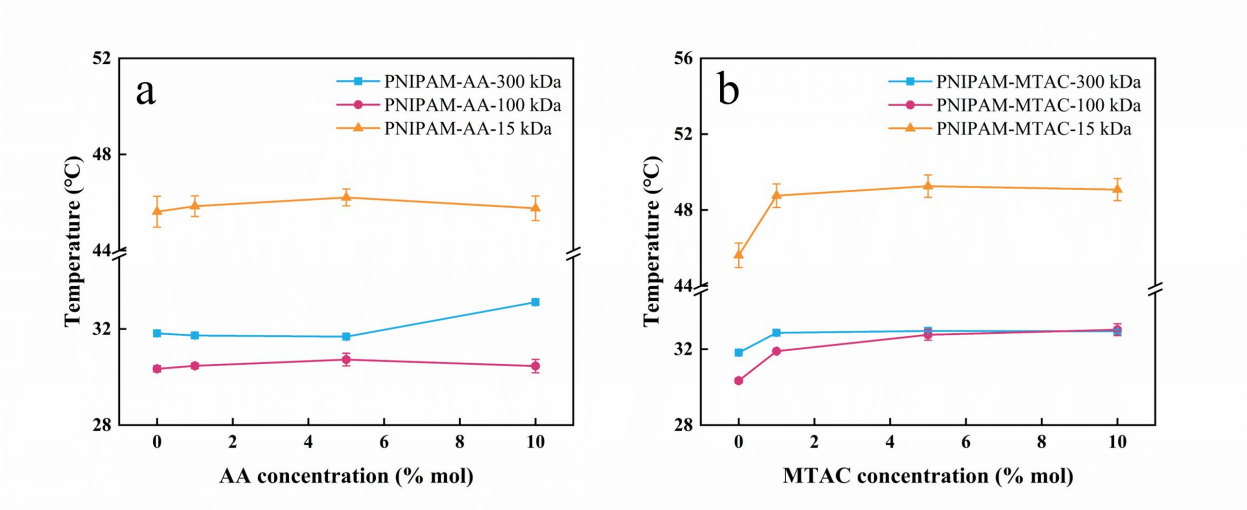

Figure 2.3. LCST of PNIPAM copolymers with AA (a) and MTAC (b) at the concentration of 100 mg/mL.

The charge of the PNIPAM-AA copolymer changed with pH (i.e., more positive at lower pH) because the degree of protonation of the AA group (carrying positive charge when protonated) increased with the decrease of pH. In contrast, the PNIPAM-MTAC copolymer had a constant charge at all pH values. The zeta potentials of the PNIPAM copolymers with AA and MTAC at various amine and MTAC contents are shown in Figure 2.4. All the data were obtained without pH adjustment. Larger MW PNIPAM homopolymers (i.e., zero AA or MTAC content with 100 and 300 kDa MW) showed almost no charge while PNIPAM-15 kDa had a significant negative charge (-21.07 mV). The pH for PNIPAM-300 kDa and PNIPAM-100 kDa were around

2.5 while the pH for PNIPAM-15 kDa was around 2.5. The polymer usually shows negative charge when its pH is over pI. For PNIPAM-AA-15 kDa, more AA in the polymer resulted in less negative charge (Figure 2.4a). However, the increase of AA content led to only a slight increase and decrease of the zeta potential for PNIPAM-AA-100 kDa and PNIPAM-AA-300 kDa, respectively. Since the AA content was based on the mol%, larger MW represented more AA in the solution, thus resulting in higher pH, which was consistent with our pH measurement results that the pH of PNIPAM without AA was around 2.5 and became 4~5 after copolymerization with AA. Meanwhile, high pH can reduce positive charge of polymers while more AA can provide more positive charge. Such an interaction of pH and AA content can cause the variation of polymer charge and further affect zeta potential of PNIPAM-AA-100 kDa and PNIPAM-AA-300 kDa with different AA contents. As shown in Figure 2.4b, the zeta potentials of PNIPAM-MTAC copolymers with different MWs increased significantly with the increase of MTAC mol% even though their charge didn't change with pH. This finding was consistent with the expected outcome that the more MTAC in the PNIPAM-MTAC copolymer resulted in more positive charge.

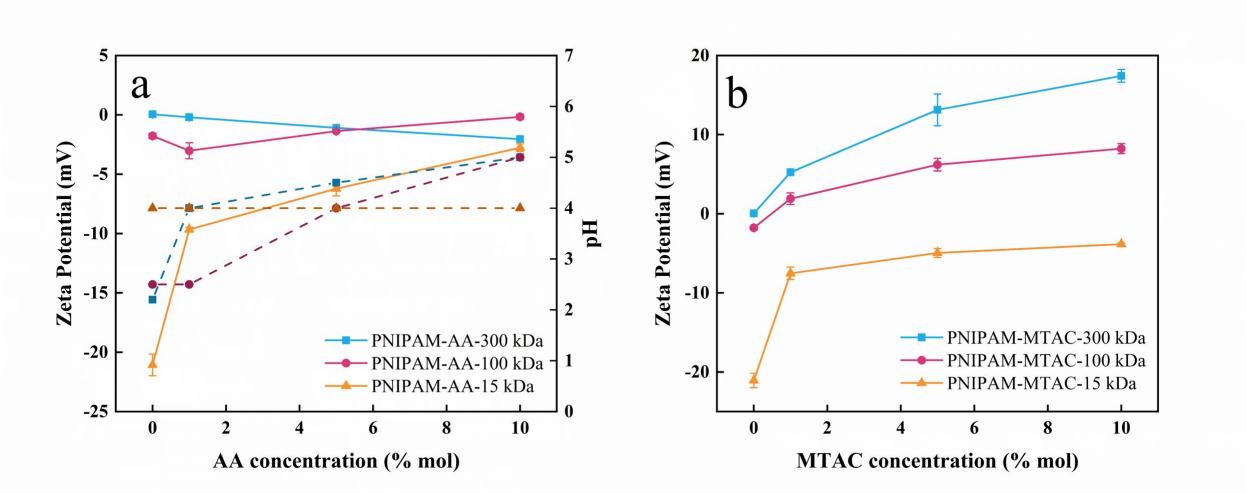

Figure 2.4. Zeta potentials of PNIPAM copolymers with varied AA (a) and MTAC (b) contents with different MWs.

2.3.3 Thermoresponsive polymer-induced microalgae harvesting

Figure 2.5a shows the UV-vis spectra for algae (UTEX 2714) and PNIPAM. The absorbance of the algae reached maximum at λ=430 nm, and PNIPAM did not display any UV-Vis absorption above λ=400 nm. Therefore, UV-vis spectroscopy was used to measure the algae OD in the presence of PINPAM in the solution. The standard curve of algae OD_{430} vs. BDW was developed in its cultivation medium (Figure 2.5b), which was used to calculate algae BDW from the measured OD_{430} values.

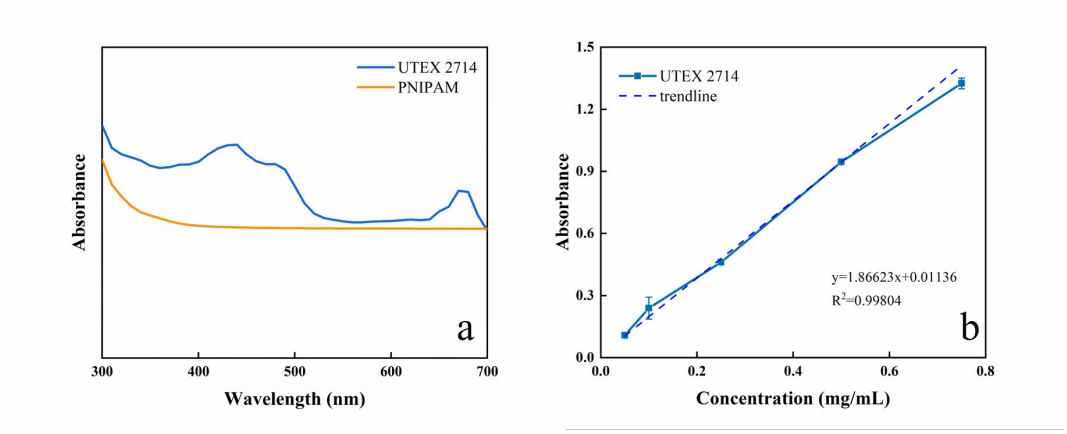

Figure 2.5. (a) UV-vis spectra for algae (UTEX 2714) and PNIPAM; and (b) standard curve for algae BDW vs. OD430 in its cultivation medium.

Figure 2.6a displays the process of TRP-induced microalgae harvesting. TRP chains change from coil to globule while simultaneously encapsulating the algae cells and separating them from the medium. As demonstrated in Figure 2.6b, the AHE increased with the increase of PNIPAM

concentration from 20 to 100 mg/mL for three PNIPAM with the MW of 15, 100 and 300 kDa, respectively, while the increasing rate were different among them. PNIPAM-300 kDa achieved a linear increase of AHE from 50% (20 mg/mL polymer) to 92% (100 mg/mL polymer), and the AHE with PNIPAM-15 kDa were similar between 20 and 40 mg/mL polymer but increased linearly from 18% to 55% with the concentration increase of PNIPAM from 40 to 100 mg/L. These findings could be explained by the fact that more TRPs in the medium can wrap more algae cells. However, PNIPAM-100 kDa only achieved numerically slight but statistically insignificant increase of AHE from 50% to 58%, which could be because PNIPAM-100 kDa prefers to form dense micro-globules, with insufficient gaps between chains to encapsulate more algae cells. In addition, the result on the effect of MW on AHE showed that higher MW achieved higher AHE at the same PNIPAM concentration. Higher MW represents longer polymer chain which could pack more algae cells and then form precipitation.

Moreover, we measured the AHE of PNIPAM-AA (Figure 2.6c) and PNIPAM-MTAC (Figure 2.6d) copolymers because the positive charges of AA and MTAC were expected to benefit the binding of algae cells to TRPs over PNIPAM (Ghernaout et al. 2020; Yin et al. 2008). As shown in Figure 2.6c, the effect of the AA content on AHE is similar across the polymers with three different MWs at the same polymer loading of 100 mg/mL. PNIPAM copolymerized with 1% mol AA reduced the AHE by 6%, 14%, and 12% for the MW of 300, 100, and 15 kDa, respectively, compared to the PNIPAM counterparts. For both MWs of 100 and 15 kDa, the increase of AA content from 1 to 5% mol increased the AHE to a similar level achieved by the PNIPAM counterparts, while further increase of AA to 10% mol decreased the AHE. For the MW of 300 kDa, 1-5% mol AA did not cause a significant change of AHE, while the AHE had a

significant decrease in the presence of 10% mol AA. In addition, PNIPAM-AA with higher MW was found to achieve higher AHE.

The effect of MTAC on the AHE of PNIPAM-MTAC copolymer varied with the MW. The presence of 1% mol MTAC in PNIPAM-MTAC-300 kDa resulted in a dramatic reduction of AHE from 90% to 35%, even less than the half of that with PNIPAM. Although further increase of the MTAC to 5% and 10% mol recovered certain AHE, the AHE was still much lower than that with PNIPAM. For PNIPAM-MTAC-100 kDa and PNIPAM-MTAC-15 kDa, the AHE kept decreasing to 38% and 22%, respectively, with the increase of MTAC content to 1% and 5%. When the MTAC content was further increased to 10% mol, their AHE was raised to a similar level of the PNIPAM counterparts. Such unexpected results indicated that copolymerization of PNIPAM with AA or MTAC could not enhance the AHE. This may be attributed to the electron repulsion on the TRP side chains, resulting in a larger spacing between TRP chains after phase transition, which is not enough to encapsulate a large quantity of algae cells.

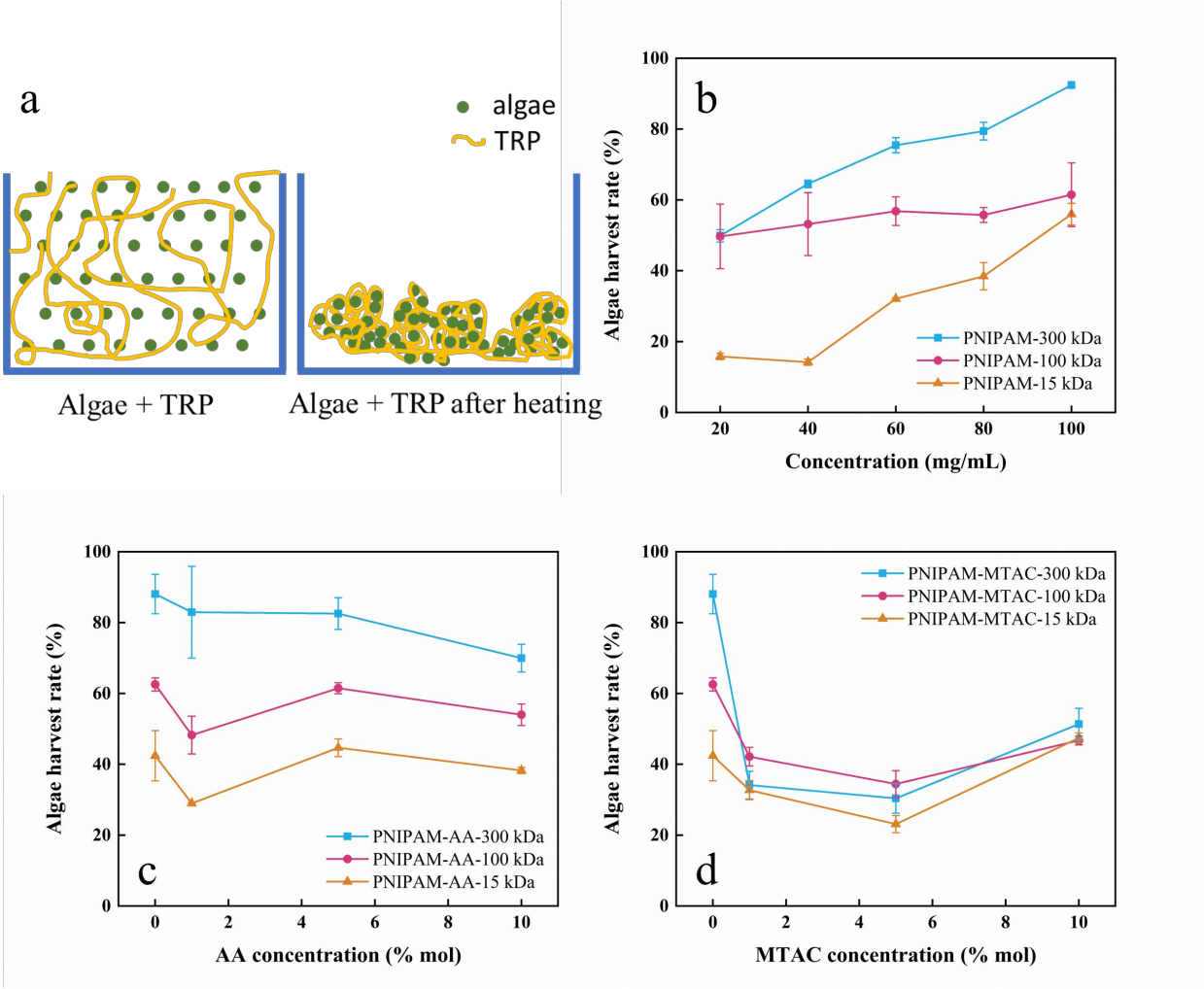

Figure 2.6. (a) Schematic diagram of the TRP-induced algae harvesting; (b) Effects of the MW and PNIPAM concentration on algae harvesting efficiency (AHE); (c) Effects of the AA content and PNIPAM-AA concentration on AHE; and (d) Effects of the MTAC content and PNIPAM-MTAC concentration on AHE.

2.4. Conclusions

In conclusion, after we successfully prepared Poly(N-isopropylacrylamide) (PNIPAM) with different properties, the effects of charge, molecular weight, amine content, and concentration on the phase change behavior were investigated. The lower critical solution temperature (LCST) of

PNIPAM increased with decreasing concentration, and the slope of the increase reduced while molecular weight (MW) got higher. With high concentration at 100 mg/mL and MW of 85 kDa, an LCST as low as 30.16 °C can be reached. Thermoresponsive polymers (TRPs) with higher MW undergo more drastic phase transitions and exhibit higher enthalpy changes. The negative charge on the surface of algae cells inspired us to add amine to PNIPAM, which may help the binding of polymer and algae cells. Modified PNIPAM with amine barely affected the LCST and did increase the positive charge on TRPs. For the application of using TRPs to harvest algae, both higher MW and concentration of the polymer can harvest more algae cells. PNIPAM-300 kDa at 100 mg/mL can harvest 92% of the algae cells in the medium. In practical applications, TRP can be applied repeatedly to expand the harvesting efficiency. However, more positive charges on the polymer did not help improve the harvesting efficiency. The mechanism of TRPs induced algae harvesting remains to be studied.

Chapter 3 - Innovative Microalgae Harvesting via Thermoresponsive Polymers: Insights into Poly(N-isopropylacrylamide) Efficacy and Mechanisms

Abstract

Microalgae-based biorefinery is promising but cost-prohibitive mainly because the algae biomass harvesting is time-consuming, energy-intensive, and costly. This work was inspired by previous research on algae biomass harvesting by co-cultivation of fungi and algae cells. The phase change progress of thermosresponsive polymers (TRPs) is similar to the self-pelletization of fungi hyphal. Poly(N-isopropylacrylamide) (PNIPAM) and its copolymers were used to investigate the ability of TRPs for harvesting microalgae biomass. Both higher molecular weight and concentration of the polymer contribute to harvesting more cells. PNIPAM-300 kDa can stably harvest more than 90% of algae cells in the culture medium. To expand the scope of TRPs use, algae strains with different sizes, culture medium, and cell wall composition have been tested as well. PNIPAM is the most suitable for *Nannochloropsis oculata* which grows in seawater with cell size of 2-10 μm and cell wall composition mainly in glucosamine. Amine induced positive charge was not helpful with algae harvesting even when the charge-shielding effect is reduced. Structure switch of TRPs after phase transition indicated that the algal cells may be encapsulated in polymers' meshwork structures, thus being harvested. The harvesting process reduced the vitality of the algae cells by more than 50%, accompanied by shrinkage and destruction of the cell wall.

Keywords: Poly(N-isopropylacrylamide) (PNIPAM); microalgae harvesting; bio-mimetics, smart polymers, stimuli-responsive

3.1. Introduction

Microalgae has been considered a promising feedstock for the 3rd generation biorefinery to produce biofuels, chemicals, food, feed, pharmaceuticals, and so on (Thanigaivel et al. 2022). Although the microalgae technology is sustainable and carbon-neutral, the cost of microalgae-based products is prohibitive (Bhatia et al. 2022). This dilemma makes current microalgae biorefinery unprofitable compared to the conventional petroleum refinery. Of the microalgae processing, algal cell harvesting accounts for a major cost contributor (Amer et al. 2011). This is because algal cells are generally small in size with negative charge on cell surface while their density is similar to water such that they usually form a uniform suspension in the culture medium (Milledge and Heaven 2013). As a result, the development of cost-efficient algal cell separation technology is essential to scale up the microalgae biorefinery.

Algae can be harvested by different types of techniques, including flocculation, centrifugation, filtration, sedimentation, and combination of some of these techniques (Singh et al. 2023), while each process has its own limitations (Ahmad et al. 2022). Inexpensive traditional chemical flocculants, such as alum, ferric chloride, and ferric sulfate, can be utilized on a large scale but often accumulate in the harvested biomass and cause product contamination as well as environmental pollution (Matter et al. 2019). Centrifugation provides contamination-free algal biomass that does not require purification before entering downstream processing. However, it is energy-intensive, resulting in high cost of algal biomass production (Najjar and Abu-Shamleh 2020). Filtration has similar shortcomings to centrifugation. Thus, new algae harvesting technologies that are cost-efficient and environmentally friendly are still needed to promote the commercialization of microalgae biorefinery.

In addition to conventional methods mentioned above, fungus-assisted microalgae bioflocculation has emerged as an efficient and economically viable approach for harvesting microalgae (Chen et al. 2018). Zhang and Hu (2012) demonstrated the co-cultivation of *Aspergillus niger* with *Chlorella vulgaris* to form cell pellets, facilitating algae harvesting. Similarly, Yang et al. (2019) highlighted the benefits of co-cultivating *Chlorella sp.* with *Aspergillus sp.* to enhance algae biomass production and harvesting efficiency. Fungus bioflocculants are a reliable method to achieve high biomass harvesting efficiency (Chu et al. 2021; Lin et al. 2022). The fungus-assisted harvesting process involves intricate interactions. Fungus, characterized by its filamentous morphology, can form spherical or ellipsoidal hyphal cellular biomass through hydrophobic interaction (Li et al. 2017; Ryan J and Russell T 2014). These structures enable self-pelletization. The secretion of extracellular polymers and the mechanism of lowering the environmental pH contribute to the efficient capture of microalgae (Bansfield et al. 2022; Velmurugan et al. 2010). However, the cultivation of fungal pellets necessitates additional nutrients in the medium, which would increase the cost (Choi et al. 2016; Oliveira, Bassin, and Cammarota 2019). Furthermore, the pathogenicity, toxicity, and/or environmental hazards associated with certain fungal strains may restrict the biomass utilization in downstream processes (Lin et al. 2022). To address these challenges, polymers that mimic fungal hyphal features present a promising alternative for microalgae harvesting (Vasistha et al. 2021). Such an approach aims to take advantage of the benefits while avoiding the drawbacks associated with the traditional fungus-assisted method, thereby enhancing the sustainability and applicability of microalgae in diverse industrial sectors.

Thermos-responsive polymers (TRPs) (e.g., poly-(N-isopropylacrylamide), PNIPAM)

undergoes a phase transition in water when temperature changes across its lower critical solution temperature (LCST) (Cao et al. 2019; Liu et al. 2022). This process is similar to fungi's self-pelletization when the polymer chains aggregate and precipitate due to hydrophobic interactions (Doberenz et al. 2020; Hogan and Mikos 2020). This is reminiscent of the use of PNIPAM to harvest microalgae cells to avoid possible safety issues. The acidic nature of the PNIPAM solution also makes it easier for the solution to reach the isoelectric point of the algae cells, thus aiding separation. Our previous work indicated that PNIPAM and its copolymers can be used to efficiently separate microalgae via some interactions between polymer and cells (Zheng et al. 2015, 2016). The phase separation behavior of TRPs can help concentrate up to ~100% of certain type of algal cells while the polymer can be recycled and reused.

This work aims at three objectives: (1) Using TRPs to simulate the process of algae harvesting via fungus-based bioflocculation; (2) Multiple properties, such as molecular weight (MW) and TRPs concentration are investigated on their effects on microalga harvesting; (3) Algae with different size, cultivation medium, and cell wall composition have also been tested to explore their effects on harvesting efficiency and their viability and cell morphology after harvest. The results are expected to lay the foundation for the development of a novel class of cost-effective and efficient microalgae harvesting methods based on TRPs.

3.2. Materials and Methods

3.2.1 Materials

N-isopropylacrylamide (NIPAM), ammonia persulfate (APS), allylamine (AA), 2-(Methacryloyloxy) ethyl trimethylammonium chloride (MTAC), tetramethylethylenediamine

(TEMED), glutaraldehyde 50% aqueous solution, paraformaldehyde, and 3-(4, 5-dimethylthiazol-2-yl)-2, 5-diphenyl tetrazolium bromide (MTT) were purchased from Fisher Scientific (Hampton, NH, USA). The microalgae cultures, including *Chlorococcum oleofaciens* (UTEX 105), *Chlorella protothecoides* (UTEX 256), *Nannochloropsis oculata* (UTEX 2164), and *Chlorella vulgaris* (UTEX 2714) culture and the media (Bristol medium, Proteose medium, and modified artificial seawater medium) were purchased from the Culture Collection of Algae at the University of Texas at Austin (Austin, TX, USA). Sodium cacodylate buffer (pH 7.4), 4% osmium tetroxide solution, and 2% uranyl acetate solution were purchased from Electron Microscopy Sciences (Hatfield, PA, USA).

3.2.2 Synthesis of PNIPAM, PNIPAM-AA, and PNIPAM-MTAC

TRPs were synthesized via the free radical emulsion polymerization of NIPAM by adding APS as an initiator. NIPAM powder of 25, 5, and 0.5 g was dissolved in 1000 mL deionized (DI) water to prepare PNIPAM with MW of 300, 100, and 15 kDa, respectively. The solution was constantly bubbled with nitrogen for 30 min to remove dissolved oxygen followed by the addition of 500 μL TEMED and 5 g APS. The nitrogen purging was continued for another 10 min before the glass bottle was sealed and left to stand stationarily at room temperature (RT) for 24 h to allow the polymerization reaction to proceed. To make TRPs with positive charge, AA and MTAC (each with the concentrations of 1, 5, and 10 mol% based on the mass of NIPAM) was dissolved in 1000 mL of DI water together with NIPAM, and the bubble, addition of TEMED and APS, another bubble and polymerization steps were repeated. The resulting TRPs were purified by dialysis against DI water for 7 days using regenerated cellulose dialysis membrane tubing (molecular weight cutoff, MWCO =10 kDa) (Spectra/Por®, Fisher Scientific,

Hampton, NH) to remove unreacted monomers. The dialyzed TRP solution was freeze-dried and stored at 4℃ until used.

3.2.3 Characterization of the synthesized thermoresponsive polymers

NMR spectrometer (Varian 400 MHz, Varian, Inc., Palo Alto, California, USA) was used to obtain the ^{1}H-NMR spectra of monomer and polymers. The NIPAM and TRP samples were dissolved in deuterated water (D_2O) at a concentration of 10 mg/mL. The measurement was conducted at 25°C, and 64 scans were obtained for signal averaging.

Differential scanning calorimetry (DSC) (Q200, TA Instrument, Schaumburg, IL) was used to determine the LCST of TRPs. Approximately 45 μL of TRP in aqueous, Bristol medium, and modified artificial sea water solutions at 100 mg/mL were weighed in aluminum pans, heated from 15 to 60℃ at a rate of 5℃·min^{-1}, and cooled down to 15℃. Three cycles were recorded to determine the LCST of each solution with DI water as a reference.

3.2.4 Microalgae harvesting by using thermoresponsive polymers

The microalgae strains used in this study were *C. oleofaciens* (UTEX 105), *C. protothecoides* (UTEX 256), *N. oculata* (UTEX 2164) and *C. vulgaris* (UTEX 2714). The properties of these strains are displayed in Table 3.1. The cultivation media were stored at 4℃ after received until used. Stock algae cultures were scraped from agar slants and transferred to liquid media to achieve an optical density of 0.1 at 670 nm (OD_{670}) for seed culture preparation. This seed culture was incubated at RT under 12-h light/dark cycles. Once the OD_{670} reached 0.2, the entire seed culture was transferred to a 500-mL flask, diluted with fresh media at a 1:5 (v/v) ratio, and incubated under the same light/dark conditions. The flasks were aerated at 0.15 liter

per minute (LPM) and stirred at 400 rpm with a magnetic bar for 12 days. Algal biomass dry weight (BDW) was determined by filtration, i.e., the cell biomass retained on the filter paper were washed with DI water for three times and dried at 80°C overnight. The BDW was calculated by subtracting the dry weight of the filter paper from the total dry weight of the filter paper and algal biomass.

Table 3.1. Properties of algae used in this research

Strain	UTEX code	Class	Size (μm)	Medium	Cell wall
Chlorococcum oleofaciens (Trainor and Bold 1953)	105	Chlorophyceae	20-35	Bristol medium (Bold 1949)	Glucose
Chlorella protothecoides (Huss et al. 1986)	256	Chlorophyceae	2-10	Proteose medium	Glucose
Nannochloropsis oculata (Hibberd 1981)	2164	Eustigmatophyceae	2-10	Modified artificial seawater medium (UTEX Culture Collection of Algae 2024)	Glucosamine
Chlorella vulgaris (González et al. 1997)	2714	Chlorophyceae	2-10	Proteose medium	Glucosamine

Note: Proteose medium was Bristol medium supplemented with 1 g/L of proteose peptone.

The wavelength corresponding to maximum absorption (λ_{max} = 430 nm) of the algae suspension was determined using the scan mode on a BioTek Epoch2 microplate reader (BioTek Instruments Inc., Winooski, VT). Optical density (OD) measurements of the algae suspension were then all taken at 430 nm. To construct a calibration curve for BDW versus OD, algae suspensions with BDW ranging from 0.05 to 1 mg/mL were prepared, and their OD_{430} values were recorded. This calibration curve was then used to determine the BDW of algae samples in subsequent experiments by measuring their OD. Samples with OD values exceeding 1.0 were

diluted and remeasured with their respective growth medium before calculation.

TRP solutions were prepared in DI water at a concentration of 200 mg/mL at RT and then mixed with the algae suspension in a 1:1 (v/v) ratio. The mixture was vortexed and heated to the specific LCST of the corresponding TRPs for 30 min to induce the phase transition from soluble to insoluble. After cooling, the supernatant was collected for OD measurement. OD values were converted to BDW using the pre-made calibration curves. The algae harvesting efficiency (AHE) was then calculated as Eq. 3.1 and biomass dry weight harvested was calculated as Eq. 3.2.

$$AHE(\%) = \frac{BDW_i - BDW_f}{BDW_i} \times 100\% \quad \text{(Equation 3.1)}$$

$$AH\ (mg/mL\ polymer) = \left(BDW_i - BDW_f\right) \Big/ 0.5\ mL \quad \text{(Equation 3.2)}$$

Where BDW_i and BDW_f are the initial and final algae BDW (mg/L), respectively.

The AHE has been tested in salt-free buffer as well to eliminate charge-shielding effect. The algae biomass was obtained by centrifugation at 3000 rpm for 10 min, the supernatant was discarded, and an equal amount of buffer was added to resuspend the biomass. The following steps are exactly the same as in the culture medium.

3.2.5 Scanning electron microscope

The PNIPAM samples were first swollen in DI water for 24 h at RT (unheated) and 35℃ (heated), and quickly frozen at -80℃ followed by immediate freeze-drying (Labconco 700402000 FreeZone 4.5L -50°C Benchtop, Labconco, Kansas City, MO, USA) under vacuum at -50℃. After the dried samples were cut with a scalpel, the cross section was sputter-coated with a thin layer of gold. The fractured surfaces of the PNIPAM samples before and after phase

change were observed by using a scanning electron microscope (SEM) (Hitachi S-3500N, Hitachi, Japan) at the operating voltage of 5.00 kV.

3.2.6 Algae cell property evaluation after harvesting with thermoresponsive polymers

Relative cell viability

Cytotoxicity of TRPs on algae cells during harvesting was assessed by using 3-(4, 5-dimethylthiazol-2-yl)-2, 5-diphenyl tetrazolium bromide (MTT) assay. The harvested algae cells were placed in a 96-well plate, and 5 replicates were prepared for each TRP. Cells were treated with 20 μL of MTT (5 mg/mL algae medium) and incubated overnight at RT. After incubation, the medium was removed by using pipette, 200 μL of dimethyl sulfoxide (DMSO) was added to each well to dissolve the purple crystals of the generated formazan. The absorbance was measured at 556 nm on a microplate reader (BioTek Epoch2, BioTek Instruments Inc., Winooski, VT). Original algae cells were analyzed by following the same process as a control group. The relative cell viability was calculated as Eq. 3.3.

$$Relative\ cell\ viability\ (\%) = \frac{OD_{sample}}{OD_{control}} \times 100\% \qquad \text{(Equation 3.3)}$$

Where OD_{sample} and $OD_{control}$ are absorbances of algae cells harvested by TRP and normal cultured algae cells, respectively.

Laser scanning confocal microscopy (LSM)

The morphology and fluorescence intensity of algae cells before and after harvesting by TRPs were observed using a laser scan confocal microscope (LSM-5 PASCAL, Zeiss,

Germany). An aliquot of 20 μL algae sample harvested with TRPs was dropped to the center of a glass slide, covered with a coverslip, and sealed with nail polish. Images were taken under a dark field.

Transmission electron microscopy (TEM)

The algae cells with and without harvesting were obtained by centrifugation at 3000 rpm for 10 min. Samples (less than 1 mm^3) were immersion-fixed in fixative containing 2% paraformaldehyde and 2% glutaraldehyde in 0.1 M sodium cacodylate buffer (pH 7.4) for 1 h at RT with constant rotation. The fixative should completely immerse the entire specimen. After fixation, cells were washed using sodium cacodylate buffer (0.1 M, pH=7.4). Post fixation was done using 2% osmium tetroxide in sodium cacodylate buffer for 1 h at RT. Samples were washed again with sodium cacodylate buffer and subsequently en bloc stained in 2% uranyl acetate (aqueous) for 1 h at RT under light protection. The cells were then washed in water and serially dehydrated with 50%, 60%, 70%, 80%, 90%, 95% and 100% acetone, respectively. Embedded samples in low viscosity epoxy after dehydration. Ultrathin sections with 60-80 nm thickness were cut using an ultramicrotome before analyzing the grids on a transmission electron microscopy (FEI CM 100, Philips/FEI, USA) operated at 100 kV.

3.2.7 Data analysis

The statistical significance of data was determined using analysis of variance (ANOVA) and least significant difference (LSD) at $\alpha = 0.05$ using SAS OnDemand for Academics analysis (SAS, NC, USA). All reported values in this study were the average of three replicates, unless specified otherwise.

3.3 Results and Discussion

3.3.1 Characterization of the synthesized thermoresponsive polymers

After preparation of PNIPAM and its copolymers, ^{1}H-NMR has been applied to confirm the success of polymer synthesis. The ^{1}H-NMR spectrum of NIPAM (Figure 3.1a) shows that peak a at 1.03 ppm was due to methyl group -CH_3, peak b at 3.85 ppm was assigned to -CH- group, and peak d at 5.59 ppm was due to the proton located on CH_2= group. Signals from 5.99-6.12 ppm were assigned to protons on CH_2= and -CH= groups. The peak at 4.66 ppm was attributed to residual water. Meanwhile, the peaks of PNIPAM (Figure 3.1b) at 1.46 ppm (-CH_2- on the polymer backbone), 1.90 ppm (-CH- on the polymer backbone), and 3.78 ppm (-CH- on the isopropyl) confirmed the opening of the carbon-carbon double bond. The integration ratio of peaks a, d, b, and c is around 6:2:1:1, corresponding to the structure of PNIPAM. Moreover, the proton signals of C=C in the initial monomer disappeared, indicating the occurrence of NIPAM polymerization. As shown in the spectrum of PNIPAM-AA (Figure 3.1c), characteristic peaks were identified for PNIPAM at 1.03 ppm (-CH_3 on the isopropyl), 1.46 ppm (-CH_2- on the polymer backbone), 1.89 ppm (-CH- on the polymer backbone), and 3.79 ppm (-CH- on the isopropyl), as well as 2.60 ppm (-CH2- protons for AA). Similar peaks a, b, c, and d at 1.03 ppm (-CH_3 on the isopropyl), 1.46 ppm (-CH_2- on the polymer backbone), 1.89 ppm (-CH- on the polymer backbone), and 3.79 (-CH- on the isopropyl), respectively, corresponding to PNIAM can be observed in the spectrum of PNIPAM-MTAC (Figure 3.1d). In addition, peaks e, f, and g at 3.14 ppm ($N^{+}CH_3$), 3.65 ppm ($N^{+}CH_2$-), and 4.39 ppm (-CH_2-) confirmed the presence of MTAC.

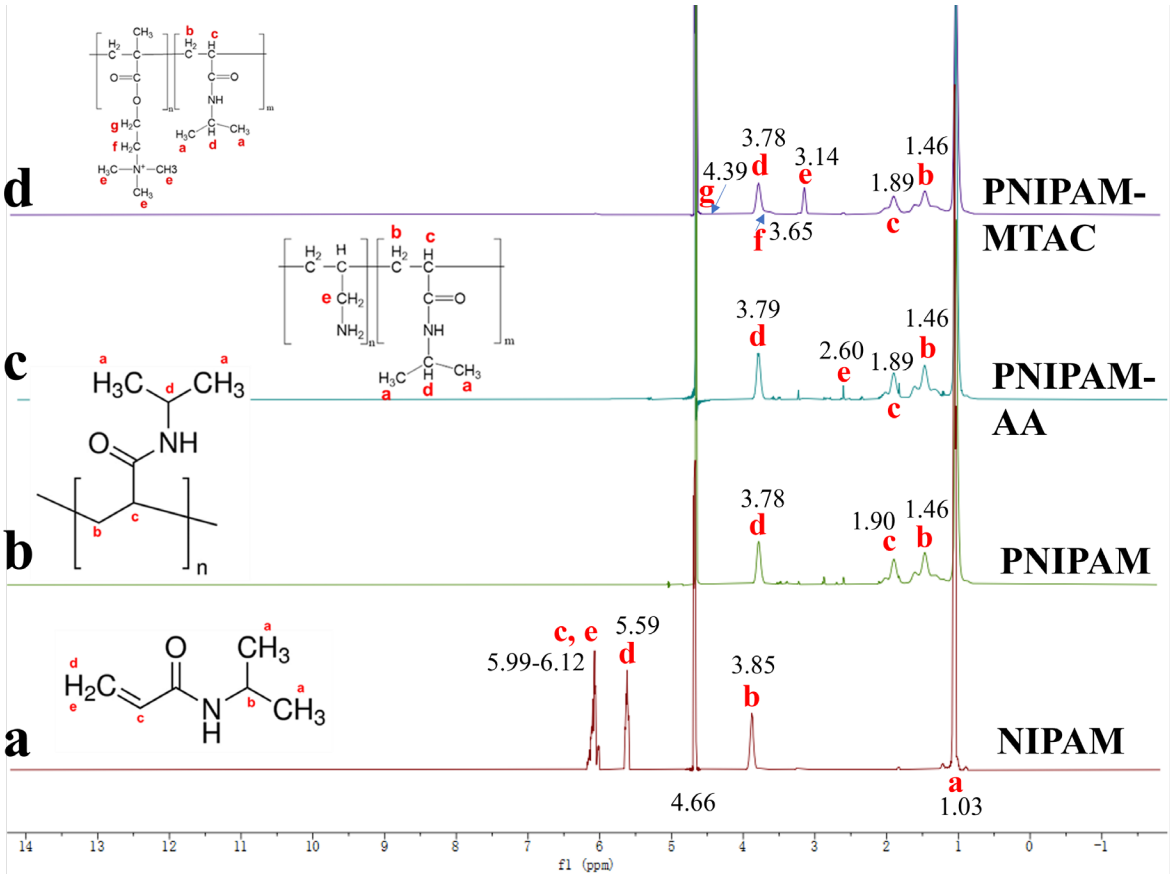

Figure 3.1. ^{1}H NMR spectrum of NIPAM (a), PNIPAM (b), PNIPAM-AA (c), and PNIPAM-MTAC (d)

The LCST of PNIPAM and its copolymers in different media are demonstrated in Figure 3.2. For PNIPAM modified with AA (a, c, e), the LCST did not change too much at different AA concentration in water except for PNIPAM-300 kDa modified with 10% mol AA (PNIPAM-300 kDa-10%AA). This may be because PNIPAM-300 kDa-10%AA had the highest AA concentration in the solution given that higher AA concentration could render higher positive charge on the side chain of the polymer, and the electrostatic interactions made it difficult for the polymer to agglomerate. But for TRPs in Bristol medium, higher AA concentration led to dramatically lower LCST with PNIPAM-15 kDa, while PNIPAM-300 kDa and PNIPAM-100

kDa retained similar LCST to that in water. Meanwhile, all the TRPs showed lower LCSTs in MASW than those in water. That because that the presence of salt in the solution shifted the LCST of TRPs to a lower temperature (Du, Wickramasinghe, and Qian 2010), given that MASW has much higher salt concentration than the Bristol medium and water. The same trend was observed for PNIPAM-MTAC. All PNIPAM-MTAC had a LCST lower than 35℃ in Bristol medium and lower than 32℃ in MASW. The lowest LCST of all the tested TRPs was 22.6℃ (even lower than the RT) which was detected for PNIPAM-100 kDa modified with 5% mol AA in MASW. Lower LCST occurring in the culture medium with high salt would benefit algae harvesting, as the energy input (raising temperature above the LCST) to initiate the TRP phase transition for algae harvesting could be reduced or avoided.

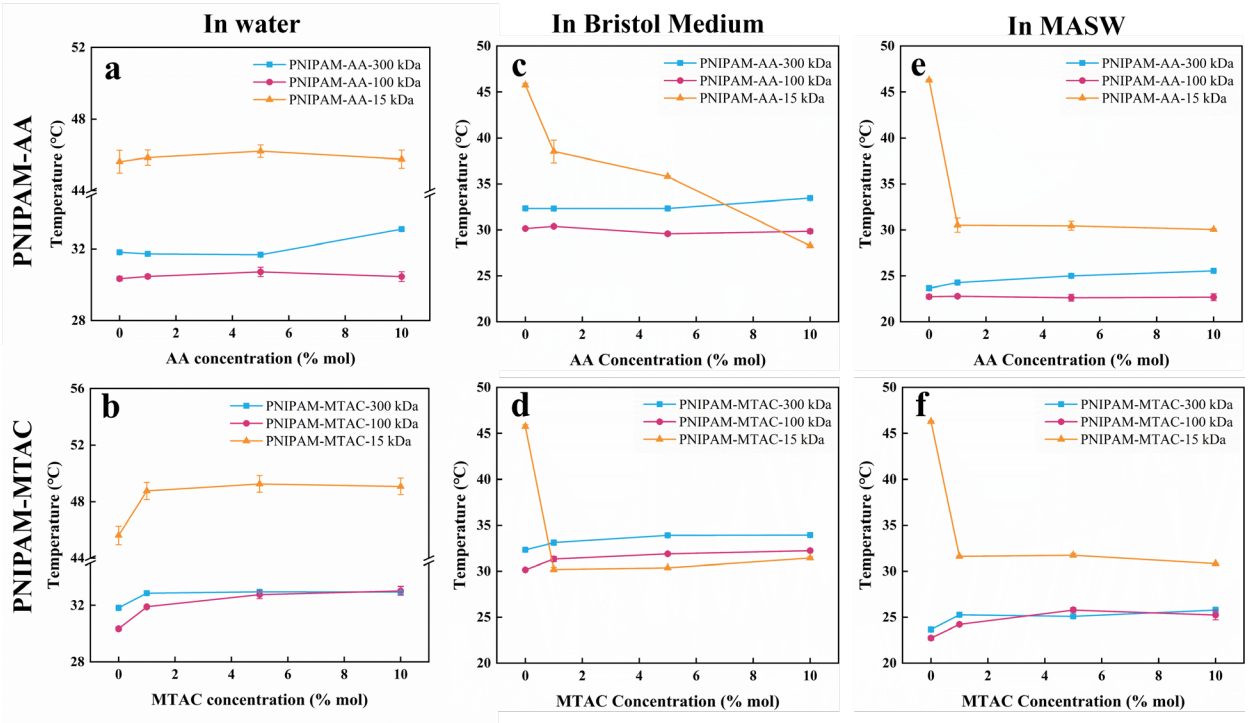

Figure 3.2. TRPs' LCST in water (a-b), Bristol medium (c-d), and modified artificial sea water (MASW) (e-f)

3.3.2 Microalgae harvesting by using thermoresponsive polymers

Figure 3.3a shows the UV-vis spectra for all four different algae strains and PNIPAM. The absorbance of all the algae had a peak at λ=430 nm, and PNIPAM did not display any UV-Vis absorption above λ=400 nm. Therefore, UV-vis spectroscopy was able to be used to measure the algae OD in the presence of PINPAM in the solution. To maintain the consistency of the experiment, 430 nm was selected for all OD analyses in all subsequent algae harvesting experiments. The standard curves for algae OD_{430} vs. BDW were developed in their cultivation media (Figure 3.3b-e), which was used to calculate algae BDW from the measured OD_{430} values. All the standard curves had an R^2>0.99, indicating their reliability.

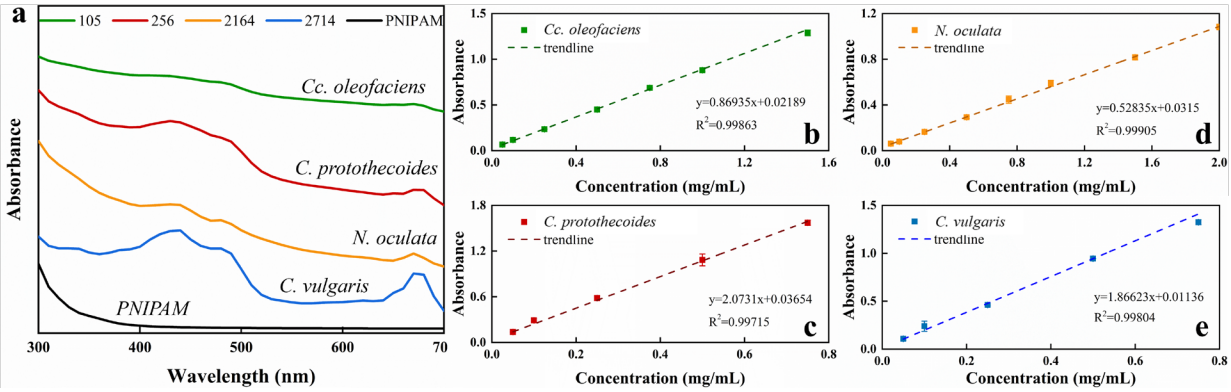

Figure 3.3. UV-vis spectra for algae strains and PNIPAM (a); and standard curve for algal BDW vs. OD_{430} in their cultivation media (b: *Cc. oleofaciens*; c: *C. protothecoides*; d: *N. oculata*; e: *C. vulgaris*)

Figure 3.4 describes the AHE after heating with TRPs. As shown in Figure 3.4a-d, PNIPAM can be used to harvest these four different algae, while the AHE varies greatly, i.e., the

lowest AHE was 0.11 mg *C. vulgaris*/mL PNIPAM-15 kDa, and the highest AHE was 1.14 mg *Cc. oleofaciens*/mL PNIPAM-300 kDa. Of the tested four stains of algae, *Cc. oleofaciens* (size = 20-35 μm) is the largest in cell size, which could make it heavier. Natural sedimentation due to gravity was observed in experiments with *Cc. oleofaciens* only, and the dotted line indicates the AHE induced by gravity. Basically, the difference between the solid line and the dotted line can help us estimate the AHE of PNIPAM for *Cc. oleofaciens*. In general, the larger MW and higher concentration of TRPs can harvest more *Cc. oleofaciens*. PNIPAM-300 kDa showed more gel-like properties and poorer liquidity than PNIPAM-100 kDa and PNIPAM-15 kDa, especially at high concentration, which made it harder for the algae to separate from the solution. PNIPAM-300 kDa achieved the best AHE of 90.71% at 100 mg/mL by counting the difference between after heating and without heating. PNIPAM-100 kDa at the concentration of 100 mg/mL enhanced the harvesting of *Cc. oleofaciens* by an additional 0.44 mg (48.50%) compared to the harvesting without heating. On the other hand, PNIPAM-15 kDa did not substantially contribute to the increased *Cc. oleofaciens* harvesting, as it naturally settled. Alternatively, the harvesting rate for *C. protothecoides* was not so related to the TRP's MW or concentration. All PNIPAM with different MW yielded a maximum of around 0.42 mg algae after heating for 30 min at their LCST, which was about 90% of algal biomass in the medium. PNIPAM-300 kDa and PNIPAM-100 kDa achieved their minimum AHE of 0.393 mg and 0.388 mg, respectively. Therefore, PNIPAM-100kDa at 20 mg/mL would be recommended for *C. protothecoides*. Unlike *C. protothecoides*, the harvesting rate for *N. oculata* rose with the increase of TRP MW but not with the concentration. It is worth mentioning that *N. oculata* is the only algae that grows in seawater. The high salt concentration of the medium may affect the collapse and dehydration of the TRPs. At a concentration of 100 mg/mL, PNIPAM-300 kDa effectively separated 0.88 mg of *N.*

oculata, accounting for approximately 87.90%. In contrast, PNIPAM-100 kDa achieved a maximum separation of 0.66 mg of *N. oculata* at a concentration of 20 mg/mL, corresponding to a separation efficiency of about 66.62%. The lower AHE at its higher concentration may be caused by the high-salt environment. The highest AHE of PNIPAM-15kDa reached 0.41 mg (41.03%) at 60 mg/mL. In addition, the AHE for *C. vulgaris* increased with the increase of MW and concentration. The TRPs separated 0.69 mg (PNIPAM-300 kDa), 0.46 mg (PNIPAM-100 kDa), and 0.42 mg (PNIPAM-15 kDa) *C. vulgaris*, which were 92.42%, 61.47%, and 55.98%, respectively. In short, TRPs are effective in separating algae from its medium and can reach more than 90% AHE for these four selected algae. Overall, PNIPAM is the most suitable for *N. oculata* which grows in seawater with cell size of 2-10 μm and cell wall composition mainly in glucosamine. PNIPAM-300 kDa can get the best results for all these 4 algae strains and its concentration has little effect on AHE. PNIPAM didn't perform as well as expected in harvesting *C. protothecoides*, and neither MW nor concentration affected its AHE. For algae in large size, such as *Cc. oleofaciens*, PNIPAM-100 kDa is recommended because it can help harvest about 50% more algae than the natural settlement. Algae with glucosamine as a major cell wall component are more sensitive to the MW of TRPs. As a result, PNIPAM-300kDa is ideal for *C. vulgaris* at 100 mg/mL.

The difficulty in microalgae harvesting is partly attributed to the repulsion between negatively charged algae cells. It was found that the repulsive force between algae cells decreased when the environmental pH was reduced, helping the microalgae to flocculate (Li et al. 2017). Filamentous fungus can secrete organic acids during growth, which can lower the pH of the culture medium (Gutarowska and Czyżowska 2009; Velmurugan et al. 2010). This

characteristic of fungus could promote the algal-fungal symbiosis to form self-flocculant, which has been taken advantage for microalgae harvesting (J. Wang et al. 2023). The TRP (e.g., PNIPAM) used in this research can also lower the pH of the solution, and the TRP with higher MW had lower pH, which may be the reason why high-MW TRPs performed better in algae harvesting.

Moreover, the AHE of PNIPAM-AA (Figure 3.4e-h) and PNIPAM-MTAC (Figure 3.4i-l) copolymers were also investigated because the positive charges of AA and MTAC were expected to benefit the binding of algae cells to TRPs over PNIPAM through electrostatic interaction (Ghernaout et al. 2020). The PNIPAM modified with AA or MTAC exhibited reduced efficiency in harvesting algae compared to the unmodified PNIPAM across all algae strains. Such results may be due to charge-shielding effect caused by the high-salt culture medium (Cruz et al. 2018), for which the positive charges on the copolymers can't interact with the negative charges on algae cells as expected. Therefore, further research is needed to clarify the mechanism of interactions between TRPs (PNIPAM and its copolymers) and algal cells in salt-free media.

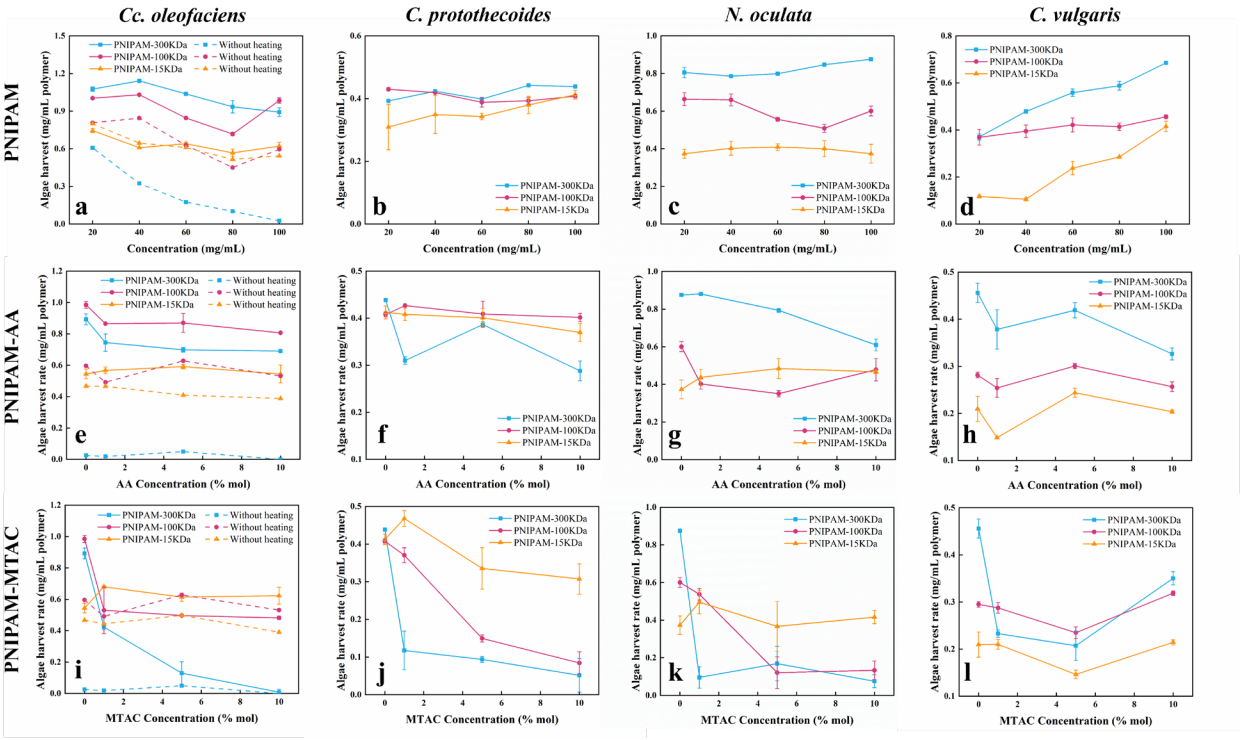

Figure 3.4. Algae harvest efficiency induced by TRPs (a: *Cc. oleofaciens* harvested by PNIPAM; b: *C. protothecoides* harvested by PNIPAM; c: *N. oculata* harvested by PNIPAM; d: *C. vulgaris* harvested by PNIPAM. e-h: algae harvested by PNIPAM-AA; i-l: algae harvested by PNIPAM-MTAC)

The AHEs for four different algae strains by TRPs in salt-free buffer (phosphate buffer) are shown in Figure 3.5. For PNIPAM-AA, the increase of AA concentration in PNIPAM-15 kDa improved the AHE for the four algae strains tested, which could be attributed to the more positive charges on the polymer. Meanwhile, more AA on PNIPAM-300 kDa and -100 kDa had different effects for different algae strains. Higher AA concentration on PNIAPM-300 kDa benefited the harvesting of *C. protothecoides* (15% improvement) and *C. vulgaris* (28% improvement) but had little positive effect on the harvesting of *Cc. oleofaciens* and *N. oculata*. Also, more AA in PNIAPM-100 kDa worsened the harvesting of *Cc. oleofaciens* and *C.*

protothecoides while having little effect on the harvesting of *N. oculata* and *C. vulgaris*. Such inconsistent trends may be because the harvesting mechanism was different from electron interaction or be attributed to the change of AA charge caused by solution pH. The positive charge of AA changes on the pH of solution, while the charge of MTAC will not change on the pH. For PNIPAM-MTAC, higher MTAC concentration on PNIPAM-15 kDa had the same effect as PNIPAM-AA in enhancing AHE. The highest improvements were 77% for *Cc. oleofaciens,* 71% for *C. protothecoides,* 17% for *N. oculata* and 36% for *C. vulgaris.* However, more MTAC on PNIPAM-300 kDa had a negative effect on harvesting. The AHEs of PNIPAM-300 kDa-MTAC were just 30%, 29%, 12% and 36% of the AHE induced by PNIPAM-300 kDa without MTAC, respectively. Also, more MTAC on PNIPAM-100 kDa harvested less *Cc. oleofaciens* and *C. protothecoides* but more *N. oculata* and *C. vulgaris* compared with PNIPAM-100 kDa without MTAC. The results indicated that more positive charge on the TRPs did not necessarily promote the algae cell binding or harvesting. Therefore, the mechanism behind the harvesting with TRPs may not be the electrostatic interaction as hypothesized. The more positive charge on TRPs with lower MW can help harvest more algae cells while the more positive charges on the higher molecular weight TRPs hinder the harvest of algae cells. During the phase change of TRPs, they could form coacervate (dense polymer-rich phase) encapsulate biomolecules such as algae cells. Excessive positive charges may result in coacervates that are not dense enough to encapsulate enough algae cells. Thus, the harvested algae may just be wrapped by agglomerated polymers without involving electrostatic interactions.

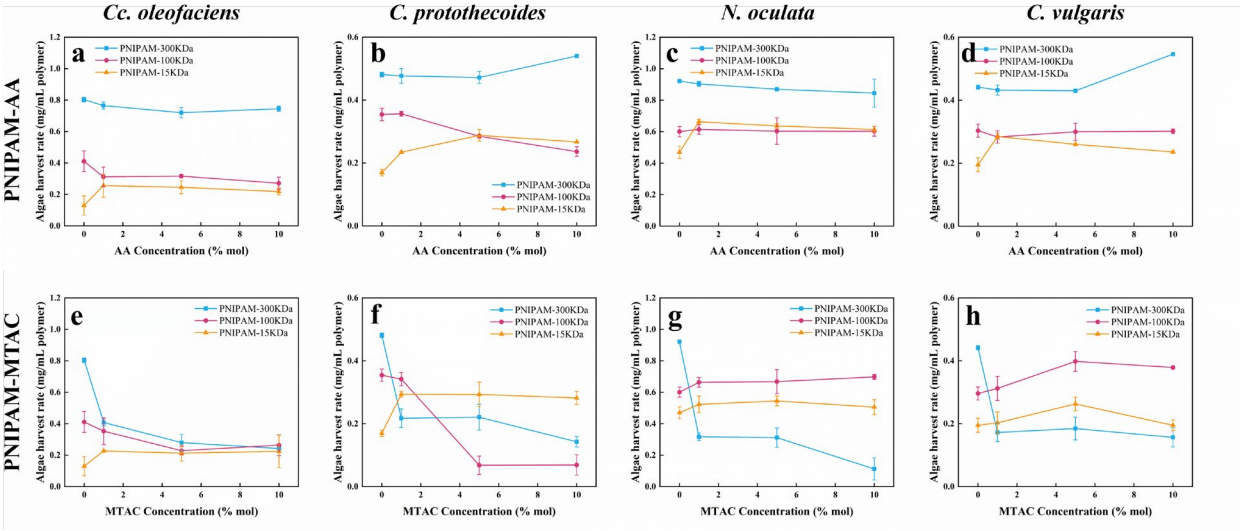

Figure 3.5. Algae harvest efficiency induced by TRPs in salt-free buffer (a: *Cc. oleofaciens* harvested by PNIPAM-AA; b: *C. protothecoides* harvested by PNIPAM-AA; c: *N. oculata* harvested by PNIPAM-AA; d: *C. vulgaris* harvested by PNIPAM-AA. e-h: algae harvested by PNIPAM-MTAC)

3.3.3. Scanning electron microscope

As shown in Figure 3.6, SEM analyses were made to investigate the cross-section structure change before and after phase transition of PNIPAM. The SEM images of PNIPAM before phase change (unheated) had sheet-like structure with one sheet stacked next to another. Zooming in on one of the slices, holes with diameter less than 1 μm can be observed. After heating, the structure of PNIPAM shifted to a three-dimensional mesh structure. The polymer's crisscross creates cavities of different sizes. The largest ones reach 15 μm in diameter, while the smallest ones are less than 2 μm. It was hypothesized that algal cells could be encapsulated in these meshwork structures during TRP phase transitions, thus being harvested.

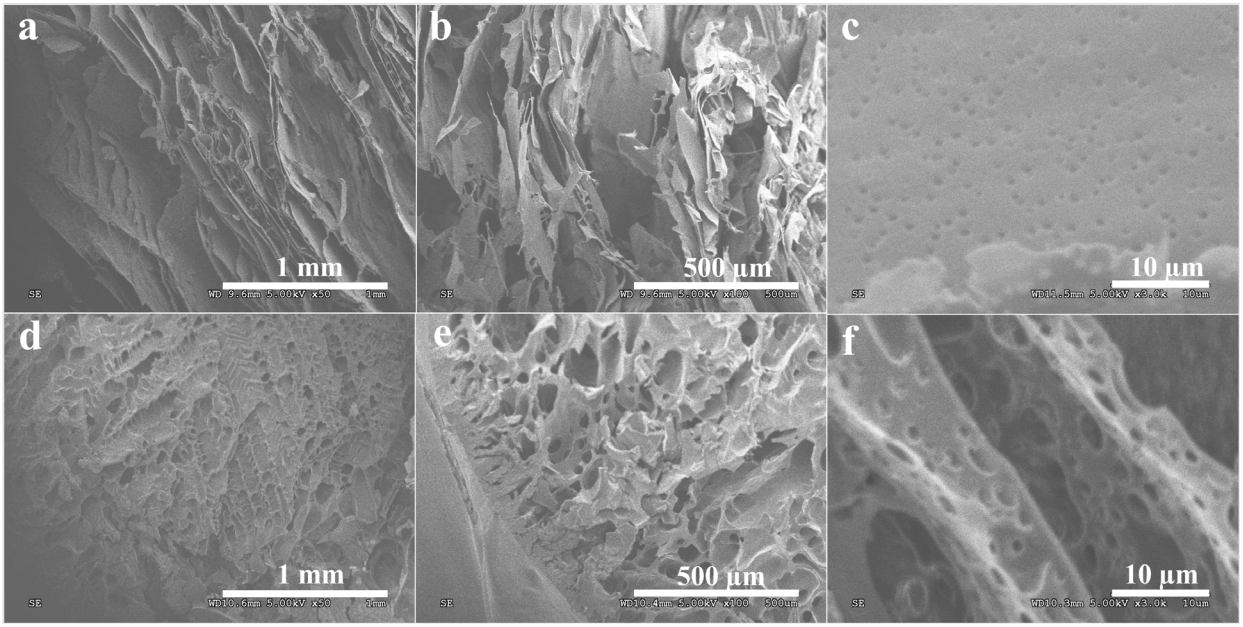

Figure 3.6. SEM of PNIPAM (a: unheated PNIPAM ×50; b: unheated PNIPAM ×100; c: unheated PNIPAM ×3000; d: heated PNIPAM ×50; e: heated PNIPAM ×100; f: heated PNIPAM ×3000)

3.3.4. Algae cell property evaluation after harvesting with thermoresponsive polymers

MTT assay was used to evaluate the cell activity of different algae cells after harvesting. As demonstrated in Figure 3.7, harvested algae cells showed significantly lower viability, and more than half of the algae were deactivated during the TRP harvesting except PNIPAM-300 kDa-10%AA. Algae harvested by PNIPAM-15 kDa without AA had much lower viability compared to other TRPs, which could be ascribed to the higher LCST of PNIPAM-15 kDa (> 45 ℃) in algae culture medium. The tested algae cells could hardly survive at such a high temperature. For *Cc. oleofaciens*, the largest algae among these 4 strains, more cells survived when harvested by

TRPs with lower MW. Shorter polymer chains have difficulty in interweaving into spaces large enough to wrap around such large cells. *C. vulgaris* had the lowest viability after harvesting by TRPs, i.e., more than 90% of the algae cells were deactivated during harvesting. Even though the cell walls are glucosamine for both *N. oculata* and *C. vulgaris*, the composites are not exactly the same. PNIPAM may have a special effect on a component of the *C. vulgaris* cell wall, which remains unclear. In summary, the viability of algae harvested by TRPs can drop below 50%, especially when the LCST of the TRP is high or when *C. vulgaris* was harvested.

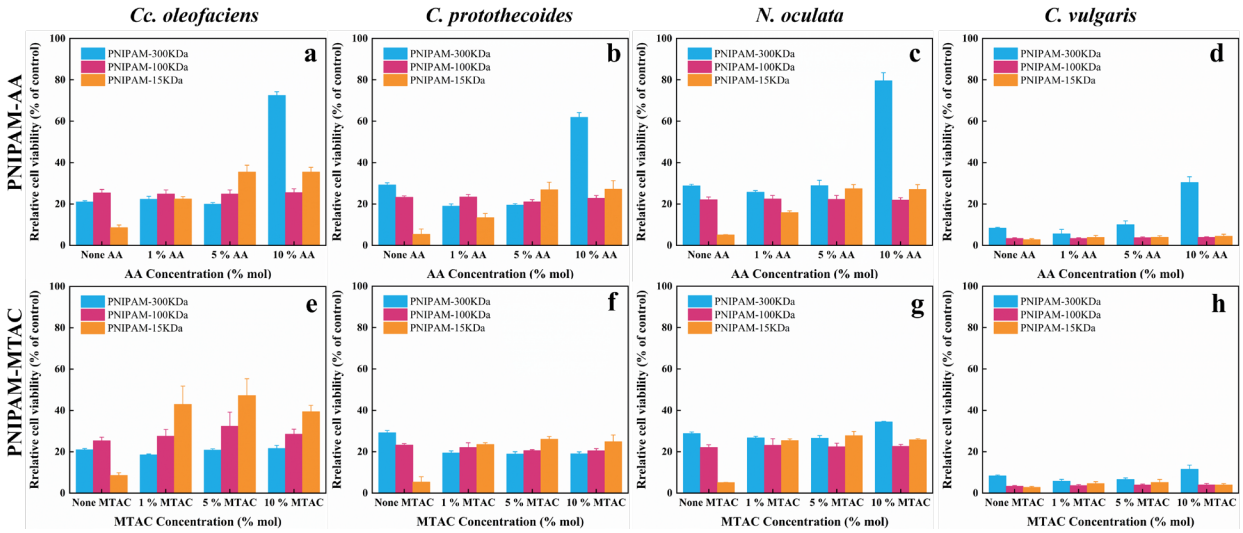

Figure 3.7. MTT assay of algae cells after harvesting (a: *Cc. oleofaciens* harvested by PNIPAM-AA; b: *C. prototheocoides* harvested by PNIPAM-AA; c: *N. oculata* harvested by PNIPAM-AA; d: *C. vulgaris* harvested by PNIPAM-AA. e-h: algae harvested by PNIPAM-MTAC)

Laser scanning confocal microscopy (LSM) was used to investigate the morphology and fluorescence intensity of algae cells before and after harvesting with TRPs. The red fluorescence shown in Figure 3.8 corresponds to the chlorophyll fluorescence in chloroplasts of algae cells.

The untreated algae cells had plump cell surfaces and strong red fluorescence, while the cell surface obviously wrinkled after harvested by TRPs and was no longer round, and the red fluorescence was significantly dimmer than that of the untreated cells. This change suggests that the TRP-induced harvesting process affected the cell walls and chloroplasts of all tested algae cells.

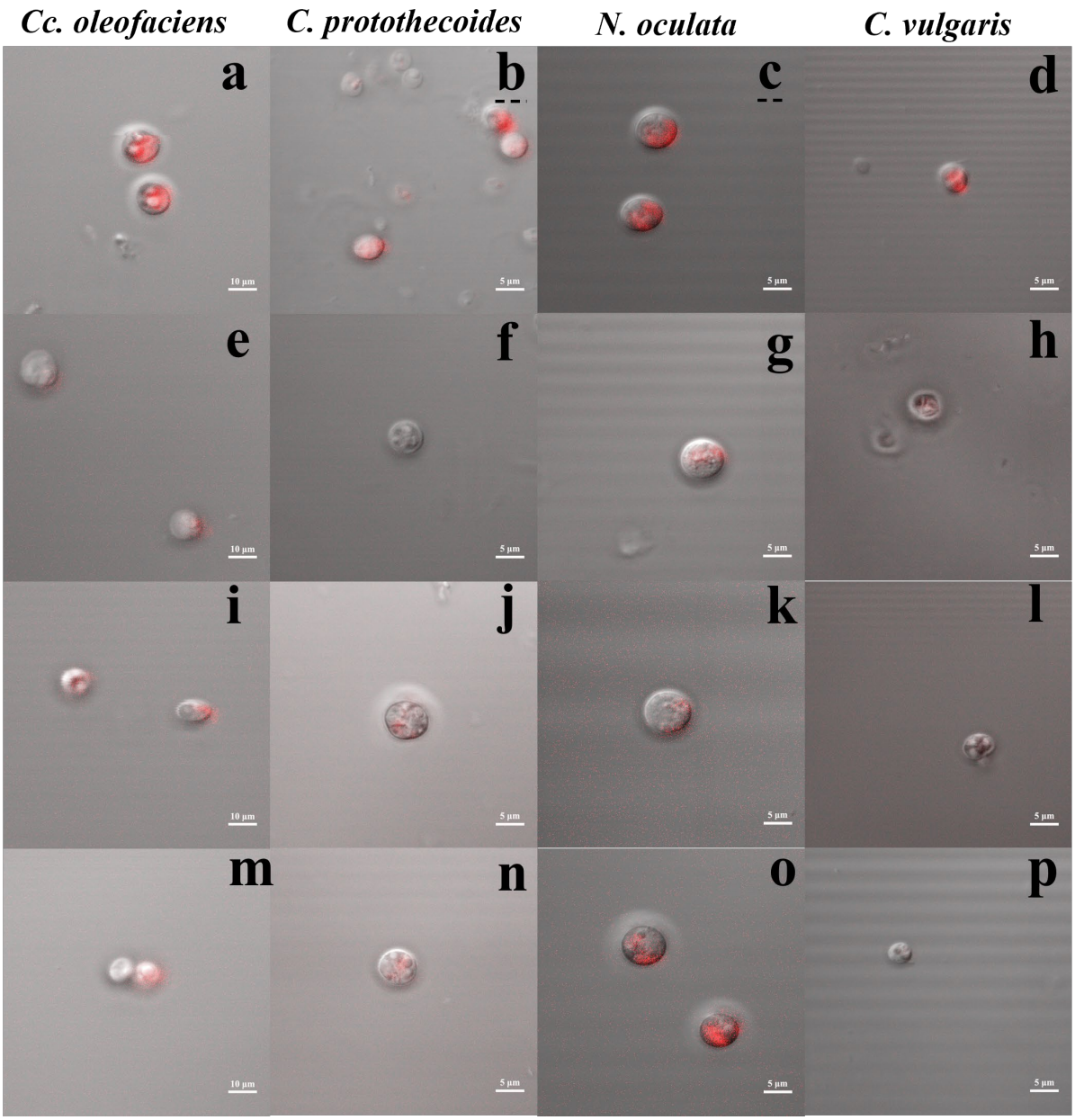

Figure 3.8. LSM images of algae cells (a: normal *Cc. oleofaciens* cells; b: normal *C. protothecoides* cells; c: normal *N. oculata* cells; d: normal *C. vulgaris* cells. e-h: algae harvested by PNIPAM. i-l: algae harvested by PNIPAM-AA. m-p: algae harvested by PNIPAM-MTAC)

TEM was performed to analyze the ultrastructural changes before and after harvesting. Normal algae cells without treatment with TRPs showed intact and round cells with smooth cell wall and clear cell organelles (Figure 3.9). TEM images for *Cc. oleofaciens* cells and *N. oculata* cells harvested by TRPs showed identical morphological changes. Both images (Figure 3.9b and f) showed the deformation and thickening of cell walls and slightly villi-like structures while the organelles inside the cells seem to be normal. Meanwhile, the TEM images for *C. protothecoides* cells harvested by PNIPAM-15 kDa showed conspicuous deformation, with almost no cellular structure visible. This is most likely caused by the high temperatures during harvesting because the LCST of PNIPAM-15 kDa is about 15℃ higher than that of other TRPs. For *C. vulgaris* cells harvested with PNIPAM-100 kDa, distinct villi-like structures and plasmolysis were observed. These phenomena indicate that the TRP harvesting process has some impact on cell morphology, but it is not enough to completely lyse the cells.

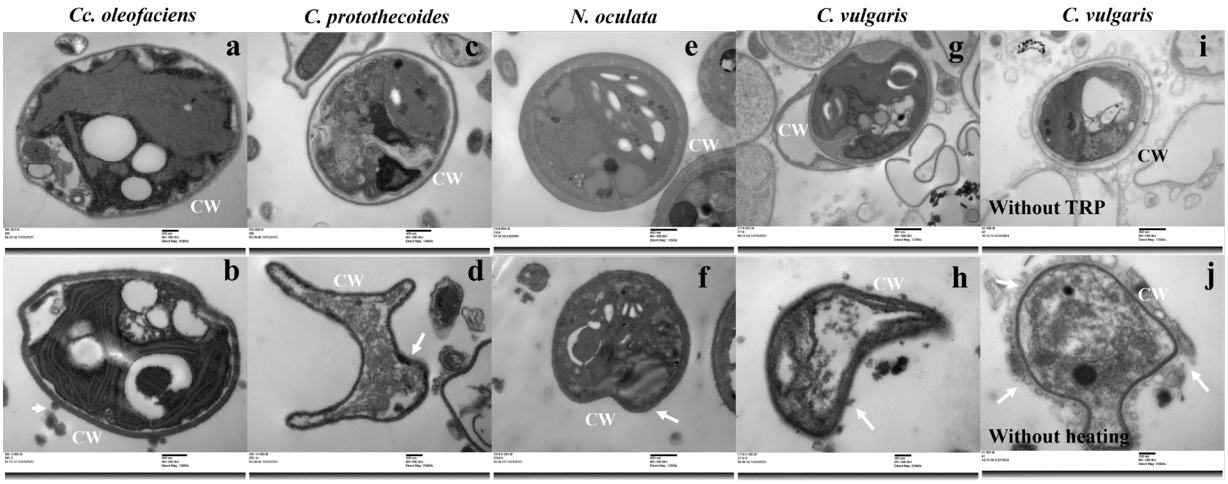

Figure 3.9. Transmission electron micrographs of (a) normal *Cc. oleofaciens* cells, (b) *Cc. oleofaciens* incubated with PNIPAM-300 kDa (32℃ for 30 min), (c) normal *C. protothecoides* cells, (d) *Cc. oleofaciens* incubated with PNIPAM-15 kDa (46℃ for 30 min), (e) normal *N. oculata* cells, (f) *N. oculata* incubated with PNIPAM-100 kDa (31℃ for 30 min), (g) normal *C. vulgaris* cells, (h) *C. vulgaris* incubated with PNIPAM-100 kDa (31℃ for 30 min), (i) *C. vulgaris* incubated at 31℃ for 30 min and (j) *C. vulgaris incubated* incubated with PNIPAM-100 kDa at 25℃ for 30 min. CW denotes the cell wall of algal cells. The arrows show the formation of villi-like structures on the cell wall after harvesting.

3.4. Conclusions

Microalgae harvesting by using thermoresponsive polymers (TRPs) can be a rapid and energy-saving method. The lower critical solution temperature (LCST) of TRPs in the algae cultivation medium was significantly lower than that in water, which made the harvesting easier. Algae harvesting efficiency depended on the molecular weight (MW) and concentration of TRPs as well as algae species (size, cultivation medium, and cell wall composition). Among four algae species, *N. oculata* was the most suitable for harvesting by poly(N-isopropylacrylamide) (PNIPAM), with optimal harvesting occurring with PNIPAM-300 kDa at 100 mg/mL. Harvesting large microalgae cells (e.g., *Cc. oleofaciens*) with TRPs was relatively low-efficient and unnecessary compared to self-sedimentation. Algae with glucosamine as a major cell wall component are more sensitive to the MW of TRPs. PNIPAM modified with amine exhibited reduced efficiency in algae harvesting even after the decrease of the charge-shielding effect caused by the high-salt culture medium, which indicated that electrostatic interaction was not the main mechanism governing algae harvesting by TRPs. The structural analysis of heated PNIPAM suggested that algae cells may be encapsulated by the agglomerated polymers. In addition to rapid harvesting, the viability of algae decreased with wrinkled and vulnerable cell

walls. The red fluorescence of cells treated by TRPs was significantly dimmer than that of untreated cells. These results suggested that all the materials inside the algal cells can potentially be released more easily. This is an important step towards sustainable commercialization of microalgae biorefinery with high return and low energy consumption.

Chapter 4 - Temperature-Induced Algae Harvesting with Grafted Poly(N-isopropylacrylamide)

Abstract

Microalgae biorefinery has a broad spectrum of applications, but the high cost of the algae harvesting process restricts the scale-up of this industry. This work developed a new method for algae harvesting by using grafted poly(N-isopropylacrylamide) (PNIPAM). PNIPAM has a temperature-induced phase change property that can be taken advantage of to capture algae cells in the cultivation medium. Grafting PNIPAM onto some substrate materials (cotton fabric, polyester sheet, polyester fabric and polystyrene flexible sheet) can make the recycling and reuse of PNIPAM more convenient and cost-efficient. The findings showed that PNIPAM-300 kDa grafted on the cotton fabric achieved the highest grafting yield (2.38 ± 0.39 mg/cm^2) and the best algae harvesting efficiency (AHE) ($72.31 \pm 0.56\%$) among all the tested grafted PNIPAM. Allowing the polymer to fully dissolve before heating to initiate algae harvesting significantly enhanced the AHE. Furthermore, PNIPAM-grafted cotton fabrics can be reused over more than 20 cycles before the AHE started decreasing. The grafted PNIPAM on substrate materials is a promising cost-efficient algae harvesting technique to promote the commercialization of microalgae biorefinery.

Keywords: Poly(N-isopropylacrylamide), microalgae harvesting, grafting, bioenergy, substrate material

4.1. Introduction

Biofuels have garnered significant attention due to their renewability and environmental benefits (Sakarika and Kornaros 2019; Thanigaivel et al. 2022; Zhao et al. 2022). Microalgae, in particular, have emerged as a leading source of commercial biofuels owing to their high biomass productivity (Brennan and Owende 2010; Hossain et al. 2019; Moshood et al. 2021). However, several fundamental challenges hinder the commercialization of microalgae biorefining, with the algae biomass harvesting being a major obstacle (Bhatia et al. 2022; Weschler et al. 2014). This difficulty arises from the intrinsic properties of algal cells which are generally small, carry negative surface charges (Moraine et al. 1979), and have a similar density to water (Lavoie and de la Noüe 1987), thus remaining uniformly suspending in the culture medium (Milledge and Heaven 2013). As a result, algal biomass harvesting is typically energy-intensive and time-consuming. To make the scale-up of microalgae biorefinery economically viable, it is essential to develop cost-effective algae harvesting technologies.

The commonly used harvesting methods, such as flocculation, centrifugation, and filtration have their own advantages and disadvantages (Ahmad et al. 2022; Singh et al. 2023). Natural flocculation is low-cost but time-consuming and inefficient (Nurdogan and Oswald 1996; Ortiz et al. 2021). Traditional chemical flocculants are cheap and highly efficient, but they can cause product contamination and/or negative impacts on the environment (Matter et al. 2019). The centrifugation method is fast with high product purity but energy-intensive, thus costly (Najjar and Abu-Shamleh 2020). Filtration is convenient but the filter needs to be replaced frequently. Our previous work has demonstrated a one-pot microalgae harvesting using poly-(N-isopropylacrylamide) (PNIPAM) (Zheng et al. 2015, 2016). PNIPAM is one of the thermos-

responsive polymers, and its solubility can be changed by temperature shift (Doberenz et al. 2020). Below the lower critical solution temperature (LCST), PNIPAM is soluble in water. Once the temperature is above its LCST, PNIPAM undergoes a phase transition and precipitates from solution (Cao et al. 2019; Liu et al. 2022). Such a phase transition process is reversible. In previous studies, when PNIPAM solution was mixed with algae culture medium and heated above the LCST (~32℃), the algal cells would precipitate along with the PNIPAM quickly. This process is energy-efficient, simple to operate, has low capital/operating costs, and does not cause environmental pollution. However, the recycling and reuse of polymers was not mentioned. Although the algal cells and PNIPAM will naturally separate after the temperature drops, this process can be greatly simplified if PNIPAM can be bound to a water-insoluble surface.

PNIPAM has been used to harvest *Chlorococcum oleofaciens*, *Chlorella protothecoides*, *Nannochloropsis oculata*, and *Chlorella vulgaris* in our previous work. Among the tested algae species, *N. oculata* had the best harvesting efficiency, with 75-88% of cells being harvested when using PNIPAM-300 kDa at 5 mg/mL-100 mg/mL. *N. oculata* belongs to the genus *Nannochloropsis* (Hibberd 1981). and has been one of the most studied microalgae species for biofuel production. It has high lipid content, high lipid productivity, fast growth and adaptability to a variety of environments (Ma et al. 2016; Okoro et al. 2019). Also, *N. oculata* is easy to genetically modify and has a desirable fatty acid profile (Su et al. 2011), which makes it a potential renewable energy source (Renaud et al. 1991). An analysis by Fasaei et al. (2018) indicated that harvesting and dewatering dilute systems using flocculants achieved the lowest energy requirements. However, due to flocculant losses, these systems ultimately had the same cost level as mechanical harvesting systems. This suggests the importance of material recycling

and reuse. PNIPAM can be grafted onto the surface of insoluble materials, thus being easily separated from water and recycled.

This work includes 3 objectives: 1): Select the PNIPAM grafting method with the highest grafting yield; 2): Graft PNIPAM onto the surface of different materials to obtain the material with the highest algae harvesting efficiency. 3): Grafted PNIPAM was reused continuously to detect degradation cycles. The results of this study are expected to demonstrate the possibility of a commercially viable microalgae harvesting technology.

4.2. Materials and Methods

4.2.1 Materials

N-isopropylacrylamide (NIPAM), ammonia persulfate (APS), tetramethylethylenediamine (TEMED), and ammonium iron (II) sulfate (Mohr's salt) were purchased from Fisher Scientific (Hampton, NH, USA). The microalga, *Nannochloropsis oculata* (UTEX 2164) culture and the medium (modified artificial seawater medium) were purchased from the Culture Collection of Algae at the University of Texas at Austin (Austin, TX, USA). The medium(UTEX Culture Collection of Algae 2024) were stocked at 4℃ after received until used.

Grafting substrate materials, including cotton fabric purchased from Valengo Fabrics, polyester (PET) sheet from Indstone, polyester fabric from Sedona Designz, and polystyrene (PS) flexible sheet from Mega Format were cut into 5 × 5 cm^2 samples, washed with acetone and water, and subsequently dried in an oven at 60℃ before measured for dry weight.

4.2.2 Polymer grafting

To simplify the recovery of PNIPAM after harvesting algae cells, PNIPAM will be grafted onto the surface of insoluble objects. Several methods and materials have been tested here. PNIPAM was first grafted on cotton fabrics using 3 different grafting methods, and then the method with the highest grafting rate was used for 3 more materials.

Room temperature Grafting: Plasma treatment was conducted on cotton fabric samples by using an atmospheric pressure plasma system (5.0 kHz RF frequency, 30 kV) for 90 s before they were immersed into a NIPAM aqueous solution in a 200-mL glass bottle. The solution was flushed with N_2 for 30 min to remove dissolved oxygen followed by the addition of APS (1g), TEMED (100 μL) and Mohr's salt (90 mg) to initiate the reaction. The glass bottle was sealed and placed at room temperature (RT) for 24 h. The grafted cotton fabric samples were washed by agitating in ultrapure water at RT for 24 h to remove unreacted monomers and un-grafted homopolymers. Then, the samples were dried at 60℃ for 24 h and weighed.

Heated grafting: All the process was same as unheated grafting except that the glass bottle was sealed and placed at 60℃ for 24 h.

Plasma initiated grafting: The cleaned dry cotton fabric samples were treated with atmospheric plasma (5.0 kHz RF frequency, 30 kV) for 90 s and immersed in a 45% NIPAM isopropanol solution followed by a treatment with plasma for 270 s to initiate the grafting. The grafted cotton fabric samples were washed by agitating in ultrapure water at RT for 24 h to remove unreacted monomers and un-grafted homopolymers. The washed samples were finally dried at 60℃ for 24 h and weighed.

The grafting yield of all substrate materials was determined by weighing the samples before and after the grafting. The amount of PNIPAM grafted on the surface of substrate materials was calculated as Eq.4.1:

$$Graft\ yield\ (mg/cm^2) = (W_1 - W_0)/A \qquad \text{(Equation 4.1)}$$

Where W_0 is the weight of dry raw substrate material, W_1 is the weight of dry substrate material with grafted polymers, and A is the substrate material surface area.

Substrate samples before and after grafted with PNIPAM were analyzed on a Fourier Transform Infrared Spectroscopy (FTIR) (PerkinElmer 400, PerkinElmer, CT, USA) on the transmission mode, and the spectra were recorded with 32 scans at a spectral resolution of 4 cm^{-1} in the range 380-4000 cm^{-1}. The surface morphology of substrate samples before and after grafting was visualized by using scanning electron microscopy (SEM) (Hitachi S-3500N, Hitachi, Japan) with 5.00 kV operating voltage.

4.2.3 Algae harvesting

The stock algae culture was scraped from agar slants and transferred to liquid medium to prepare the seed culture, and the optical density of the seed culture was 0.1 at 670 nm (OD_{670}). The seed culture was incubated at RT under the 12-h light/dark cycle and the OD_{670} was monitored every day. Once the OD_{670} reached 0.2, it was transferred to a 500-mL flask, diluted with fresh medium at a 1:5 (v/v) ratio, and incubated under the 12-h light/dark cycles. Meanwhile, the medium was bubbled with humid air at 0.15 liter per minute (LPM) and stirred at 400 rpm with a magnetic stirring bar for 12 days before used for harvesting test.

Algal biomass dry weight (BDW) was determined by filtration with a filter paper (0.22 μm pore size), washing the biomass with deionized (DI) water, and drying at 80°C overnight. BDW was calculated by subtracting the dry weight of the filter paper from the total dry weight of the filter paper and algal biomass.

One-time harvest

Each piece of substrate material with grafted PNIPAM was placed directly into 20 mL algae culture medium and heated to 35°C in a water bath for 30 min. The OD of the algae suspension before and after heating were measured at 430 nm on a microplate reader (BioTek Epoch2, BioTek Instruments Inc., Winooski, VT). The OD values were then converted to biomass dry weight (BDW) using the premade calibration curves (y = 0.52835x + 0.0315, where x is the OD and y is the BDW). The algae harvesting efficiency (AHE) was calculated as Eq. 2:

$$AHE(\%) = \frac{BDW_i - BDW_f}{BDW_i} \times 100\% \qquad \text{(Equation 4.2)}$$

Where BDW_i and BDW_f are the algae BDW before and after heating (mg/L), respectively.

In the subsequent experiments, the polymer was allowed to dissolve for 20 min after placing the grafted material in the algae culture medium, and the rest was the same as above.

Multiple harvests

Each piece of PNIPAM-grafted substrate material was placed into 20 mL algae culture medium for 20 min for the polymer to fully dissolve, and heated to 35°C in a water bath for 30 min. After the substrate material was taken out with harvested algae cells, put it directly into a new 20 mL algae culture medium for 20 min for the polymer to cool down and returned soluble

followed by heating to 35°C for 30 min again, and repeat this process. The OD_{430} values before and after harvesting were measured and converted to BDW. The AHE was also calculated as Eq. 2.

The elution step was added after removing the algae harvested material. The material was grasped with forceps, shaken in clean water for 3 s, and then placed in new medium.

4.2.4 Data analysis

The statistical significance of the collected data was determined with analysis of variance (ANOVA) and least significant difference (LSD) at $\alpha = 0.05$ by using SAS OnDemand for Academics analysis (SAS, NC, USA). All reported values in this study are the average of three replicates, unless specified otherwise.

4.3. Results and Discussion

4.3.1 PNIPAM grafting on fabric substrate materials

The grafting yields of cotton fabrics prepared through the three grafting methods were measured and compared in Figure 4.1a. The PNIPAM-grafted cotton using the heated grafting method achieved the highest grafting yield of 3.25 ± 0.57 mg/cm^2. Generally, the grafting copolymerization is competing with homo-polymerization of PNIPAM. The plasma treatment before grafting helped the copolymerization occur while the heating made homo-polymerization progress easier. The APS added before polymerization is usually used as an initiator, and its persulfate bonds can be broken down to free radicals especially after heating. Therefore, the grafting yield for heated grafting methods is about 12 times higher than that of the RT grafting.

For the plasma-initiated grafting, the cold plasma produced free radicals on the cotton surface, but it restricts the occurrence of homo-polymerization at the same time. Since the heated grafting had a significantly higher grafting yield than other methods, the heated grafting method was used for the following experiments unless specified, otherwise.

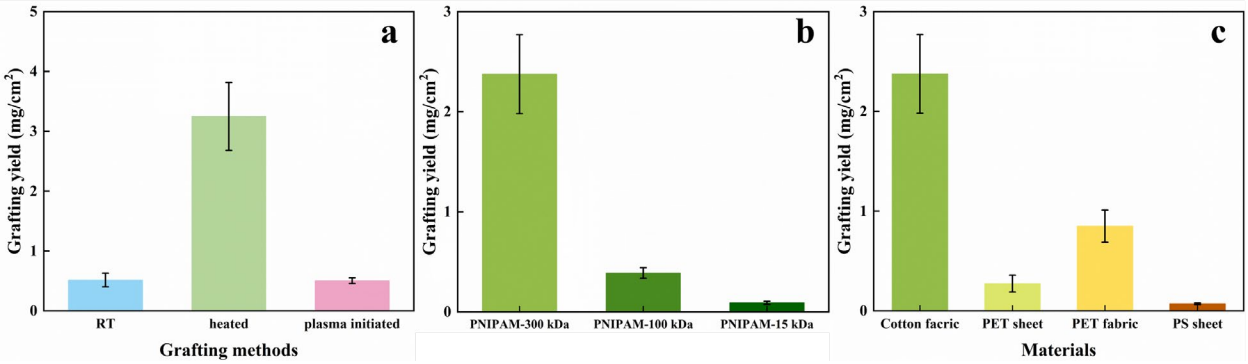

Figure 4.1. Grafting yield of PNIPAM onto cotton by using various methods (a); grafting yield of PNIPAM with various MWs onto cotton (b); grafting yield of PNIPAM-300 kDa onto various substrate materials (c).

PNIPAM of different MWs were grafted on the cotton fabric by using heated grafting method. The MW of PNIPAM was controlled by adjusting the concentration of the NIPAM monomer in solution. Their grafting yields are shown in Figure 4.1b. The PNIPAM with high MW has higher grafting yield. Although atmospheric plasma was used to activate the surface, the grafting of NIPAM onto cotton surfaces was still generally accompanied by the formation of PNIPAM homopolymers. After cold plasma pretreatment, a certain number of sites available for graft copolymerization are provided. In the subsequent grafting reaction, the higher NIPAM concentration is only responsible for homopolymerization, that is, increasing the chain length of the polymer. The grafting yields of PNIPAM-100 kDa and PNIPAM-15 kDa were too low to

achieve the ideal polymer concentration during harvesting. Therefore, PNIPAM-300 kDa was the only PNIPAM used in the following experiments.

Other substrate materials such as PET sheet, PET fabric and PS flexible sheets were also grafted with PNIPAM-300 kDa by using heated grafting method. The graft yields on different substrate materials are presented in Figure 4.1c. PET Fabric had the 2nd highest grafting yield of around 0.85 ± 0.16 mg/cm^3, about one third of the grafting yield of cotton fabric, which could be due to their different chemical structures and/or the interaction between PNIPAM and substrate materials. Cotton has much more C-O and C=O groups, which are susceptible to free radical formation. The grafting yields for both PET sheet and fabric showed significant difference even though both are polyesters. PET fabric had more than three times the grafting yield of PET sheet. This finding could indicate that the fibers are woven in such a way that more functional groups could be exposed and then react with NIPAM. The PS had the lowest yield (0.071 ± 0.008 mg/cm^3) of all four substrate materials. Unlike PET or cotton, PS doesn't have C-O or C=O groups that contribute to the free radical formation. In short, cotton can be grafted with most PNIPAM among four experimental samples, and fabric can be grafted with more PNIPAM than sheet made of the same material.

4.3.2 Characterization of grafted substrate materials

FTIR spectra

The comparison of FTIR spectra for the original and grafted cotton (with different grafting methods) is shown in Figure 4.2a to investigate the success of PNIPAM grafting on cotton. The peaks in the region 3500-3100 cm^{-1} represent the polymeric hydroxyl groups (Sun et al. 2018) in

the spectra for the original cotton (black line), plasma treated cotton (gray line), PNIPAM (blue line), and all the grafted cotton. The peaks observed around 1200-1000 cm^{-1} correspond to the stretching of C-O and C=O groups (Yang et al. 2012). The FTIR spectra for RT grafted cotton (yellow line) were similar to the original cotton (i.e., the difference is too small to be detected by FTIR), which is most likely due to the low grafting yield of this method. The heated grafted cotton (red line), and plasma initiated grafted cotton (green line) show stronger peaks at 1639 cm^{-1} and 1537 cm^{-1} (representing typical amide groups stretch vibrations in PNIPAM chains) than the original cotton, while these two peaks are absent in the plasma treated cotton spectrum. The peak at 2970 cm^{-1} observed in the spectra for PNIPAM, heated grafted cotton and plasma initiated grafted cotton, which is not found for the original cotton, can be attributed to the asymmetric stretching of $-CH_3$ groups in PNIPAM. Nevertheless, the difference between cotton before and after grafting strongly suggests the presence of the PNIPAM on the grafted cotton surface, and the heated grafting results in the highest grafting yield compared to the other two methods.

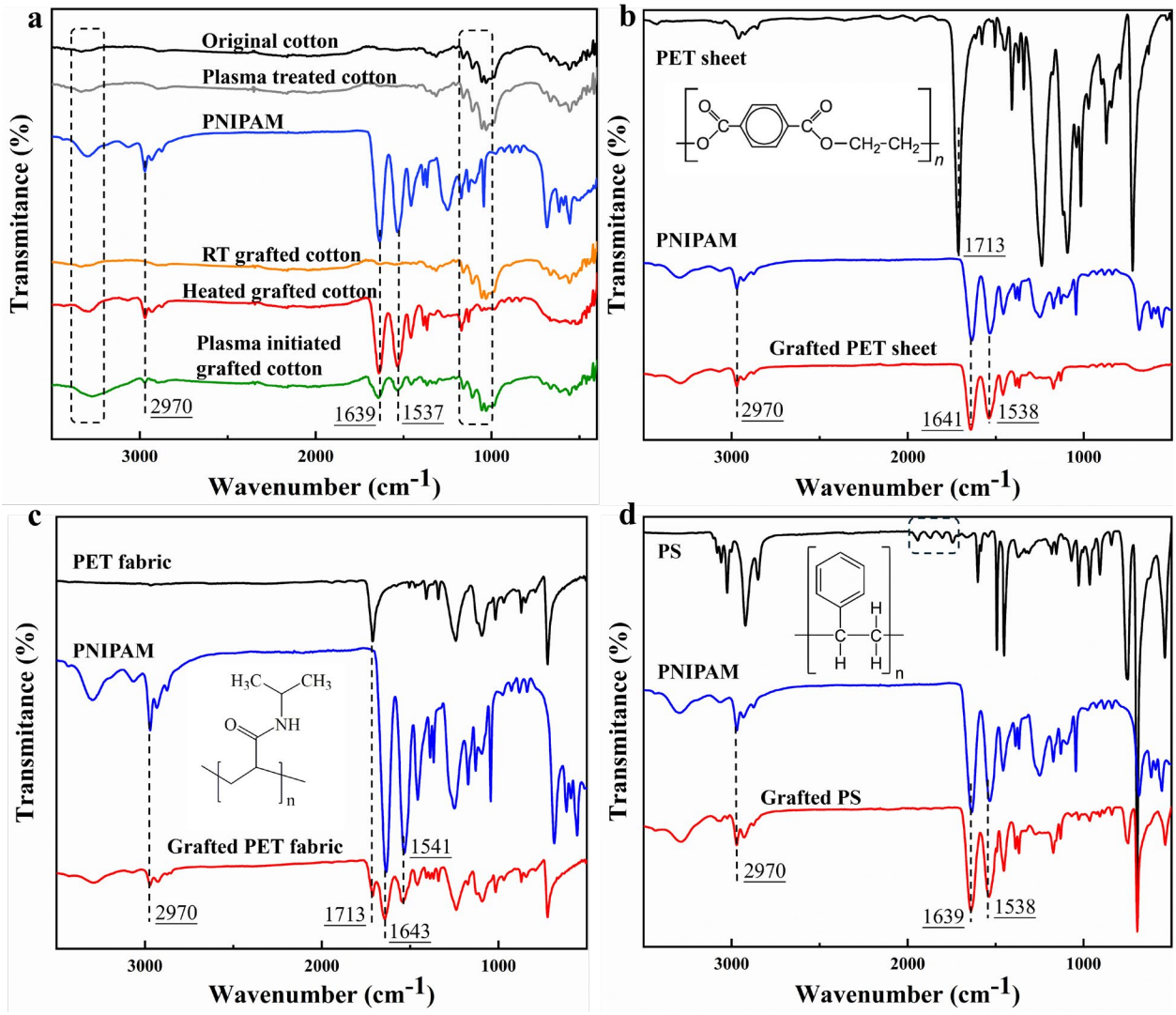

Figure 4.2. FTIR spectra for PNIPAM-grafted cotton fabric (a), PNIPAM-grafted PET sheet (b), PNIPAM-grafted PET fabric (c), and PNIPAM-grafted PS sheet (d).

Furthermore, PNIPAM was grafted on three more substrate materials, PET, PET fabric, and PS. The FTIR spectra for the original PET/PET fabric/PS (black line) and PNIPAM-grafted PET/PET fabric/PS (red line) are demonstrated in Figures 4.2b, 4.2c, and 4.2d. For the black lines in Figures 4.2b and 4.2c, the peak at 1713 cm^{-1} is attributed to the C=O stretching of ester.

This peak disappeared in the grafted PET but still was observed in the grafted PET fabric. The reason for this finding could be that the PET sheet has a smooth surface, and PNIPAM grafted on it completely covered the PET surface, blocking the detection of the peak. As shown in Figure 4.2d for the original PS, a series of peaks were observed in the range of 2000 cm^{-1} to 1700 cm^{-1}, which represents aromatic overtones. The peak around 2970 cm^{-1} is present in the spectra of all grafted substrate materials, indicating the -CH_3 groups in PNIPAM chains. The peaks at around 1640 cm^{-1} and 1540 cm^{-1} suggest the N-H vibrations in PNIPAM. In sum, the differences between the original PET/PET fabric/PS and the PNIPAM-grafted counterparts confirmed the grafting of PNIPAM on the substrate material surfaces.

Scanning electron microscope

SEM analyses were made to investigate the surface morphology change before and after PNIPAM grafting. The SEM image of the original cotton fiber (Figure 4.3a-c) shows a clean and smooth surface, while the cotton fiber with RT grafting (Figure 4.3d-f) has some obvious tentacle-like protrusions, with the diameter ranging from 6 to 7 μm. A much different surface structure was observed for heated grafting cotton fiber (Figure 4.3g-i) where the polymer seems to cover the original cotton fiber. There are obvious mesh structures next to the faintly visible cotton fibers. It should be noticed that these images were collected after freeze-drying, meaning that that this is the state of the polymer in solution. Nevertheless, the heated grafting had much more polymers grafted on cotton fiber than the RT grafting. For the plasma-initiated grafting (Figure 4.3j-l), fine filaments were found on the fabric. The difference in polymer diameter from RT and heated graft may be due to the different volume of monomer solution when the reaction happened. For both RT grafting and heated grafting, the interactions occurred in bottle with

sufficient monomer available. While for plasma-initiated grafting, the cotton fabric was immersed in the monomer solution and then taken out. There was only a small amount of monomer solution (those left on the fabric) that can participate in the reaction during plasma-initiated grafting. Thus, the obvious polymer structure on grafted cotton indicated that PNIPAMs were successfully grafted on the cotton fabric surface through all three grafting methods where the heated grafting achieved the best grafting performance among them.

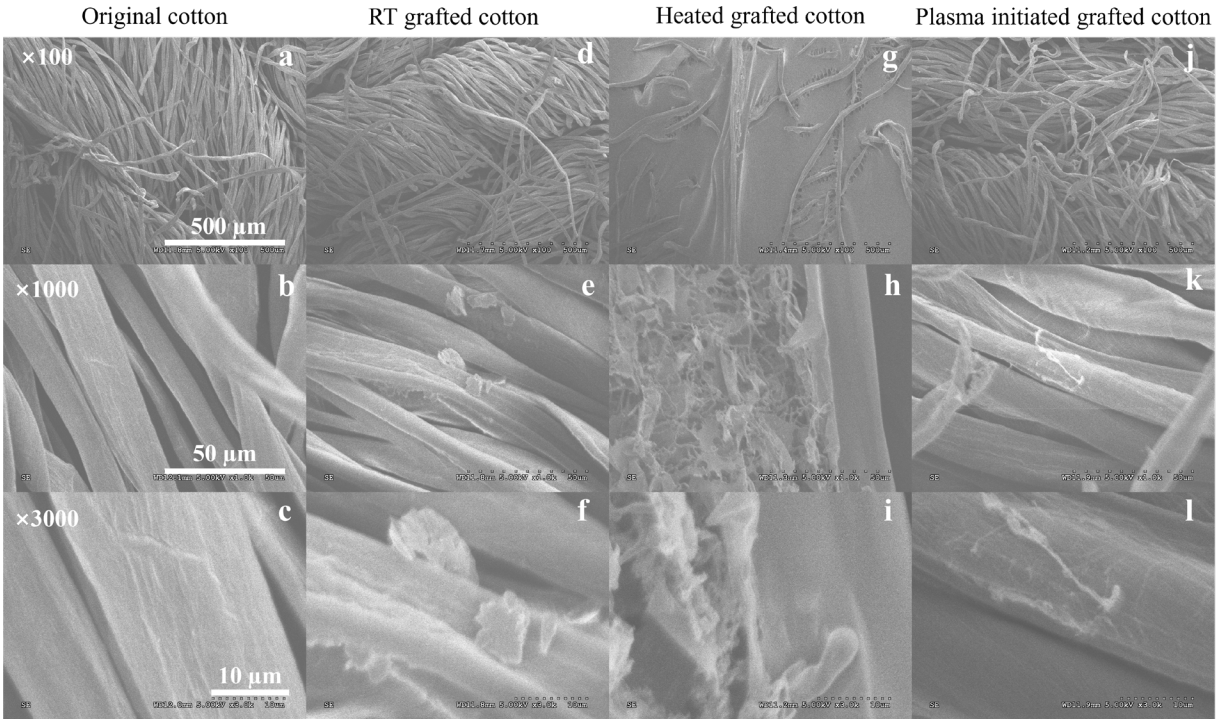

Figure 4.3. SEM images for the original (a-c), RT grafted (d-f), heated grafted (g-i), and plasma initiated grafted (j-l) cotton fabrics. Scale bar: 500 µm for ×100 (a, d, g, j), 50 µm for ×1000 (b, e, h, k), and 10 µm for ×3000 (c, f, I, l).

Surface morphology of the original PET/PET fabric/PS and the PNIPAM-grafted PET/PET fabric/PS have been analyzed through SEM as well. As shown in Figure 4.4, both original PET

sheet (Figure 4.4a) and PET fabric (Figure 4.4c) have clean and smooth surfaces as the original cotton fabric. However, the original PS (Figure 4.4e) shows a certain roughness, which could be due to the acetone prewashing. After grafting with PNIPAM, homogeneous and dense polymer structure were observed on the surface of PET sheet (Figure 4.4b), PET fabric (Figure 4.4d), and PS (Figure 4.4f) while PNIPAM covered the original surface of PET sheet and PS sheet completely. In addition, the polymer was distributed along the fiber on the PET fabric. In sum, SEM images visually proved that PNIPAMs were successfully grafted on PET, PET fabric, and PS surface.

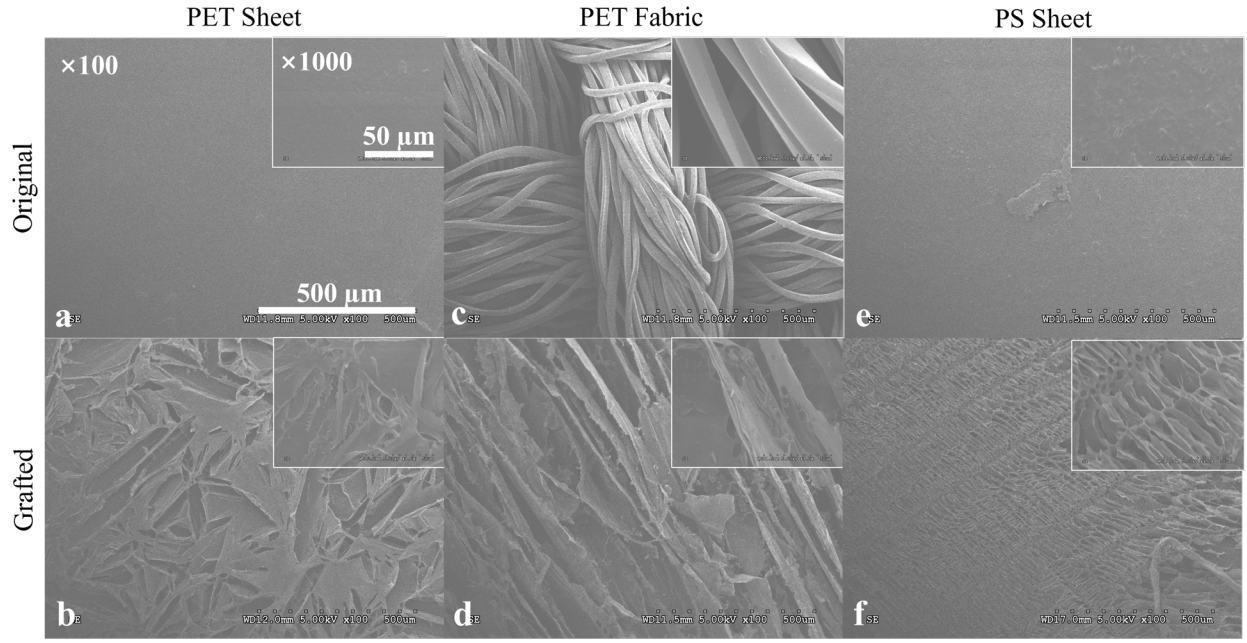

Figure 4.4. SEM images for the original and grafted PET sheet (a-b), PET fabric (c-d), and PS sheet (e-f). Scale bar: 500 µm for ×100 and 50 µm for ×1000.

4.3.3 Microalgae harvesting by using grafted PNIPAM on different substrate

materials

The grafted PNIPAM on cotton fabric and other substrate materials were tested for their ability to harvest algae cells. Each piece of substrate material with grafted PNIPAM was placed in the algae culture medium, followed by heating in a water bath immediately without waiting for PNIPAM to dissolve. Figure 4.5a describes the AHE of PNIPAM-grafted cotton fabric with different MWs. Higher MW polymer grafted on the cotton harvested more algae cells. The highest AHE achieved by PNIPAM-300 kDa was only around 42%, much lower than 90% obtained by bulk polymer from Chapter 3, while PNIPAM-100 kDa and PNIPAM-15 kDa harvested only about 12% and 6% of algae cells in the algae medium, respectively. For PNIPAM-300 kDa grafted on other substrate materials, the AHE was low as well. PNIPAM grafted on PET sheet, PET fabric, and PS sheet harvested only approx. 12%, 19%, and 18% of the algae cells, respectively (Figure 4.5b). This unsatisfactory AHE may be due to the low concentration of polymer in the culture medium. Although the grafting yield is as high as the PNIPAM-300 kDa on cotton fabric, which is 2.38 ± 0.39 mg/cm^2, the final concentration was just about 3 mg/mL. However, 5 mg/mL of bulk PNIPAM-300 kDa dissolved directly in culture medium can get around 75% of the algae cells according to our previous work. So, the extremely low AHE for grafted PNIPAM may also be because the polymer was not fully dissolved. The grafted polymer was immersed directly into the culture medium and then heated immediately. In this case, the polymer may not have enough time to fully unfold in the liquid and contact the cells before phase transition.

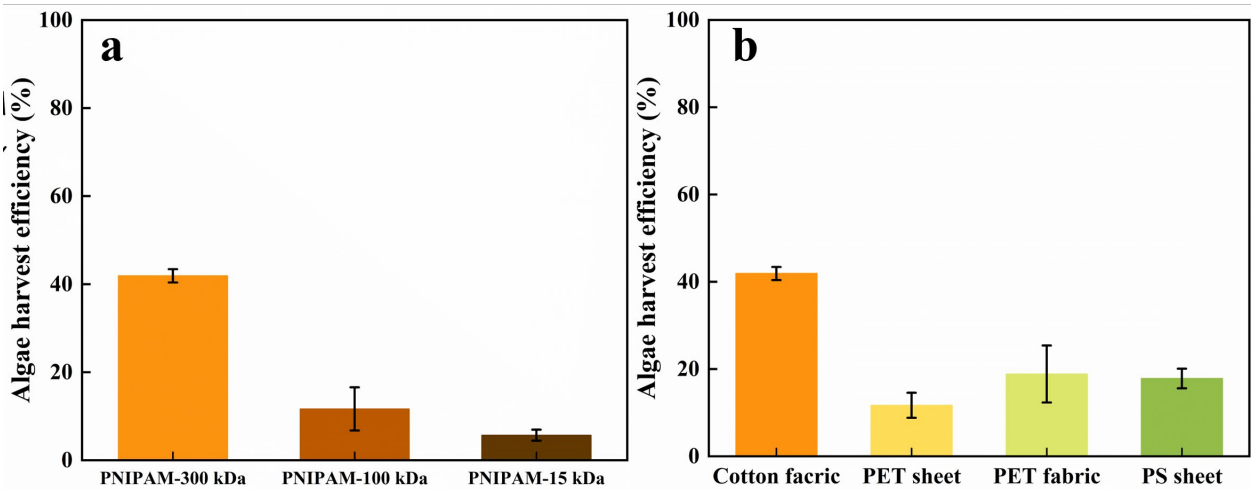

Figure 4.5. Immediate algae harvesting efficiency by using PNIPAM-grafted cotton fabric with different MW (a) and using different substrate materials with grafted PNIPAM (b).

In another algae harvesting scenario, the polymer grafted on the substrate materials was immersed in the culture medium for 20 min until it dissolved before heating. As shown in Figure 4.6, all the AHEs were increased significantly compared to those achieved by immediate heating (as shown in Figure 4.5), which indicates the importance of polymer dissolution in algae harvesting. Of the tested MWs, PNIPAM-300 kDa grafted on the cotton fabric harvested the most algal cells, that was 72.31 ± 0.56% (Figure 4.6a), which is comparable to the AHE (around 75% at 5 mg/mL) for the non-grafted polymer. Such a reduction of the AHE could be caused by the restricted movement of one end of the polymer due to grafting. Under normal conditions, the PNIPAM chains were folded into global. But with one end fixed, the chains are not as flexible as normal. PNIPAM-300 kDa on the PET fabric obtained the second most algae cells, which was 49.64 ± 3.48%, while the PS sheet had the lowest AHE of only 20.58 ± 2.35%. The AHEs for PNIPAM with different MWs and grafted on different substrate materials were consistent with

the trend of PNIPAM grafting yield. The grafting yield reflected the concentration of the polymer in the solution since the grafted polymers were directly submerged into the culture medium. The only exception was that the grafting yield of PNIPAM-15 kDa on cotton cloth was lower than that of PNIAPM-300 kDa on PET sheet, but its AHE was higher. This may be because the structure of the fabric benefited the capture of some algae cells, but the smooth surface of the sheet helped little with algae harvesting. In conclusion, the dissolution of PNIPAM is essential to promote algae harvesting, and PNIPAM-300 kDa grafted on the cotton fabric achieved the highest AHE.

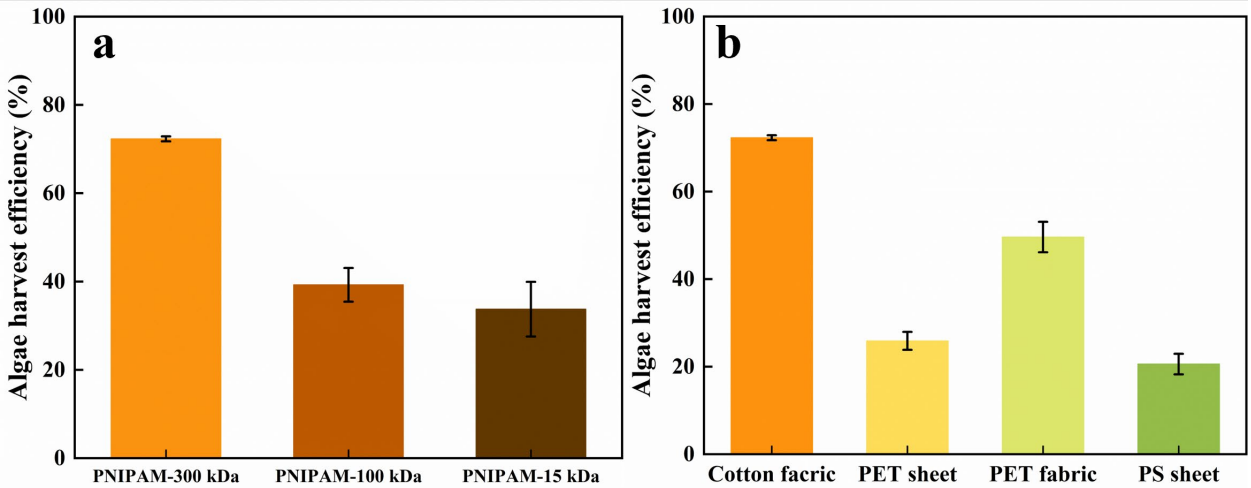

Figure 4.6. Effect of PNIPAM dissolution on algae harvesting efficiency by using PNIPAM-grafted cotton fabric with different MW (a) and using PNIPAM-grafted other materials (b).

The cotton fabric grafted with PNIPAM-300 kDa with the best AHE, was used to study the polymer degradation cycle. The AHE of consecutive harvesting using a single grafted substrate material is shown in Figure 4.7a. After one harvesting, the grafted sample with algal cells was

directly placed into the next algae culture medium. The results showed a continuously decreasing AHE, with only around 10% AHE by the grafted cotton for the tenth cycle. This could mainly be because the AHE was calculated as the BDW ratio between the algae medium before and after harvesting. Continuous harvesting was equivalent to the addition of the algae cells obtained in the previous round to the new batch of culture medium, i.e., the algae concentration kept increasing for subsequent harvesting cycle. However, the ability of PNIPAM to capture algal cells is limited. Assuming that the number of cells harvested each time is the same, as the algae concentration continues to rise, the number of algae cells left in the culture medium will only increase. This leads to higher and higher BDW_f in the calculation, but BDWi remains unchanged, and AHE naturally declined. To eliminate the impact of this situation, a post-harvest elution step was added to the degradation cycle evaluation after each harvesting cycle (Figure 4.7b). As it can be seen from Figure 4.7c, the AHE became much more stable after more than 20 continuous harvesting cycles by adding the elution step. During the first 24 harvesting cycles, the AHE remained around 70% with the maximum of 74.20 ± 0.23%. In actual operation, it was found that the AHE decreased slightly after multiple harvesting cycles in a short period of time, while the AHE returned to the initial level after an overnight rest. After 25 cycles, the AHE had a significant decrease to 63.02 ± 1.43%. The second AHE significant drop to 53.48 ± 1.53% occurred after 27 cycles. Although the AHE rebounded briefly afterwards, it never exceeded 60% again, and the overall trend was still downward. By the 40th cycle, the AHE was only 45.29 ± 0.69%, about 60% of the initial value. In summary, by adding a washing step after each harvesting cycle, the grafted cotton fabric can be used continuously for more than 20 times and extending the rest time between two harvesting cycles is helpful to retain the AHE.

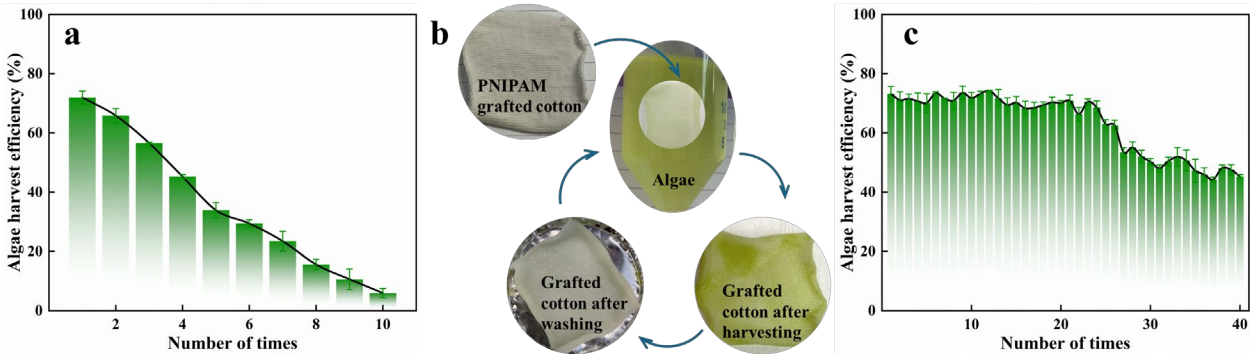

Figure 4.7. Algae harvesting efficiency (AHE) of consecutive harvesting cycles using PNIPAM-300 kDa grafted on cotton fabric (a); Schematic for the improved continuous algae harvesting process using grafted cotton (b); and AHE of consecutive multiple harvest with addition of the elution step (c).

4.4. Conclusions

The temperature-induced phase change behavior of poly-(N-isopropylacrylamide) (PNIPAM) can be used to capture algae cells in the cultivation medium. Cotton fabric, polyester (PET) sheet, PET fabric, and polystyrene flexible sheet were chosen as substrate materials for PNIPAM grafting. The grafting yield was the highest when the substrate materials were first treated with plasma and then reacted at 60°C. The grafting yield of fabric was higher than that of sheets, and cotton fabric had the highest yield, which was 2.38 ± 0.39 mg/cm^2. The microstructure of fabric was more suitable for polymer binding, and the cotton fabric had more active groups than PET fabric. In the application to algae harvesting, it was found that directly immersing the grafted material into the algae culture medium was not sufficient to achieve its full efficacy. The dissolution of the grafted PNIPAM prior to heating to induce phase transition is critical to achieve higher algae harvesting efficiency. Of all the tested substrate materials, PNIPAM-300 kDa grafted on cotton fabric performed the best, and harvested 72.31 ± 0.56%

algae cells. Moreover, the PNIPAM-grafted cotton fabric can be continuously reused for more than 20 times with stable harvesting efficiency. This technique is a new energy-effective method for harvesting algae biomass, and the success of this technique could promote the commercialization of algae biorefinery.

Chapter 5 - Conclusions and recommendations

This thesis presents a comprehensive investigation into the development and application of a novel technique for harvesting algal biomass utilizing thermoresponsive polymers (TRPs). This method is designed to address the complex challenges inherent in microalgae-based biorefineries. The innovative approach demonstrates the potential to achieve low-cost and high efficiency harvesting of algal biomass, thereby advancing the technological landscape of cost-effective algal cell separation. The primary objectives of this study are threefold: (1) to establish the relationship between TRP characteristics and algal harvesting efficiency; (2) to elucidate the fundamental principles underlying the interaction between TRPs and algal cells; and (3) to explore the grafting of polymers onto appropriate substrate surfaces to facilitate large-scale reuse of TRPs.

Reliable and economical harvesting methods for algal biomass are crucial for the viability of microalgae biorefineries. Previous research has indicated that poly(N-isopropylacrylamide) (PNIPAM) and its copolymers can effectively harvest algae; however, their durability and broader applicability (for more algae strains) require further exploration. Additionally, the mechanisms governing the interactions between TRPs and algal cells warrant further investigation.

In this study, TRPs with varying properties were synthesized, and the effects of charge, molecular weight, amine content, and concentration on phase transition behavior were analyzed. At a concentration of 100 mg/mL and a molecular weight of 85 kDa, the lower critical solution temperature (LCST) was observed to reach 30.16 °C. Notably, the LCST of TRPs in algal culture media is significantly lower than that in deionized water, facilitating the harvesting

process. For applications targeting *Chlorella vulgaris*, *Chlorococcum oleofaciens*, *Chlorella protothecoides*, and *Nannochloropsis oculata*, increased molecular weight and concentration correlate with enhanced harvesting efficiency. PNIPAM (300 kDa) achieved over 90% algae harvesting efficiency across all tested strains at a concentration of 100 mg/mL, with *N. oculata* being particularly amenable to PNIPAM-based harvesting. Algae with glucosamine-rich cell walls exhibited greater sensitivity to the molecular weight of TRPs. The rapid harvesting process resulted in the shrinkage and fragility of algal cell walls, suggesting that cellular contents may be more readily released. This advancement represents a significant step toward the sustainable commercialization of microalgae biorefineries, characterized by high returns and low energy consumption.

Furthermore, PNIPAM was grafted onto various substrates, including cotton fabric, PET sheets, PET fabric, and polystyrene sheets. The highest grafting rates were observed when substrates were treated with plasma prior to reaction at 60 °C, with cotton fabric achieving a grafting rate of 2.38 mg/cm². It was determined that direct immersion of the grafted materials into algal culture media was insufficient to maximize harvesting efficiency. Dissolving the grafted PNIPAM prior to heating to induce phase transition was critical for achieving optimal harvesting efficiency. Among all tested substrates, PNIPAM (300 kDa) grafted onto cotton fabric demonstrated superior performance, successfully harvesting 72% of algal cells. Additionally, PNIPAM-grafted cotton fabric exhibited the capability for over 20 reuse cycles while maintaining stable harvesting efficiency.

In conclusion, TRPs such as PNIPAM are capable of harvesting over 90% of algal biomass from culture media across multiple strains. The use of seawater media and glucosamine-rich cell

walls enhances harvesting efficiency. The harvesting mechanism appears to involve the encapsulation of algal cells by aggregated polymer chains. Grafting PNIPAM onto cotton fabric facilitates recycling, allowing for extensive reuse before a decline in harvesting efficiency occurs. This technology represents an energy-efficient method for algal biomass harvesting, with the potential to significantly enhance the commercialization of microalgae biorefineries.

Recommendations for future work:

- It is advisable to expand the range of applicable algal species to include additional genera, which may enhance the versatility and overall effectiveness of the harvesting technique.
- Future research should focus on modifying the thermoresponsive polymer to achieve higher harvesting efficiencies and faster algal harvesting efficiencies, thereby optimizing the process for various applications.
- Conducting a comprehensive economic assessment of this technology is essential to determine its viability and cost-effectiveness in real-world applications, which will support its commercialization.
- Efforts should be made to improve the grafting process of the TRP onto substrate materials to increase the number of reuse cycles, thereby enhancing the sustainability and cost-efficiency of the harvesting method.
- It is important to explore the application of this technology on a larger scale, as this will help to assess its feasibility and performance in industrial settings.

- A thorough evaluation of the extraction process, particularly regarding the degradation of algal cell walls during harvesting, will provide insights into the impacts on cell integrity and product yield.

- Lastly, an analysis of the extraction of downstream products from harvested algal biomass should be undertaken to better understand the overall benefits and potential applications of this harvesting method.

References

Abdelkarim, Omnia H., Rene H. Wijffels, and Maria J. Barbosa. 2024. "Microalgal Lipid Production: A Comparative Analysis of Nannochloropsis and Microchloropsis Strains." *Journal of Applied Phycology*. doi: 10.1007/s10811-024-03318-7.

Ahmad, Muhammad Talba, Mohamed Shariff, Fatimah Md. Yusoff, Yong Meng Goh, and Sanjoy Banerjee. 2020. "Applications of Microalga Chlorella Vulgaris in Aquaculture." *Reviews in Aquaculture* 12(1):328–46. doi: 10.1111/raq.12320.

Ahmad, Shamshad, Kashifa Iqbal, Richa Kothari, Har Mohan Singh, Ahmet Sari, and V. V. Tyagi. 2022. "A Critical Overview of Upstream Cultivation and Downstream Processing of Algae-Based Biofuels: Opportunity, Technological Barriers and Future Perspective." *Journal of Biotechnology* 351:74–98. doi: 10.1016/j.jbiotec.2022.03.015.

Alam, Md. Asraful, Zhongming Wang, and Zhenhong Yuan. 2017. "Generation and Harvesting of Microalgae Biomass for Biofuel Production." Pp. 89–111 in *Prospects and Challenges in Algal Biotechnology*, edited by B. N. Tripathi and D. Kumar. Singapore: Springer.

Al-Hoqani, Umaima, Rosanna Young, and Saul Purton. 2016. "The Biotechnological Potential of Nannochloropsis." *Perspectives in Phycology* 4. doi: 10.1127/pip/2016/0065.

Amer, Luke, Birendra Adhikari, and John Pellegrino. 2011. "Technoeconomic Analysis of Five Microalgae-to-Biofuels Processes of Varying Complexity." *Bioresource Technology* 102(20):9350–59. doi: 10.1016/j.biortech.2011.08.010.

Ammar, Saad H., Hussein J. Khadim, and Ahmed Isam Mohamed. 2018. "Cultivation of

Nannochloropsis Oculata and *Isochrysis Galbana* Microalgae in Produced Water for Bioremediation and Biomass Production." *Environmental Technology & Innovation* 10:132–42. doi: 10.1016/j.eti.2018.02.002.

Anbuchezhian, Ramasamy, Valliappan Karuppiah, and Zhiyong Li. 2015. "Prospect of Marine Algae for Production of Industrially Important Chemicals." Pp. 195–217 in *Algal Biorefinery: An Integrated Approach*, edited by D. Das. Cham: Springer International Publishing.

Arora, Neha, Enlin Lo, and George P. Philippidis. 2022. "A Two-Prong Mutagenesis and Adaptive Evolution Strategy to Enhance the Temperature Tolerance and Productivity of *Nannochloropsis Oculata*." *Bioresource Technology* 364:128101. doi: 10.1016/j.biortech.2022.128101.

Bansfield, Danielle, Kristian Spilling, Anna Mikola, and Jonna Piiparinen. 2022. "Bioflocculation of Euglena Gracilis via Direct Application of Fungal Filaments: A Rapid Harvesting Method." *Journal of Applied Phycology* 34(1):321–34. doi: 10.1007/s10811-021-02651-5.

Bayat Tork, Mahya, Rasoul Khalilzadeh, and Hasan Kouchakzadeh. 2017. "Efficient Harvesting of Marine *Chlorella Vulgaris* Microalgae Utilizing Cationic Starch Nanoparticles by Response Surface Methodology." *Bioresource Technology* 243:583–88. doi: 10.1016/j.biortech.2017.06.181.

Bhatia, Latika, Rakesh K. Bachheti, Vijay Kumar Garlapati, and Anuj K. Chandel. 2022. "Third-Generation Biorefineries: A Sustainable Platform for Food, Clean Energy, and

Nutraceuticals Production." *Biomass Conversion and Biorefinery* 12(9):4215–30. doi: 10.1007/s13399-020-00843-6.

Bhatt, Ankita, Mitali Khanchandani, Mohit Singh Rana, and Sanjeev Kumar Prajapati. 2022. "Techno-Economic Analysis of Microalgae Cultivation for Commercial Sustainability: A State-of-the-Art Review." *Journal of Cleaner Production* 370:133456. doi: 10.1016/j.jclepro.2022.133456.

Bischofberger, Irmgard, Davide. CE Calzolari, and Veronique Trappe. 2014. "Co-Nonsolvency of PNiPAM at the Transition between Solvation Mechanisms." *Soft Matter* 10(41):8288–95. doi: 10.1039/C4SM01345J.

Bold, Harold C. 1949. "The Morphology of Chlamydomonas Chlamydogama, Sp. Nov." *Bulletin of the Torrey Botanical Club* 76(2):101–8. doi: 10.2307/2482218.

Borowitzka, Michael A. 1995. "Microalgae as Sources of Pharmaceuticals and Other Biologically Active Compounds." *Journal of Applied Phycology* 7(1):3–15. doi: 10.1007/BF00003544.

Borowitzka, Michael A. 2013. "High-Value Products from Microalgae—Their Development and Commercialisation." *Journal of Applied Phycology* 25(3):743–56. doi: 10.1007/s10811-013-9983-9.

Branco-Vieira, Monique, Teresa M. Mata, Antonio A. Martins, Marcos Aurelio Vasconcelos de Freitas, and Nídia S. Caetano. 2020. "Economic Analysis of Microalgae Biodiesel Production in a Small-Scale Facility." *Energy Reports* 6:325–32. doi:

10.1016/j.egyr.2020.11.156.

Brennan, Liam, and Philip Owende. 2010. “Biofuels from Microalgae—A Review of Technologies for Production, Processing, and Extractions of Biofuels and Co-Products.” *Renewable and Sustainable Energy Reviews* 14(2):557–77. doi: 10.1016/j.rser.2009.10.009.

Caetano, Nídia S., Antonio A. Martins, Malihe Gorgich, Daniel Medina Gutiérrez, Thiago J. Ribeiro, and Teresa M. Mata. 2020. “Flocculation of Arthrospira Maxima for Improved Harvesting.” *Energy Reports* 6:423–28. doi: 10.1016/j.egyr.2019.08.083.

Candido, Camila, and Ana Teresa Lombardi. 2017. “Growth of Chlorella Vulgaris in Treated Conventional and Biodigested Vinasses.” *Journal of Applied Phycology* 29(1):45–53. doi: 10.1007/s10811-016-0940-2.

Cao, Meiwen, Yu Wang, Xuzhi Hu, Haoning Gong, Ruiheng Li, Henry Cox, Jing Zhang, Thomas A. Waigh, Hai Xu, and Jian Ren Lu. 2019. “Reversible Thermoresponsive Peptide–PNIPAM Hydrogels for Controlled Drug Delivery.” *Biomacromolecules* 20(9):3601–10. doi: 10.1021/acs.biomac.9b01009.

Cha, Kwang Hyun, Hee Ju Lee, Song Yi Koo, Dae-Geun Song, Dong-Un Lee, and Cheol-Ho Pan. 2010. “Optimization of Pressurized Liquid Extraction of Carotenoids and Chlorophylls from Chlorella Vulgaris.” *Journal of Agricultural and Food Chemistry* 58(2):793–97. doi: 10.1021/jf902628j.

Chatsungnoen, Tawan, and Yusuf Chisti. 2019. “Chapter 11 - Flocculation and

Electroflocculation for Algal Biomass Recovery." Pp. 257–86 in *Biofuels from Algae (Second Edition)*, *Biomass, Biofuels, Biochemicals*, edited by A. Pandey, J.-S. Chang, C. R. Soccol, D.-J. Lee, and Y. Chisti. Elsevier.

Chen, Jie, Lijian Leng, Chensong Ye, Qian Lu, Min Addy, Jinghan Wang, Jin Liu, Paul Chen, Roger Ruan, and Wenguang Zhou. 2018. "A Comparative Study between Fungal Pellet- and Spore-Assisted Microalgae Harvesting Methods for Algae Bioflocculation." *Bioresource Technology* 259:181–90. doi: 10.1016/j.biortech.2018.03.040.

Chew, Kit Wayne, Shir Reen Chia, Pau Loke Show, Tau Chuan Ling, Shalini S. Arya, and Jo-Shu Chang. 2018. "Food Waste Compost as an Organic Nutrient Source for the Cultivation of *Chlorella Vulgaris*." *Bioresource Technology* 267:356–62. doi: 10.1016/j.biortech.2018.07.069.

Chisti, Yusuf. 2007. "Biodiesel from Microalgae." *Biotechnology Advances* 25(3):294–306. doi: 10.1016/j.biotechadv.2007.02.001.

Chisti, Yusuf. 2013. "Constraints to Commercialization of Algal Fuels." *Journal of Biotechnology* 167(3):201–14. doi: 10.1016/j.jbiotec.2013.07.020.

Chisti, Yusuf. 2018. "Chapter 2 - Society and Microalgae: Understanding the Past and Present." Pp. 11–21 in *Microalgae in Health and Disease Prevention*, edited by I. A. Levine and J. Fleurence. Academic Press.

Choi, Yun-Nam, Hyun Uk Cho, Joseph Christian Utomo, Dong Yoon Shin, Hye Kyung Kim, and Jong Moon Park. 2016. "Efficient Harvesting of Synechocystis Sp. PCC 6803 with

Filamentous Fungal Pellets." *Journal of Applied Phycology* 28(4):2225–31. doi: 10.1007/s10811-015-0787-y.

Chu, Ruoyu, Shuangxi Li, Liandong Zhu, Zhihong Yin, Dan Hu, Chenchen Liu, and Fan Mo. 2021. "A Review on Co-Cultivation of Microalgae with Filamentous Fungi: Efficient Harvesting, Wastewater Treatment and Biofuel Production." *Renewable and Sustainable Energy Reviews* 139:110689. doi: 10.1016/j.rser.2020.110689.

Chua, Elvis T., and Peer M. Schenk. 2017. "A Biorefinery for *Nannochloropsis*: Induction, Harvesting, and Extraction of EPA-Rich Oil and High-Value Protein." *Bioresource Technology* 244:1416–24. doi: 10.1016/j.biortech.2017.05.124.

Coronado-Reyes, Jesús Alberto, Juan Alfonso Salazar-Torres, Beatriz Juárez-Campos, and Juan Carlos González-Hernández. 2020. "*Chlorella Vulgaris,* a Microalgae Important to Be Used in Biotechnology: A Review." *Food Science and Technology* 42:e37320. doi: 10.1590/fst.37320.

Cruz, Megan A., Daniel L. Morris, John P. Swanson, Mangaldeep Kundu, Steven G. Mankoci, Thomas C. Leeper, and Abraham Joy. 2018. "Efficient Protein Encapsulation within Thermoresponsive Coacervate-Forming Biodegradable Polyesters." *ACS Macro Letters* 7(4):477–81. doi: 10.1021/acsmacrolett.8b00118.

Danquah, Michael K., Brendan Gladman, Navid Moheimani, and Gareth M. Forde. 2009. "Microalgal Growth Characteristics and Subsequent Influence on Dewatering Efficiency." *Chemical Engineering Journal* 151(1):73–78. doi: 10.1016/j.cej.2009.01.047.

Deckers, Marie, Dieter Deforce, Marie-Alice Fraiture, and Nancy H. C. Roosens. 2020. "Genetically Modified Micro-Organisms for Industrial Food Enzyme Production: An Overview." *Foods* 9(3):326. doi: 10.3390/foods9030326.

Del Río, Esperanza, Elena García-Gómez, José Moreno, Miguel G. Guerrero, and Mercedes García-González. 2017. "Microalgae for Oil. Assessment of Fatty Acid Productivity in Continuous Culture by Two High-Yield Strains, *Chlorococcum Oleofaciens* and *Pseudokirchneriella Subcapitata*." *Algal Research* 23:37–42. doi: 10.1016/j.algal.2017.01.003.

Díaz-Santos, Encarnación, Marta Vila, Marta de la Vega, Rosa León, and Javier Vigara. 2015. "Study of Bioflocculation Induced by *Saccharomyces Bayanus* Var. *Uvarum* and Flocculating Protein Factors in Microalgae." *Algal Research* 8:23–29. doi: 10.1016/j.algal.2014.12.013.

Doberenz, Falko, Kui Zeng, Christian Willems, Kai Zhang, and Thomas Groth. 2020. "Thermoresponsive Polymers and Their Biomedical Application in Tissue Engineering – a Review." *Journal of Materials Chemistry B* 8(4):607–28. doi: 10.1039/C9TB02052G.

Du, Hongbo, Ranil Wickramasinghe, and Xianghong Qian. 2010. "Effects of Salt on the Lower Critical Solution Temperature of Poly (N-Isopropylacrylamide)." *The Journal of Physical Chemistry B* 114(49):16594–604. doi: 10.1021/jp105652c.

Dubini, Alexandra, and David Gonzalez-Ballester. 2016. "Biohydrogen from Microalgae." Pp. 165–93 in *Algae Biotechnology: Products and Processes*, edited by F. Bux and Y. Chisti. Cham: Springer International Publishing.

Elkelawy, Medhat, Hagar Alm-Eldin Bastawissi, E. A. El Shenawy, Mohammed Taha, Hitesh Panchal, and Kishor Kumar Sadasivuni. 2021. “Study of Performance, Combustion, and Emissions Parameters of DI-Diesel Engine Fueled with Algae Biodiesel/Diesel/n-Pentane Blends.” *Energy Conversion and Management: X* 10:100058. doi: 10.1016/j.ecmx.2020.100058.

Endo, Hiroshi. 1977. “Growth Yields of Chlorella Regularis in Dark-Heterotrophic Continuous Cultures Using Acetate : Studies on Chlorella Regularis, Heterotrophic Fast-Growing Strain (III) :” *Journal of Fermentation Technology* 55(4):369–79.

Ettl, Hanuš, and Georg Gärtner. 2013. *Syllabus der Boden-, Luft- und Flechtenalgen*. Springer-Verlag.

Farooq, Wasif, Myounghoon Moon, Byung-gon Ryu, William I. Suh, Anupama Shrivastav, Min S. Park, Sanjiv K. Mishra, and Ji-Won Yang. 2015. “Effect of Harvesting Methods on the Reusability of Water for Cultivation of Chlorella Vulgaris, Its Lipid Productivity and Biodiesel Quality.” *Algal Research* 8:1–7. doi: 10.1016/j.algal.2014.12.007.

Fasaei, Farnoosh, Johannes Hendrik Bitter, Petronella Margaretha Slegers, and Anton J. B. Van Boxtel. 2018. “Techno-Economic Evaluation of Microalgae Harvesting and Dewatering Systems.” *Algal Research* 31:347–62. doi: 10.1016/j.algal.2017.11.038.

Gallardo-Rodríguez, J., A. Sánchez-Mirón, F. García-Camacho, L. López-Rosales, Y. Chisti, and E. Molina-Grima. 2012. “Bioactives from Microalgal Dinoflagellates.” *Biotechnology Advances* 30(6):1673–84. doi: 10.1016/j.biotechadv.2012.07.005.

Gantar, Miroslav, and Zorica Svirčev. 2008. “Microalgae and Cyanobacteria: Food for Thought.” *Journal of Phycology* 44(2):260–68. doi: 10.1111/j.1529-8817.2008.00469.x.

Gatenby, Robert A. 2019. “The Role of Cell Membrane Information Reception, Processing, and Communication in the Structure and Function of Multicellular Tissue.” *International Journal of Molecular Sciences* 20(15):3609. doi: 10.3390/ijms20153609.

Gendy, Tahani S., and Seham A. El-Temtamy. 2013. “Commercialization Potential Aspects of Microalgae for Biofuel Production: An Overview.” *Egyptian Journal of Petroleum* 22(1):43–51. doi: 10.1016/j.ejpe.2012.07.001.

Gerardo, Michael L., Sofie Van Den Hende, Han Vervaeren, Thea Coward, and Stephen C. Skill. 2015. “Harvesting of Microalgae within a Biorefinery Approach: A Review of the Developments and Case Studies from Pilot-Plants.” *Algal Research* 11:248–62. doi: 10.1016/j.algal.2015.06.019.

Ghernaout, Djamel, Noureddine Elboughdiri, Saad Ghareba, and Alsamani Salih. 2020. “Coagulation Process for Removing Algae and Algal Organic Matter—An Overview.” *Open Access Library Journal* 7(4):1–21. doi: 10.4236/oalib.1106272.

González, Luz Estela, Rosa Olivia Cañizares, and Sandra Baena. 1997. “Efficiency of Ammonia and Phosphorus Removal from a Colombian Agroindustrial Wastewater by the Microalgae *Chlorella Vulgaris* and *Scenedesmus Dimorphus*.” *Bioresource Technology* 60(3):259–62. doi: 10.1016/S0960-8524(97)00029-1.

Gouveia, Luísa, Anabela Raymundo, Ana Paula Batista, Isabel Sousa, and José Empis. 2006.

"Chlorella Vulgaris and Haematococcus Pluvialis Biomass as Colouring and Antioxidant in Food Emulsions." *European Food Research and Technology* 222(3):362–67. doi: 10.1007/s00217-005-0105-z.

Gutarowska, Beata, and Agata Czyżowska. 2009. "The Ability of Filamentous Fungi to Produce Acids on Indoor Building Materials." *Annals of Microbiology* 59(4):807–13. doi: 10.1007/BF03179227.

Hajinajaf, Nima, Abbas Mehrabadi, and Omid Tavakoli. 2021. "Practical Strategies to Improve Harvestable Biomass Energy Yield in Microalgal Culture: A Review." *Biomass and Bioenergy* 145:105941. doi: 10.1016/j.biombioe.2020.105941.

Halim, Ronald, Brendan Gladman, Michael K. Danquah, and Paul A. Webley. 2011. "Oil Extraction from Microalgae for Biodiesel Production." *Bioresource Technology* 102(1):178–85. doi: 10.1016/j.biortech.2010.06.136.

Harun, Razif, Jason W. S. Yip, Selvakumar Thiruvenkadam, Wan A. W. A. K. Ghani, Tamara Cherrington, and Michael K. Danquah. 2014. "Algal Biomass Conversion to Bioethanol – a Step-by-Step Assessment." *Biotechnology Journal* 9(1):73–86. doi: 10.1002/biot.201200353.

Heasman, M., J. Diemar, W. O'connor, T. Sushames, and L. Foulkes. 2000. "Development of Extended Shelf-Life Microalgae Concentrate Diets Harvested by Centrifugation for Bivalve Molluscs – a Summary." *Aquaculture Research* 31(8–9):637–59. doi: 10.1046/j.1365-2109.2000.318492.x.

Henderson, Rita, Simon A. Parsons, and Bruce Jefferson. 2008. “The Impact of Algal Properties and Pre-Oxidation on Solid–Liquid Separation of Algae.” *Water Research* 42(8):1827–45. doi: 10.1016/j.watres.2007.11.039.

Heredia-Arroyo, Tamarys, Wei Wei, and Bo Hu. 2010. “Oil Accumulation via Heterotrophic/Mixotrophic Chlorella Protothecoides.” *Applied Biochemistry and Biotechnology* 162(7):1978–95. doi: 10.1007/s12010-010-8974-4.

Hibberd, David J. 1981. “Notes on the Taxonomy and Nomenclature of the Algal Classes Eustigmatophyceae and Tribophyceae (Synonym Xanthophyceae).” *Botanical Journal of the Linnean Society* 82(2):93–119. doi: 10.1111/j.1095-8339.1981.tb00954.x.

Hogan, Katie J., and Antonios G. Mikos. 2020. “Biodegradable Thermoresponsive Polymers: Applications in Drug Delivery and Tissue Engineering.” *Polymer* 211:123063. doi: 10.1016/j.polymer.2020.123063.

Hossain, Nazia, Teuku Meurah Indra Mahlia, and Rahman Saidur. 2019. “Latest Development in Microalgae-Biofuel Production with Nano-Additives.” *Biotechnology for Biofuels* 12(1):125. doi: 10.1186/s13068-019-1465-0.

Huo, Shuhao, Zhongming Wang, Shunni Zhu, Fengjie Cui, Bin Zou, Wenhua You, Zhenhong Yuan, and Renjie Dong. 2014. “Optimization of Alkaline Flocculation for Harvesting of Scenedesmus Quadricauda #507 and Chaetoceros Muelleri #862.” *Energies* 7(9):6186–95. doi: 10.3390/en7096186.

Huss, Volker A. R., Richard Dörr, Ulrike Grossmann, and Erich Kessler. 1986.

"Deoxyribonucleic Acid Reassociation in the Taxonomy of the Genus Chlorella." *Archives of Microbiology* 145(5):329–33. doi: 10.1007/BF00470866.

Hussian, Mohamed, and Abd Ellatif. 2018. "The Role of Microalgae in Renewable Energy Production: Challenges and Opportunities." doi: 10.5772/intechopen.73573.

Inomata, Hiroshi, Shuichi Goto, and Shozaburo Saito. 1990. "Phase Transition of N-Substituted Acrylamide Gels." *Macromolecules* 23(22):4887–88. doi: 10.1021/ma00224a023.

Japar, Azima Syafaini, Nur Mutmainnah Azis, Mohd Sobri Takriff, and Nazlina Haiza Mohd Yasin. 2017. "Application of Different Techniques to Harvest Microalgae." *Transactions on Science and Technology* 4(2):98–108.

Javed, Fahed, Muhammad Aslam, Naim Rashid, Zufishan Shamair, Asim Laeeq Khan, Muhammad Yasin, Tahir Fazal, Ainy Hafeez, Fahad Rehman, Muhammad Saif Ur Rehman, Zakir Khan, Javed Iqbal, and Aqeel Ahmed Bazmi. 2019. "Microalgae-Based Biofuels, Resource Recovery and Wastewater Treatment: A Pathway towards Sustainable Biorefinery." *Fuel* 255:115826. doi: 10.1016/j.fuel.2019.115826.

Kagan, Michael L., and Ray A. Matulka. 2015. "Safety Assessment of the Microalgae *Nannochloropsis Oculata*." *Toxicology Reports* 2:617–23. doi: 10.1016/j.toxrep.2015.03.008.

Kawasaki, Yuriko, Takashi Nakada, and Masaru Tomita. 2015. "Taxonomic Revision of Oil-Producing Green Algae, Chlorococcum Oleofaciens (Volvocales, Chlorophyceae), and Its Relatives." *Journal of Phycology* 51(5):1000–1016. doi: 10.1111/jpy.12343.

Kay, Robert A., and Larry L. Barton. 1991. “Microalgae as Food and Supplement.” *Critical Reviews in Food Science and Nutrition* 30(6):555–73. doi: 10.1080/10408399109527556.

Kent, Megan, Heather M. Welladsen, Arnold Mangott, and Yan Li. 2015. “Nutritional Evaluation of Australian Microalgae as Potential Human Health Supplements.” *PLOS ONE* 10(2):e0118985. doi: 10.1371/journal.pone.0118985.

Kim, Dong-Yeon, Kyubock Lee, Jiye Lee, Young-Hee Lee, Jong-In Han, Ji-Yeon Park, and You-Kwan Oh. 2017. “Acidified-Flocculation Process for Harvesting of Microalgae: Coagulant Reutilization and Metal-Free-Microalgae Recovery.” *Bioresource Technology* 239:190–96. doi: 10.1016/j.biortech.2017.05.021.

Krishnamoorthy, Nageshwari, Yuwalee Unpaprom, Rameshprabu Ramaraj, Gaanty Pragas Maniam, Natanamurugaraj Govindan, Thirugnanam Arunachalam, and Balasubramanian Paramasivan. 2021. “Recent Advances and Future Prospects of Electrochemical Processes for Microalgae Harvesting.” *Journal of Environmental Chemical Engineering* 9(5):105875. doi: 10.1016/j.jece.2021.105875.

Kumar, Adepu K., Shaishav Sharma, Aesha Patel, Gaurav Dixit, and Ekta Shah. 2019. “Comprehensive Evaluation of Microalgal Based Dairy Effluent Treatment Process for Clean Water Generation and Other Value Added Products.” *International Journal of Phytoremediation* 21(6):519–30. doi: 10.1080/15226514.2018.1537248.

Kumar, Niwas, Chiranjib Banerjee, Sangeeta Negi, and Pratyoosh Shukla. 2023. “Microalgae Harvesting Techniques: Updates and Recent Technological Interventions.” *Critical Reviews in Biotechnology* 43(3):342–68. doi: 10.1080/07388551.2022.2031089.

Kwon, Hyuckjin, Mingshou Lu, Eun Yeol Lee, and Jinwon Lee. 2014. “Harvesting of Microalgae Using Flocculation Combined with Dissolved Air Flotation.” *Biotechnology and Bioprocess Engineering* 19(1):143–49. doi: 10.1007/s12257-013-0433-y.

Lavoie, Alain, and J. de la Noüe. 1987. “Harvesting of Scenedesmus Obliquus in Wastewaters: Auto- or Bioflocculation?” *Biotechnology and Bioengineering* 30(7):852–59. doi: 10.1002/bit.260300707.

Lee, Jimin, Dae-Hyun Cho, Rishiram Ramanan, Byung-Hyuk Kim, Hee-Mock Oh, and Hee-Sik Kim. 2013. “Microalgae-Associated Bacteria Play a Key Role in the Flocculation of *Chlorella Vulgaris*.” *Bioresource Technology* 131:195–201. doi: 10.1016/j.biortech.2012.11.130.

Lee, Young-Chul, Bohwa Kim, Wasif Farooq, Jane Chung, Jong-In Han, Hyun-Jae Shin, Sang Hwa Jeong, Ji-Yeon Park, Jin-Suk Lee, and You-Kwan Oh. 2013. “Harvesting of Oleaginous Chlorella Sp. by Organoclays.” *Bioresource Technology* 132:440–45. doi: 10.1016/j.biortech.2013.01.102.

Lee, Yuan-Kun. 1997. “Commercial Production of Microalgae in the Asia-Pacific Rim.” *Journal of Applied Phycology* 9(5):403–11. doi: 10.1023/A:1007900423275.

Li, Gang, Zhitao Lu, Jiang Zhang, Huan Li, Yuguang Zhou, Ali Mohammed Ibrahim Zayan, and Zhigang Huang. 2020. “Life Cycle Assessment of Biofuel Production from Microalgae Cultivated in Anaerobic Digested Wastewater.” *International Journal of Agricultural and Biological Engineering* 13(1):241–46. doi: 10.25165/j.ijabe.20201301.4178.

Li, Shuangxi, Tianyi Hu, Yanzhe Xu, Jingyi Wang, Ruoyu Chu, Zhihong Yin, Fan Mo, and Liandong Zhu. 2020. “A Review on Flocculation as an Efficient Method to Harvest Energy Microalgae: Mechanisms, Performances, Influencing Factors and Perspectives.” *Renewable and Sustainable Energy Reviews* 131:110005. doi: 10.1016/j.rser.2020.110005.

Li, Tianrui, Jiangjun Hu, and Liandong Zhu. 2021. “Self-Flocculation as an Efficient Method to Harvest Microalgae: A Mini-Review.” *Water* 13(18):2585. doi: 10.3390/w13182585.

Li, Yi, Yanting Xu, Lei Liu, Ping Li, Yue Yan, Tong Chen, Tianling Zheng, and Hailei Wang. 2017. “Flocculation Mechanism of *Aspergillus Niger* on Harvesting of *Chlorella Vulgaris* Biomass.” *Algal Research* 25:402–12. doi: 10.1016/j.algal.2017.06.001.

Li, Yuqin, Yuanyuan Luo, Rong Zhou, Xiaohong Zuo, Yong Zhang, Zhenyao Wang, Xuan Li, Xing Zhang, Zihao Qin, and Carol Sze Ki Lin. 2024. “Coculture of *Chlorella Protothecoides* and *Coccomyxa Subellipsoidea* Enhances Cell Growth and Lipid Accumulation: An Effective Strategy for Biodiesel Production.” *Chemical Engineering Journal* 486:150302. doi: 10.1016/j.cej.2024.150302.

Lin, Weizhong, Lining Chen, Zexing Tan, Zhenqi Deng, and Hui Liu. 2022. “Application of Filamentous Fungi in Microalgae-Based Wastewater Remediation for Biomass Harvesting and Utilization: From Mechanisms to Practical Application.” *Algal Research* 62:102614. doi: 10.1016/j.algal.2021.102614.

Lin, Zhong, Yunfeng Xu, Zhen Zhen, Yu Fu, Yueqiao Liu, Wenyan Li, Chunling Luo, Aizhong Ding, and Dayi Zhang. 2015. “Application and Reactivation of Magnetic Nanoparticles

in Microcystis Aeruginosa Harvesting." *Bioresource Technology* 190:82–88. doi: 10.1016/j.biortech.2015.04.068.

Liu, Jia, Lei Jiang, Sirui He, Jie Zhang, and Wei Shao. 2022. "Recent Progress in PNIPAM-Based Multi-Responsive Actuators: A Mini-Review." *Chemical Engineering Journal* 433:133496. doi: 10.1016/j.cej.2021.133496.

Liu, Jiexia, Yi Zhu, Yujun Tao, Yuanming Zhang, Aifen Li, Tao Li, Ming Sang, and Chengwu Zhang. 2013. "Freshwater Microalgae Harvested via Flocculation Induced by pH Decrease." *Biotechnology for Biofuels* 6(1):98. doi: 10.1186/1754-6834-6-98.

Liu, Jin, and Feng Chen. 2016. "Biology and Industrial Applications of Chlorella: Advances and Prospects." Pp. 1–35 in *Microalgae Biotechnology*, edited by C. Posten and S. Feng Chen. Cham: Springer International Publishing.

Lordan, Sinéad, R. Paul Ross, and Catherine Stanton. 2011. "Marine Bioactives as Functional Food Ingredients: Potential to Reduce the Incidence of Chronic Diseases." *Marine Drugs* 9(6):1056–1100. doi: 10.3390/md9061056.

Lü, Jing, Con Sheahan, and Pengcheng Fu. 2011. "Metabolic Engineering of Algae for Fourth Generation Biofuels Production." *Energy & Environmental Science* 4(7):2451–66.

Ma, Xiao-Nian, Tian-Peng Chen, Bo Yang, Jin Liu, and Feng Chen. 2016. "Lipid Production from Nannochloropsis." *Marine Drugs* 14(4):61. doi: 10.3390/md14040061.

Malakootian, Mohammad, Behnam Hatami, Shidwash Dowlatshahi, and Ahmad Rajabizadeh. 2016. "Growth and Lipid Accumulation in Response to Different Cultivation

Temperatures in Nannochloropsis Oculata for Biodiesel Production."

Maliwat, Gian Carlo, Stephanie Velasquez, Jan Lorie Robil, Merab Chan, Rex Ferdinand Traifalgar, Melchor Tayamen, and Janice A. Ragaza. 2017. "Growth and Immune Response of Giant Freshwater Prawn Macrobrachium Rosenbergii (De Man) Postlarvae Fed Diets Containing Chlorella Vulgaris (Beijerinck)." *Aquaculture Research* 48(4):1666–76. doi: 10.1111/are.13004.

Maltsev, Yevhen, Svetlana Maltseva, and Irina Maltseva. 2022. "Diversity of Cyanobacteria and Algae During Primary Succession in Iron Ore Tailing Dumps." *Microbial Ecology* 83(2):408–23. doi: 10.1007/s00248-021-01759-y.

Maltseva, Irina, Aleksandr Yakoviichuk, Svetlana Maltseva, Svetlana Cherkashina, Maxim Kulikovskiy, and Yevhen Maltsev. 2024. "Biochemical and Antioxidant Characteristics of Chlorococcum Oleofaciens (Chlorophyceae, Chlorophyta) under Various Cultivation Conditions." *Plants* 13(17):2413. doi: 10.3390/plants13172413.

Maruyama, Isao, Takashi Nakao, Ikuro Shigeno, Yotaro Ando, and Kazutsugu Hirayama. 1997. "Application of Unicellular Algae Chlorella Vulgaris for the Mass-Culture of Marine Rotifer Brachionus." Pp. 133–38 in *Live Food in Aquaculture*, edited by A. Hagiwara, T. W. Snell, E. Lubzens, and C. S. Tamaru. Dordrecht: Springer Netherlands.

Matter, Bui, Jung, Seo, Kim, Lee, and Oh. 2019. "Flocculation Harvesting Techniques for Microalgae: A Review." *Applied Sciences* 9(15):3069. doi: 10.3390/app9153069.

Matter, Ibrahim A., Osama M. Darwesh, and Mohamed F. Eida. 2018. "Harvesting of

Microalgae Scenedesmus Obliquus Using Chitosan-Alginate Dual Flocculation System." *Bioscience Research* 15(1):540–48.

Melis, Anastasios, and Thomas Happe. 2001. "Hydrogen Production. Green Algae as a Source of Energy." *Plant Physiology* 127(3):740–48. doi: 10.1104/pp.010498.

Milledge, John J., and Sonia Heaven. 2013. "A Review of the Harvesting of Micro-Algae for Biofuel Production." *Reviews in Environmental Science and Bio/Technology* 12(2):165–78. doi: 10.1007/s11157-012-9301-z.

Mohamed, Zakaria A. 2008. "Polysaccharides as a Protective Response against Microcystin-Induced Oxidative Stress in Chlorella Vulgaris and Scenedesmus Quadricauda and Their Possible Significance in the Aquatic Ecosystem." *Ecotoxicology* 17(6):504–16. doi: 10.1007/s10646-008-0204-2.

Montingelli, Maria E., Silvia Tedesco, and Abdul Ghani Olabi. 2015. "Biogas Production from Algal Biomass: A Review." *Renewable and Sustainable Energy Reviews* 43:961–72. doi: 10.1016/j.rser.2014.11.052.

Moraine, R., G. Shelef, A. Meydan, and A. Levi. 1979. "Algal Single Cell Protein from Wastewater Treatment and Renovation Process." *Biotechnology and Bioengineering* 21(7):1191–1207. doi: 10.1002/bit.260210709.

Moshood, Taofeeq D., Gusman Nawanir, and Fatimah Mahmud. 2021. "Microalgae Biofuels Production: A Systematic Review on Socioeconomic Prospects of Microalgae Biofuels and Policy Implications." *Environmental Challenges* 5:100207. doi:

10.1016/j.envc.2021.100207.

Najjar, Yousef S. H., and Amer Abu-Shamleh. 2020. “Harvesting of Microalgae by Centrifugation for Biodiesel Production: A Review.” *Algal Research* 51:102046. doi: 10.1016/j.algal.2020.102046.

Narayanan, Mathiyazhagan. 2024. “Marine Algae Biomass: A Viable and Renewable Resource for Biofuel Production: A Review.” *Algal Research* 82:103687. doi: 10.1016/j.algal.2024.103687.

Negassa, Lalise Wadajo, Majid Mohiuddin, and Girum Ayalneh Tiruye. 2021. “Treatment of Brewery Industrial Wastewater and Generation of Sustainable Bioelectricity by Microbial Fuel Cell Inoculated with Locally Isolated Microorganisms.” *Journal of Water Process Engineering* 41:102018. doi: 10.1016/j.jwpe.2021.102018.

Nguyen, Thanh Tien, Yoshimitsu Uemura, Vijendren Krishnan, and Nadila Abdul Khalid. 2017. “Autoflocculation of Scenedesmus Quadricauda: Effects of Aeration Rate, Aeration Gas CO2 Concentration and Medium Nitrogen Concentration.” *International Journal of Biomass and Renewables* 6(1):11–17. doi: 10.61762/ijbrvol6iss1art4546.

Nguyen, Thi Dong Phuong, Matthieu Frappart, Pascal Jaouen, Jérémy Pruvost, and Patrick Bourseau. 2014. “Harvesting Chlorella Vulgaris by Natural Increase in pH: Effect of Medium Composition.” *Environmental Technology* 35(11):1378–88. doi: 10.1080/09593330.2013.868531.

Ningrum, Eva, Zela Marni Safitri, Muhammad Asyam Dzaky, Suprapto Suprapto, Achmad

Dwitama Karisma, and Hikmatun Ni'mah. 2022. "The Effect of Temperatures and Monomer Ratios on the Characteristic of Anionic and Cationic Gel-Based Adsorbents." *IOP Conference Series: Earth and Environmental Science* 963(1):012035. doi: 10.1088/1755-1315/963/1/012035.

Nurdogan, Yakup, and William J. Oswald. 1996. "Tube Settling of High-Rate Pond Algae." *Water Science and Technology* 33(7):229–41. doi: 10.1016/0273-1223(96)00358-7.

O'Grady, John, and John A. Morgan. 2011. "Heterotrophic Growth and Lipid Production of Chlorella Protothecoides on Glycerol." *Bioprocess and Biosystems Engineering* 34(1):121–25. doi: 10.1007/s00449-010-0474-y.

Okeke, Emmanuel Sunday, Onome Ejeromedoghene, Charles Obinwanne Okoye, Timothy Prince Chidike Ezeorba, Raphael Nyaruaba, Chukwudozie Kingsley Ikechukwu, Abiodun Oladipo, and Joshua Iseoluwa Orege. 2022. "Microalgae Biorefinery: An Integrated Route for the Sustainable Production of High-Value-Added Products." *Energy Conversion and Management: X* 16:100323. doi: 10.1016/j.ecmx.2022.100323.

Okoro, Victor, Ulugbek Azimov, Jose Munoz, Hector H. Hernandez, and Anh N. Phan. 2019. "Microalgae Cultivation and Harvesting: Growth Performance and Use of Flocculants - A Review." *Renewable and Sustainable Energy Reviews* 115:109364. doi: 10.1016/j.rser.2019.109364.

Oliveira, Helena R., Isabelli D. Bassin, and Magali C. Cammarota. 2019. "Bioflocculation of Cyanobacteria with Pellets of *Aspergillus Niger*: Effects of Carbon Supplementation, Pellet Diameter, and Other Factors in Biomass Densification." *Bioresource Technology*

294:122167. doi: 10.1016/j.biortech.2019.122167.

Ortiz, Antonio, María Jesús García-Galán, Joan García, and Rubén Díez-Montero. 2021. "Optimization and Operation of a Demonstrative Full Scale Microalgae Harvesting Unit Based on Coagulation, Flocculation and Sedimentation." *Separation and Purification Technology* 259:118171. doi: 10.1016/j.seppur.2020.118171.

Pahl, Stephen L., Andrew K. Lee, Theo Kalaitzidis, Peter J. Ashman, Suraj Sathe, and David M. Lewis. 2013. "Harvesting, Thickening and Dewatering Microalgae Biomass." Pp. 165–85 in *Algae for Biofuels and Energy*, edited by M. A. Borowitzka and N. R. Moheimani. Dordrecht: Springer Netherlands.

Park, Jason. B. K., Rupert J. Craggs, and Andy Shilton. 2011. "Recycling Algae to Improve Species Control and Harvest Efficiency from a High Rate Algal Pond." *Water Research* 45(20):6637–49. doi: 10.1016/j.watres.2011.09.042.

Peng, Chengrong, Shuangshuang Li, Jiaoli Zheng, Shun Huang, and Dunhai Li. 2017. "Harvesting Microalgae with Different Sources of Starch-Based Cationic Flocculants." *Applied Biochemistry and Biotechnology* 181(1):112–24. doi: 10.1007/s12010-016-2202-9.

Peter, Angela Paul, Kit Wayne Chew, Ashok Pandey, Sie Yon Lau, Saravanan Rajendran, Huong Yong Ting, Heli Siti Halimatul Munawaroh, Nguyen Van Phuong, and Pau Loke Show. 2023. "Artificial Intelligence Model for Monitoring Biomass Growth in Semi-Batch *Chlorella Vulgaris* Cultivation." *Fuel* 333:126438. doi: 10.1016/j.fuel.2022.126438.

Přibyl, Pavel, Vladislav Cepák, and Vilém Zachleder. 2012. "Production of Lipids in 10 Strains of Chlorella and Parachlorella, and Enhanced Lipid Productivity in Chlorella Vulgaris." *Applied Microbiology and Biotechnology* 94(2):549–61. doi: 10.1007/s00253-012-3915-5.

Radin Mohamed, Radin Maya Saphira, Adel Ali Saeed Al-Gheethi, and Amir Hashim Mohd Kassim, eds. 2019. *Management of Greywater in Developing Countries*. Vol. 87. Cham: Springer International Publishing.

Rahmani, Abdellatif, Djamal Zerrouki, Lahcène Djafer, and André Ayral. 2017. "Hydrogen Recovery from the Photovoltaic Electroflocculation-Flotation Process for Harvesting *Chlorella Pyrenoidosa* Microalgae." *International Journal of Hydrogen Energy* 42(31):19591–96. doi: 10.1016/j.ijhydene.2017.06.123.

Rajabi Islami, Houman, and Reza Assareh. 2020. "Enhancement Effects of Ferric Ion Concentrations on Growth and Lipid Characteristics of Freshwater Microalga *Chlorococcum Oleofaciens* KF584224.1 for Biodiesel Production." *Renewable Energy* 149:264–72. doi: 10.1016/j.renene.2019.12.067.

Randrianarison, Gilbert, and Muhammad Aqeel Ashraf. 2017. "Microalgae: A Potential Plant for Energy Production." *Geology, Ecology, and Landscapes* 1(2):104–20. doi: 10.1080/24749508.2017.1332853.

Rasdi, Nadiah W., and Jian G. Qin. 2015. "Effect of N:P Ratio on Growth and Chemical Composition of Nannochloropsis Oculata and Tisochrysis Lutea." *Journal of Applied Phycology* 27(6):2221–30. doi: 10.1007/s10811-014-0495-z.

Rashid, Naim, Saif Ur Rehman, and Jong-In Han. 2013. “Rapid Harvesting of Freshwater Microalgae Using Chitosan.” *Process Biochemistry* 48(7):1107–10. doi: 10.1016/j.procbio.2013.04.018.

Ratomski, Patryk, and Małgorzata Hawrot-Paw. 2021. “Influence of Nutrient-Stress Conditions on Chlorella Vulgaris Biomass Production and Lipid Content.” *Catalysts* 11(5):573. doi: 10.3390/catal11050573.

Rayati, Marzie, Houman Rajabi Islami, and Mehdi Shamsaie Mehrgan. 2020. “Light Intensity Improves Growth, Lipid Productivity, and Fatty Acid Profile of Chlorococcum Oleofaciens (Chlorophyceae) for Biodiesel Production.” *BioEnergy Research* 13(4):1235–45. doi: 10.1007/s12155-020-10144-5.

Renaud, Susan M., David L. Parry, Luong-Van Thinh, Chao-yang Kuo, Amanda Padovan, and Nadine Sammy. 1991. “Effect of Light Intensity on the Proximate Biochemical and Fatty Acid Composition of Isochrysis Sp. and Nannochloropsis Oculata for Use in Tropical Aquaculture.” *Journal of Applied Phycology* 3(1):43–53. doi: 10.1007/BF00003918.

Rodríguez-Castillo, Gabriel, Carla Amarelo-Santos, Maritza Guerrero-Barrantes, Alberto Delgado dos Reis, Gabriel Rodríguez-Castillo, Carla Amarelo-Santos, Maritza Guerrero-Barrantes, and Alberto Delgado dos Reis. 2016. “Study of Morphological and Phisiological Characteristics of Chlorella Protothecoides Oriented to Lipid Production for Biofuel.” *Revista Tecnología En Marcha* 29:3–11. doi: 10.18845/tm.v29i6.2897.

Roy, Madonna, and Kaustubha Mohanty. 2019. “A Comprehensive Review on Microalgal Harvesting Strategies: Current Status and Future Prospects.” *Algal Research* 44:101683.

doi: 10.1016/j.algal.2019.101683.

Ru, Irene Tiong Kai, Yeong Yik Sung, Malinna Jusoh, Mohd Effendy Abdul Wahid, and Thilahgavani Nagappan. 2020. “Chlorella Vulgaris: A Perspective on Its Potential for Combining High Biomass with High Value Bioproducts.” *Applied Phycology* 1(1):2–11. doi: 10.1080/26388081.2020.1715256.

Ryan J, Powell, and Hill Russell T. 2014. “Mechanism of Algal Aggregation by Bacillus Sp. Strain RP1137.” *American Society for Microbiology* 80(13):4042–50. doi: 10.1128/AEM.00887-14.

Safi, Carl, Bachar Zebib, Othmane Merah, Pierre-Yves Pontalier, and Carlos Vaca-Garcia. 2014. “Morphology, Composition, Production, Processing and Applications of *Chlorella Vulgaris*: A Review.” *Renewable and Sustainable Energy Reviews* 35:265–78. doi: 10.1016/j.rser.2014.04.007.

Sakarika, Myrsini, and Michael Kornaros. 2019. “Chlorella Vulgaris as a Green Biofuel Factory: Comparison between Biodiesel, Biogas and Combustible Biomass Production.” *Bioresource Technology* 273:237–43. doi: 10.1016/j.biortech.2018.11.017.

Savvidou, Maria G., Maria Myrto Dardavila, Ioulia Georgiopoulou, Vasiliki Louli, Haralambos Stamatis, Dimitris Kekos, and Epaminondas Voutsas. 2021. “Optimization of Microalga Chlorella Vulgaris Magnetic Harvesting.” *Nanomaterials* 11(6):1614. doi: 10.3390/nano11061614.

Scherbina, Vyacheslav, Irina Andreevna Maltseva, and Anatoliy Solonenko. 2014. “Peculiarities

of Postpyrogene Development of Algae in Steppe Biocenoses at Askania Nova Biospheric National Park." *Contemporary Problems of Ecology* 7(2):187–91. doi: 10.1134/S1995425514020140.

Sharma, Rekha. 2012. "Effects of Culture Conditions on Growth and Biochemical Profile of Chlorella Vulgaris." *Journal of Plant Pathology & Microbiology* 03(05). doi: 10.4172/2157-7471.1000131.

Sharmila, V. Godvin, J. Rajesh Banu, M. Dinesh Kumar, Somanathan Adish Kumar, and Gopalakrishnan Kumar. 2022. "Algal Biorefinery towards Decarbonization: Economic and Environmental Consideration." *Bioresource Technology* 364:128103. doi: 10.1016/j.biortech.2022.128103.

Shen, Xiao-Fei, Qi-Wen Qin, Shao-Kai Yan, Jia-Le Huang, Kun Liu, and Shou-Biao Zhou. 2019. "Biodiesel Production from Chlorella Vulgaris under Nitrogen Starvation in Autotrophic, Heterotrophic, and Mixotrophic Cultures." *Journal of Applied Phycology* 31(3):1589–96. doi: 10.1007/s10811-019-01765-1.

Shen, Ying, Yan Cui, and Wenqiao Yuan. 2013. "Flocculation Optimization of Microalga Nannochloropsis Oculata." *Applied Biochemistry and Biotechnology* 169(7):2049–63. doi: 10.1007/s12010-013-0123-4.

Shi, Ye, Chongbo Ma, Lele Peng, and Guihua Yu. 2015. "Conductive 'Smart' Hybrid Hydrogels with PNIPAM and Nanostructured Conductive Polymers." *Advanced Functional Materials* 25(8):1219–25. doi: 10.1002/adfm.201404247.

Singh, Har Mohan, Mriduta Sharma, V. V. Tyagi, Kajol Goria, D. Buddhi, Atul Sharma, Frank Bruno, Shane Sheoran, and Richa Kothari. 2023. “Potential of Biogenic and Non-Biogenic Waste Materials as Flocculant for Algal Biomass Harvesting: Mechanism, Parameters, Challenges and Future Prospects.” *Journal of Environmental Management* 337:117591. doi: 10.1016/j.jenvman.2023.117591.

Specht, Elizabeth A., and Stephen P. Mayfield. 2014. “Algae-Based Oral Recombinant Vaccines.” *Frontiers in Microbiology* 5. doi: 10.3389/fmicb.2014.00060.

Su, Chia-Hung, Liang-Jung Chien, James Gomes, Yu-Sheng Lin, Yuan-Kun Yu, Jhang-Song Liou, and Rong-Jhih Syu. 2011. “Factors Affecting Lipid Accumulation by Nannochloropsis Oculata in a Two-Stage Cultivation Process.” *Journal of Applied Phycology* 23(5):903–8. doi: 10.1007/s10811-010-9609-4.

Sui, Yixing, Yu Jiang, Michele Moretti, and Siegfried E. Vlaeminck. 2020. “Harvesting Time and Biomass Composition Affect the Economics of Microalgae Production.” *Journal of Cleaner Production* 259:120782. doi: 10.1016/j.jclepro.2020.120782.

Sukenik, Assaf, Yael Carmeli, and Tamar Berner. 1989. “Regulation of Fatty Acid Composition by Irradiance Level in the Eustigmatophyte Nannochloropsis Sp.” *Journal of Phycology* 25(4):686–92. doi: 10.1111/j.0022-3646.1989.00686.x.

Sun, Xiaohang, Emiel DenHartog, Xiangwu Zhang, and Marian McCord. 2018. “Study of Poly(N-Isopropylacrylamide) Grafted Cotton Fabrics Initiated by Atmospheric Pressure Plasma.” *Applied Surface Science* 453:182–91. doi: 10.1016/j.apsusc.2018.05.056.

Sun, Zheng, Zhi-gang Zhou, Henri Gerken, Feng Chen, and Jin Liu. 2015. “Screening and Characterization of Oleaginous *Chlorella* Strains and Exploration of Photoautotrophic *Chlorella Protothecoides* for Oil Production.” *Bioresource Technology* 184:53–62. doi: 10.1016/j.biortech.2014.09.054.

Suparmaniam, Uganeeswary, Man Kee Lam, Yoshimitsu Uemura, Jun Wei Lim, Keat Teong Lee, and Siew Hoong Shuit. 2019. “Insights into the Microalgae Cultivation Technology and Harvesting Process for Biofuel Production: A Review.” *Renewable and Sustainable Energy Reviews* 115:109361. doi: 10.1016/j.rser.2019.109361.

Tabarsa, Mehdi, Il-Shik Shin, Ju Hun Lee, Utoomporn Surayot, WooJung Park, and SangGuan You. 2015. “An Immune-Enhancing Water-Soluble α-Glucan from Chlorella Vulgaris and Structural Characteristics.” *Food Science and Biotechnology* 24(6):1933–41. doi: 10.1007/s10068-015-0255-0.

Tan, Xin Bei, Man Kee Lam, Yoshimitsu Uemura, Jun Wei Lim, Chung Yiin Wong, and Keat Teong Lee. 2018. “Cultivation of Microalgae for Biodiesel Production: A Review on Upstream and Downstream Processing.” *Chinese Journal of Chemical Engineering* 26(1):17–30. doi: 10.1016/j.cjche.2017.08.010.

Tang, Li, Jia Ke Jin, Anjun Qin, Wang Zhang Yuan, Yu Mao, Ju Mei, Jing Zhi Sun, and Ben Zhong Tang. 2009. “A Fluorescent Thermometer Operating in Aggregation-Induced Emission Mechanism: Probing Thermal Transitions of PNIPAM in Water.” *Chemical Communications* 0(33):4974–76. doi: 10.1039/B907382E.

Thanigaivel, Sundaram, Sundaram Vickram, Nibedita Dey, Govindarajan Gulothungan,

Ramasamy Subbaiya, Muthusamy Govarthanan, Natchimuthu Karmegam, and Woong Kim. 2022. “The Urge of Algal Biomass-Based Fuels for Environmental Sustainability against a Steady Tide of Biofuel Conflict Analysis: Is Third-Generation Algal Biorefinery a Boon?” *Fuel* 317:123494. doi: 10.1016/j.fuel.2022.123494.

Trainor, Francis R., and Harold C. Bold. 1953. “Three New Unicellular Chlorophyceae from Soil.” *American Journal of Botany* 40(10):758–67. doi: 10.2307/2438272.

Tran, Clara T. H., Alexey Kondyurin, Wojciech Chrzanowski, Marcela M. M. Bilek, and David R. McKenzie. 2014. “Increasing Binding Density of Yeast Cells by Control of Surface Charge with Allylamine Grafting to Ion Modified Polymer Surfaces.” *Colloids and Surfaces B: Biointerfaces* 122:537–44. doi: 10.1016/j.colsurfb.2014.07.026.

Úbeda, Bárbara, José Ángel Gálvez, Mónica Michel, and Ana Bartual. 2017. “Microalgae Cultivation in Urban Wastewater: *Coelastrum* Cf. *Pseudomicroporum* as a Novel Carotenoid Source and a Potential Microalgae Harvesting Tool.” *Bioresource Technology* 228:210–17. doi: 10.1016/j.biortech.2016.12.095.

UTEX Culture Collection of Algae. 2024. “Modified Artificial Seawater Medium.” *UTEX Culture Collection of Algae*. Retrieved August 11, 2024 (https://utex.org/products/modified-artificial-seawater-medium).

Valverde, Federico, Francisco J. Romero-Campero, Rosa León, Miguel G. Guerrero, and Aurelio Serrano. 2016. “New Challenges in Microalgae Biotechnology.” *European Journal of Protistology* 55:95–101. doi: 10.1016/j.ejop.2016.03.002.

Vasistha, S., A. Khanra, M. Clifford, and M. P. Rai. 2021. “Current Advances in Microalgae Harvesting and Lipid Extraction Processes for Improved Biodiesel Production: A Review.” *Renewable and Sustainable Energy Reviews* 137:110498. doi: 10.1016/j.rser.2020.110498.

Velmurugan, Palanivel, Seralathan Kamala-Kannan, Vellingiri Balachandar, Perumalsamy Lakshmanaperumalsamy, Jong-Chan Chae, and Byung-Taek Oh. 2010. “Natural Pigment Extraction from Five Filamentous Fungi for Industrial Applications and Dyeing of Leather.” *Carbohydrate Polymers* 79(2):262–68. doi: 10.1016/j.carbpol.2009.07.058.

Wan, Chun, Xin-Qing Zhao, Suo-Lian Guo, Md. Asraful Alam, and Feng-Wu Bai. 2013. “Bioflocculant Production from *Solibacillus Silvestris* W01 and Its Application in Cost-Effective Harvest of Marine Microalga *Nannochloropsis Oceanica* by Flocculation.” *Bioresource Technology* 135:207–12. doi: 10.1016/j.biortech.2012.10.004.

Wang, Chao, Yangyang Yang, Jun Hou, Peifang Wang, Lingzhan Miao, Xun Wang, and Laodong Guo. 2020. “Optimization of Cyanobacterial Harvesting and Extracellular Organic Matter Removal Utilizing Magnetic Nanoparticles and Response Surface Methodology: A Comparative Study.” *Algal Research* 45:101756. doi: 10.1016/j.algal.2019.101756.

Wang, Junjun, Qinghua Tian, Weimin Zeng, Guanzhou Qiu, and Li Shen. 2023. “Insights about Fungus-Microalgae Symbiotic System in Microalgae Harvesting and Wastewater Treatment: A Review.” *Renewable and Sustainable Energy Reviews* 182:113408. doi: 10.1016/j.rser.2023.113408.

Wang, Kexin, Kuan Shiong Khoo, Hui Yi Leong, Dillirani Nagarajan, Kit Wayne Chew, Huong Yong Ting, Anurita Selvarajoo, Jo-Shu Chang, and Pau Loke Show. 2022. "How Does the Internet of Things (IoT) Help in Microalgae Biorefinery?" *Biotechnology Advances* 54:107819. doi: 10.1016/j.biotechadv.2021.107819.

Wang, Shuang, Jiangyi Zhou, Yifei Zhang, Sirong He, Sivakumar Esakkimuthu, Kai Zhu, Sunel Kumar, Gaojin Lv, and Xun Hu. 2023. "Biochar Assisted Cultivation of *Chlorella Protothecoides* for Adsorption of Tetracycline and Electrochemical Study on Self-Cultured *Chlorella Protothecoides*." *Bioresource Technology* 389:129810. doi: 10.1016/j.biortech.2023.129810.

Wang, Xuan, Yaoli Zhang, Changlei Xia, Ali Alqahtani, Ashutosh Sharma, and Arivalagan Pugazhendhi. 2023. "A Review on Optimistic Biorefinery Products: Biofuel and Bioproducts from Algae Biomass." *Fuel* 338:127378. doi: 10.1016/j.fuel.2022.127378.

Wells, Mark L., Philippe Potin, James S. Craigie, John A. Raven, Sabeeha S. Merchant, Katherine E. Helliwell, Alison G. Smith, Mary Ellen Camire, and Susan H. Brawley. 2017. "Algae as Nutritional and Functional Food Sources: Revisiting Our Understanding." *Journal of Applied Phycology* 29(2):949–82. doi: 10.1007/s10811-016-0974-5.

Weschler, Matthew K., William J. Barr, Willie F. Harper, and Amy E. Landis. 2014. "Process Energy Comparison for the Production and Harvesting of Algal Biomass as a Biofuel Feedstock." *Bioresource Technology* 153:108–15. doi: 10.1016/j.biortech.2013.11.008.

Williams, Del. 2009. "Algenol Biofuels Announces Plan to Build and Operate a Pilot-Scale

Algae-Based Integrated Biorefinery." *Journal of Canadian Petroleum Technology* 48(8):6–8.

Wu, Qingyu, Shi Yin, Guoying Sheng, and Jiamo Fu. 1994. "New discoveries in study on hydrocarbons from thermal degradation of heterotrophically yellowing alga." *Science in China Series B, Chemistry, life sciences & earth sciences* (3).

Xu, Han, Xiaoling Miao, and Qingyu Wu. 2006. "High Quality Biodiesel Production from a Microalga *Chlorella Protothecoides* by Heterotrophic Growth in Fermenters." *Journal of Biotechnology* 126(4):499–507. doi: 10.1016/j.jbiotec.2006.05.002.

Yamamoto, Maki, Mariko Fujishita, Aiko Hirata, and Shigeyuki Kawano. 2004. "Regeneration and Maturation of Daughter Cell Walls in the Autospore-Forming Green Alga Chlorella Vulgaris (Chlorophyta, Trebouxiophyceae)." *Journal of Plant Research* 117(4):257–64. doi: 10.1007/s10265-004-0154-6.

Yamamoto, Maki, Ippei Kurihara, and Shigeyuki Kawano. 2005. "Late Type of Daughter Cell Wall Synthesis in One of the Chlorellaceae, Parachlorella Kessleri (Chlorophyta, Trebouxiophyceae)." *Planta* 221(6):766–75. doi: 10.1007/s00425-005-1486-8.

Yanase, Keiichi, Richard Buchner, and Takaaki Sato. 2020. "Microscopic Insights into the Phase Transition of Poly(N-Isopropylacrylamide) in Aqueous Media: Effects of Molecular Weight and Polymer Concentration." *Journal of Molecular Liquids* 302:112025. doi: 10.1016/j.molliq.2019.112025.

Yang, Hengrui, A. Catarina C. Esteves, Haijin Zhu, Dujin Wang, and John H. Xin. 2012. "In-

Situ Study of the Structure and Dynamics of Thermo-Responsive PNIPAAm Grafted on a Cotton Fabric." *Polymer* 53(16):3577–86. doi: 10.1016/j.polymer.2012.05.053.

Yang, Jia, Xin Li, Hongying Hu, Xue Zhang, Yin Yu, and Yongsheng Chen. 2011. "Growth and Lipid Accumulation Properties of a Freshwater Microalga, *Chlorella Ellipsoidea* YJ1, in Domestic Secondary Effluents." *Applied Energy* 88(10):3295–99. doi: 10.1016/j.apenergy.2010.11.029.

Yang, Limin, Huankai Li, and Qin Wang. 2019. "A Novel One-Step Method for Oil-Rich Biomass Production and Harvesting by Co-Cultivating Microalgae with Filamentous Fungi in Molasses Wastewater." *Bioresource Technology* 275:35–43. doi: 10.1016/j.biortech.2018.12.036.

Yeh, Kuei-Ling, and Jo-Shu Chang. 2011. "Nitrogen Starvation Strategies and Photobioreactor Design for Enhancing Lipid Content and Lipid Production of a Newly Isolated Microalga Chlorella Vulgaris ESP-31: Implications for Biofuels." *Biotechnology Journal* 6(11):1358–66. doi: 10.1002/biot.201000433.

Yen, Hong-Wei, Pin-Wen Chen, and Li-Juan Chen. 2015. "The Synergistic Effects for the Co-Cultivation of Oleaginous Yeast-*Rhodotorula Glutinis* and Microalgae-*Scenedesmus Obliquus* on the Biomass and Total Lipids Accumulation." *Bioresource Technology* 184:148–52. doi: 10.1016/j.biortech.2014.09.113.

Yin, Meizhen, Ke Ding, Radu A. Gropeanu, Jie Shen, Rüdiger Berger, Tanja Weil, and Klaus Müllen. 2008. "Dendritic Star Polymers for Efficient DNA Binding and Stimulus-Dependent DNA Release." *Biomacromolecules* 9(11):3231–38. doi: 10.1021/bm800797j.

Yoo, Chan, Hyun-Joon La, Sun-Chang Kim, and Hee-Mock Oh. 2015. “Simple Processes for Optimized Growth and Harvest of Ettlia Sp. by pH Control Using CO2 and Light Irradiation.” *Biotechnology and Bioengineering* 112(2):288–96. doi: 10.1002/bit.25362.

Yun, Chol-Jin, Kum-Ok Hwang, Song-Su Han, and Hyong-Guan Ri. 2019. “The Effect of Salinity Stress on the Biofuel Production Potential of Freshwater Microalgae Chlorella Vulgaris YH703.” *Biomass and Bioenergy* 127:105277. doi: 10.1016/j.biombioe.2019.105277.

Zanella, Lorenzo, and Fabio Vianello. 2020. “Microalgae of the Genus *Nannochloropsis*: Chemical Composition and Functional Implications for Human Nutrition.” *Journal of Functional Foods* 68:103919. doi: 10.1016/j.jff.2020.103919.

Zhang, Jianguo, and Bo Hu. 2012. “A Novel Method to Harvest Microalgae via Co-Culture of Filamentous Fungi to Form Cell Pellets.” *Bioresource Technology* 114:529–35. doi: 10.1016/j.biortech.2012.03.054.

Zhang, Jilai, Qianqian Xiang, Lin Shen, Jian Ling, Chuanhua Zhou, Jinming Hu, and Liqiang Chen. 2020. “Surface Charge-Dependent Bioaccumulation Dynamics of Silver Nanoparticles in Freshwater Algae.” *Chemosphere* 247:125936. doi: 10.1016/j.chemosphere.2020.125936.

Zhao, Fangchao, Xixi Han, Zhuang Shao, Zhichao Li, Zongxue Li, and Dong Chen. 2022. “Effects of Different Pore Sizes on Membrane Fouling and Their Performance in Algae Harvesting.” *Journal of Membrane Science* 641:119916. doi: 10.1016/j.memsci.2021.119916.

Zheng, Yi, Mark Roberts, Jesse Kelly, Ning Zhang, and Terry Walker. 2015. “Harvesting Microalgae Using the Temperature-Activated Phase Transition of Thermoresponsive Polymers.” *Algal Research* 11:90–94. doi: 10.1016/j.algal.2015.06.006.

Zheng, Yi, Rui Xiao, and Mark Roberts. 2016. “Polymer-Enhanced Enzymatic Microalgal Cell Disruption for Lipid and Sugar Recovery.” *Algal Research* 14:100–108. doi: 10.1016/j.algal.2016.01.010.

Zhu, Liandong, Zhaohua Li, and Erkki Hiltunen. 2018. “Microalgae Chlorella Vulgaris Biomass Harvesting by Natural Flocculant: Effects on Biomass Sedimentation, Spent Medium Recycling and Lipid Extraction.” *Biotechnology for Biofuels* 11(1):183. doi: 10.1186/s13068-018-1183-z.

Appendix A - Copyright permission for Figure 1.1

JOHN WILEY AND SONS LICENSE
TERMS AND CONDITIONS

Oct 28, 2024

This Agreement between Xuexue Wang ("You") and John Wiley and Sons ("John Wiley and Sons") consists of your license details and the terms and conditions provided by John Wiley and Sons and Copyright Clearance Center.

License Number	5897820756807
License date	Oct 28, 2024
Licensed Content Publisher	John Wiley and Sons
Licensed Content Publication	Journal of Phycology
Licensed Content Title	Taxonomic revision of oil-producing green algae, Chlorococcum oleofaciens (Volvocales, Chlorophyceae), and its relatives
Licensed Content Author	Yuriko Kawasaki, Takashi Nakada, Masaru Tomita
Licensed Content Date	Sep 13, 2015
Licensed Content Volume	51
Licensed Content Issue	5
Licensed Content Pages	17
Type of use	Dissertation/Thesis
Requestor type	University/Academic
Format	Electronic

Appendix B - Copyright permission for Figure 1.3

ELSEVIER LICENSE
TERMS AND CONDITIONS

Oct 28, 2024

This Agreement between XUEXUE WANG ("You") and Elsevier ("Elsevier") consists of your license details and the terms and conditions provided by Elsevier and Copyright Clearance Center.

License Number	5897831120926
License date	Oct 28, 2024
Licensed Content Publisher	Elsevier
Licensed Content Publication	Renewable and Sustainable Energy Reviews
Licensed Content Title	Morphology, composition, production, processing and applications of Chlorella vulgaris: A review
Licensed Content Author	Carl Safi,Bachar Zebib,Othmane Merah,Pierre-Yves Pontalier,Carlos Vaca-Garcia
Licensed Content Date	Jul 1, 2014
Licensed Content Volume	35
Licensed Content Issue	n/a
Licensed Content Pages	14
Start Page	265
End Page	278
Type of Use	reuse in a thesis/dissertation

Appendix C - Copyright permission for Chapter 2

ELSEVIER LICENSE
TERMS AND CONDITIONS

Nov 04, 2024

This Agreement between Xuexue Wang ("You") and Elsevier ("Elsevier") consists of your license details and the terms and conditions provided by Elsevier and Copyright Clearance Center.

License Number	5901991480948
License date	Nov 04, 2024
Licensed Content Publisher	Elsevier
Licensed Content Publication	Bioresource Technology
Licensed Content Title	Microalgae aggregation induced by thermoresponsive polymers
Licensed Content Author	Xuexue Wang,Donovan Mafukidze,Yi Zheng
Licensed Content Date	Jan 1, 2025
Licensed Content Volume	415
Licensed Content Issue	n/a
Licensed Content Pages	1
Start Page	131650
End Page	
Type of Use	reuse in a thesis/dissertation
Portion	full article